Hydrogeochemical Characteristics of the Ngatamariki Geothermal Field and a Comparison with the Orakei Korako Thermal Area, Taupo Volcanic Zone, New Zealand.

A thesis submitted in partial fulfilment of the requirements for the

Degree of

Master of Science in Geology

at the

University of Canterbury

By

Jeremy Mark O'Brien

2010

Frontispiece

"When the water starts boiling it is foolish to turn off the heat"

~Nelson Mandela~

Abstract

The Ngatamariki Geothermal Field is located 20 km north of Taupo in the Taupo Volcanic Zone and has a boundary of 12 km^2 as delineated by magneto-telluric surveys (Urzua 2008). Rhyolitic deposits, derived from the Maroa Volcanic Centre, dominate the geology of the area with the 186 AD (Wilson et al. 2009) Taupo pumice mantling stream valleys in the area. The majority of thermal features at Ngatamariki are located along the Orakonui Stream on the western boundary of the field; the stream area is dominated by a 50x30 m geothermal pool filling a hydrothermal eruption crater. This crater was formed during a hydrothermal eruption in 1948, with a subsequent eruption in April 2005. Orakei Korako is located 7 km north of Ngatamariki and has one of the largest collections of thermal features in New Zealand. The geology at Orakei Korako is similar to Ngatamariki, but the area is dominated by a series of south-west trending normal faults which create sinter terraces on the eastern bank of Lake Ohakuri.

Water samples from springs and wells at Ngatamariki and Orakei Korako were taken to assess the nature of both fields. Spring waters at Ngatamariki have chloride contents of 56 to 647 mg/l with deep waters from wells ranging from 1183 to 1574 mg/l. This variation is caused by mixing of deep waters with a steam heated groundwater, above clay caps within the reservoir. Stable isotopic results ($\delta^{18}O$ and δD) suggest that reservoir waters are meteoric waters mixed with magmatic (andesitic) water at Ngatamariki.

Reservoir water chemistry at Orakei Korako exhibits low chloride contents, which is anomalous in the Taupo Volcanic Zone. Chloride content in well and spring waters is similar ranging from 546 to 147 mg/l, due to mixing of reservoir fluids with a 'hot water' diluent at depth. Isotopic compositions of spring waters suggest that they are meteoric waters which mix with magmatic (rhyolitic) water, more enriched in $\delta^{18}O$ and δD than 'andesitic' water.

Relationships between major ion concentrations and known subsurface geology suggest there is no hydraulic connection between the two fields.

Table of Contents

List of Figures

Chapter 1

Chapter 2

Chapter 3

List of Tables

Acknowledgments

Firstly I would like to thank my supervisors Prof. Jim Cole and Dr Travis Horton for your time and advice. Jim for always having an open door, an open mind to my sometimes wild trains of thought, countless edits and for blossoming my interest into initially volcanology and then geothermal systems. Travis for also always having an open door, for help with getting my head round geochemical concepts and the analysis of the samples here at Canterbury.

Huge thanks to Mighty River Power for jointly sponsoring me with the Tertiary Education Commission for the Enterprise Scholarship, keeping me afloat over the past two years and for analysis. Tom Powell my supervisor at Mighty River Power for getting me started in the field and taking the time to look over my work and help me with technical concepts. Also Karl Spinks for his guidance and help while Tom was extremely busy.

Thanks to the Somerville's and Craig and the team at Orakei Korako for access to my field areas throughout the last couple of years.

Clinton Rissmann for taking the time to help me get started in the field and for all the help getting my head around the concepts I have found difficult to understand. James Campbell and Tim Rutherford for being great not only great mates but great field assistants.

Stephen Brown and Bruce Mountain for XRD analysis here at Canterbury and water analysis at GNS Wairakei respectively.

The staff and students in the geology department at the University of Canterbury also need mention for creating such a friendly environment to work in and for the great camaraderie on fieldtrips and on social occasions.

Thanks to the boys from Memorial Ave for the good times and a chilled environment, making it easy to get on with the task at hand.

Last but not least my parents, Mark and Margaret for the guidance and support throughout my time at university and Mel for her support and friendship, you always keep things in perspective for me and have been my rock during the past couple of years, I love you all!

Chapter 1: Introduction

1.1 Overview

Age and duration of geothermal systems is important in understanding and evaluating energy and mineral potential of active and fossil systems (Arehart et al. 2002). The Taupo Volcanic Zone (TVZ) encompasses 23 geothermal systems, with 17 high temperature systems (<250^{o}C) producing a natural heat output of 4200 +/- 500 MW (Bibby et al. 1995). TVZ shows one of the highest intensities worldwide of crustal heat transfer among currently active large-scale rhyolitic volcanism, similar to that of Yellowstone (Giggenbach 1995). Energy outputs for the Ngatamariki and Orakei Korako areas are 40 and 340 MW respectively. Geothermal areas in TVZ occur in two linear zones 20 km apart, on its western and eastern margins (Kissling & Weir 2005), with 75% of the heat output occurring on the eastern side (Bibby et al. 1995).

The Ngatamariki and Orakei Korako geothermal fields are located about 20 and 27 km north of Taupo respectively, in central TVZ. Both are on the eastern margins of the 340 ka Whakamaru Caldera (Figure 1.1).

Geothermal exploration and the development of geothermal reservoirs for power generation are important for New Zealand. Geothermal power provides a renewable source of base load energy, which will bolster the national grid; creating more stability in drought conditions, when the main hydro generators cannot generate as much power. However only 5 of the 23 known fields in the TVZ have been developed for power generation, they are Wairakei, Ohaaki, Rotokawa, Mokai and Kawerau (Figure 1.1).

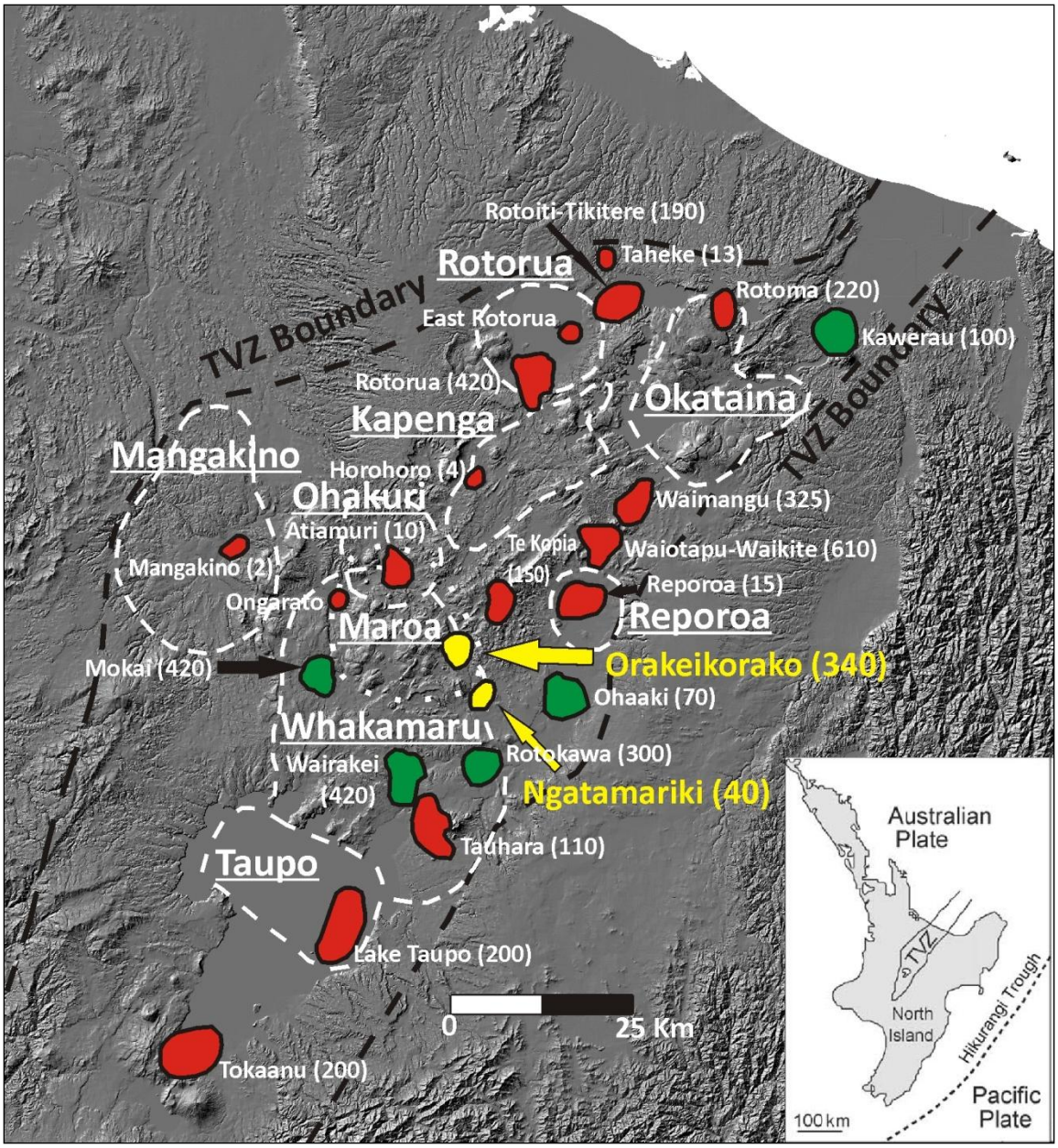

Figure 1.1: Location of geothermal fields and calderas (dashed areas with names underlined) within the TVZ (Maroa is dotted because it is a dome complex). Names of geothermal areas are in smaller font with numbers representing the heat output of each field in MW. Red areas represent geothermal areas, green represent sites currently used for geothermal energy generation and the yellow areas represent the field area for this study. The inset in the bottom right corner shows the location of the map within the North Island of New Zealand. (Adapted from Cole et. al, 2009, Werner and Cardellini, 2006 and Kissling and Weir, 2005)

Soil gas surveys and analysis of geothermal fluids have been used to determine the characteristics of geothermal fields. This is because they can help in determining the type, potential and near surface permeability of a particular field (Werner & Cardellini 2006). The characteristics of a given geothermal field's heat source can be determined by analyzing isotopic, trace and major compositions of soil gases and fluids, which can also provide important information on the composition of geothermal gasses being emitted into the atmosphere from a geothermal system (Christenson et al. 2002).

1.2 T.V.Z

1.2.1 Geology and Structure

The Taupo Volcanic Zone (TVZ) has long been recognised as an active arc/back-arc system related to the westward subduction of the Pacific Plate beneath the Australian Plate (Karig 1970) (Figure 1.1). The subduction of the Pacific Place beneath the Australian Plate in this fashion has formed the Taupo-Hikurangi arc-trench system (Cole & Lewis 1981).

The TVZ is a complex volcano-tectonic depression in New Zealand's North Island of Quaternary intra-arc rifting and calc-alkaline volcanism which began around 2 Ma (Houghton et al. 1995). It is 300 km long and up to 60 km wide and is dominated by rhyolitic volcanism.
There are three main segments; the southwest and northeast segments characterised by andesitic to dacitic volcanoes with no rhyolitic calderas and the central area containing bimodal rhyolite/basalt volcanoes dominated by calderas (Houghton et al. 1995). The activity within these segments is related to a thinner crust only around 15 km thick (Bibby et al. 1995). At the centre of TVZ is the Taupo Fault Belt, a series of northeast trending normal faults related to the intrusion of magma into shallow crust, creating the heat source for the TVZ (Wilson et al. 1995; Kissling & Weir 2005). The fault zone creates zones of high fracture permeability which often host intense geothermal activity, especially where the fractures interact with NE-SW trending regional faults. (eg. Paeroa and Kaingaroa Faults)

Volcanic activity in the central TVZ is dominated by large calderas; these have produced more than 15,000 km^3 of material over the last 1.6 Ma. Eight main calderas have produced the bulk of the material (calderas—Rotorua, Okataina, Kapenga, Reporoa, Ohakuri, Mangakino, Whakamaru and Taupo). The oldest of these are the Mangakino (active c.1.6-1.0 Ma) and Kapenga (earliest activity dated at 1.0 Ma) calderas, which are both located in the western TVZ (Wilson et al. 1995) (Figure 1.1).

1.2.2 Geothermal Systems

Geothermal systems are comprised of three main elements: 1) A heat Source, 2) A permeable rock reservoir and 3) Water to carry the heat from the reservoir to the surface of the earth (Figure 2) or may be referred to as a natural process where heat is transferred from within a confined volume of the Earth's crust (heat source) to the surface (heat sink) (Goff & Janik 2000; Hochstein & Browne 2000) As mentioned above the TVZ encompasses numerous high

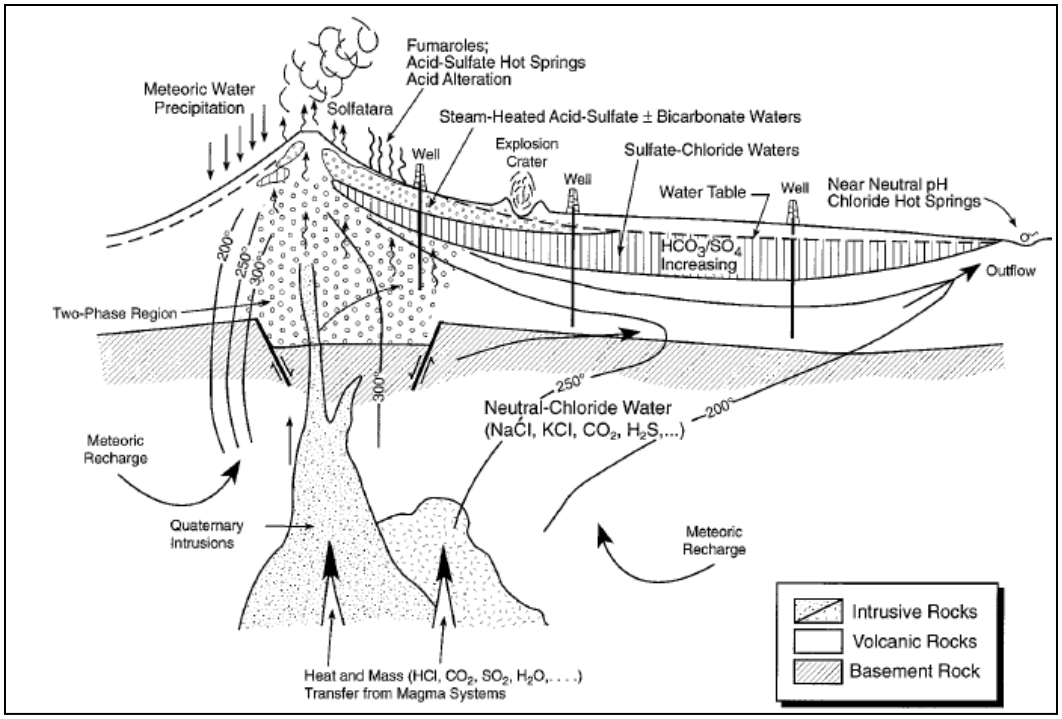

Figure 1.2: Conceptual model of a geothermal system hosted by an andesitic stratovolcano (Goff & Janik 2000).

temperature (<250 ^{o}C) geothermal systems which are split into two linear zones about 20 km apart on the eastern and western edges of the TVZ (Kissling & Weir 2005) (Figure 1.1). The systems have a natural heat output of 4200 +/- 500 MW channelled through these zones with negligible heat flow occurring outside (Bibby et al. 1995).

The heat flow from the 23 recognised systems ranges from < 1 MW (Motuoapa) to 540 MW at Waiotapu, with over 40 percent of the heat flow coming from only four fields each with heat flows greater than 400 MW at Wairakei, Waiotapu, Rotorua and Mokai (Bibby et al. 1995). Electrical resistivity surveys indicate that there are areas of high electrical resistivity between geothermal fields which suggests these areas have undergone hydrothermal alteration (Bibby et al. 1995). The implication of this is that geothermal systems have been confined to their present active locations since the onset of volcanism in the TVZ, it is also thought that once a hydrothermal plume is formed they are long-lasting systems (Kissling & Weir 2005).

Geothermal systems are typically 5 – 25 km^2 in area in TVZ. This is delineated by electrical resistivity studies, measured at depths between 0.5 and 1 km deep. The rising geothermal plumes show low resistivity compared with surrounding shallow geological units acting as aquitards, shallow groundwater aquifers and surface groundwater (Bibby et al. 1995; Kissling & Weir 2005). This phenomena is seen at Ngatamariki where the geothermal plume interacts with the local shallow groundwater and surface groundwater, resulting in a resistivity boundary of 12 km^2 in extent (Bennie 1983; Urzua 2008).

Temperatures of geothermal systems in TVZ range from around 300 ^{o}C in western TVZ (326 ^{o}C at Mokai) to 265 ^{o}C in eastern TVZ (Kissling & Weir 2005). In deeper geothermal wells low-temperature gradients are seen (~20 ^{o}C/km). The extrapolation of these gradients to depth suggests that at 8 km depth temperatures may be in the range of 350 – 400 ^{o}C, consistent with the brittle ductile transition at this depth (Kissling & Weir 2005).

Due to changes in volcanic activity in the TVZ over the past 2 Ma it is not clear whether or not the present day systems are representative of how they may have been in the past. There is, however, evidence that some geothermal fields have been active for several hundred thousand years. Based on fragments of hydrothermally altered material found in younger sediments at Wairakei, an age of 0.5 Ma has been given to the field (Grindley 1965). It is also suggested that the presence of hydrothermal mineral veins in greywacke fragments at Kawerau means that the system has been active for at least 0.2 Ma (Browne 1979). Other examples of geothermal fields demonstrating stability include the Wairakei field which seems to have remained active through the 186 AD Taupo eruption (Wilson et al. 2009) and the Waimangu field surviving the 1886 Mt Tarawera eruption which caused dramatic changes in the area (Kissling & Weir 2005).

1.3 Scope for Thesis

The scope for this study is to constrain the nature of the geothermal system at Ngatamariki by using chemical analysis of water from the deep reservoir (wells) and the surface (springs and seeps). This will allow the processes occurring during fluid ascent and the nature of the system at depth to be attained. This will be carried out by analysing the major ions in waters from springs, wells and surrounding fresh water, which will also give clues as to the effects the geothermal system has on the natural groundwater system. Stable isotopic analysis will also be carried out on the waters to determine what type of water is recharging the geothermal system and if any magmatic influence is evident. Results from this analysis will be compared to similar results from waters at Orakei Korako to determine the nature of water chemistry for the area and create a hydrogeological model across the two areas.

Chapter 2: Chemistry and Geothermal Systems

2.1 Types of Geothermal Systems

Geothermal systems can be categorised is two different ways, either by temperature or enthalpy (high (>150 ^{o}C) vs low (<150 ^{o}C)) (Nicholson 1993) or by geologic and tectonic association. The latter can be spilt into four broad groups (Chandrasekharam & Bundschuh 2008):

1. Geothermal systems associated with **active volcanism and tectonism** (mostly subduction related); examples include TVZ (Figure 2.1), Philippines, Indonesia and North, Central and South America. These systems are generally high temperature/high enthalpy systems (>150 ^{o}C). A good example of this is TVZ, where the Pacific plate is subducted below the Australian plate creating a volcanic arc; the associated magma bodies provide the heat source for the TVZ.
2. Geothermal systems associated with **continental collision**, the best example of this type of system is the Himalayan geothermal belt which extends along the Indus suture zone between the Indian and Eurasian plates.
3. Geothermal systems associated with **active volcanism in continental rift systems**; geothermal systems in Kenya, Eritrea and Ethiopia fall into this category.
4. Geothermal Systems associated with **continental rift systems not associated with volcanism**; these types of systems are located in India and at Larderello in Italy.

In addition to the above there are geothermal systems associated with large sedimentary basins or 'geopressured reservoirs'. These systems are located in large sedimentary basins where a large amount of sediment has been deposited over a relatively short period of geological time. Due to the difficulty of removing the fluids from the sedimentary pores, pore pressures become extremely high and can approach lithostatic pressures. The geothermal gradient in such reservoirs can approach ~75 ^{o}C/km for burial depths of 2 to 3 km (Chandrasekharam & Bundschuh 2008).

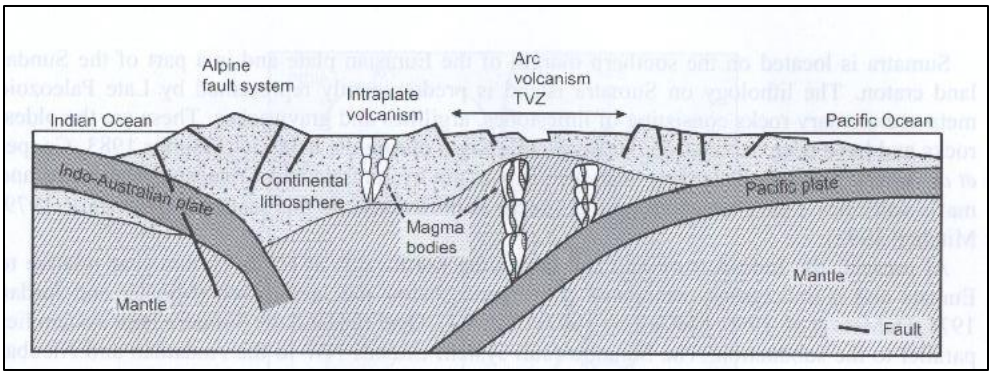

Figure 2.1: Idealized cross section of the tectonic setting of geothermal systems in New Zealand. Magmatic intrusions and upwelling mantle provide the heat source for the geothermal systems in TVZ (Chandrasekharam & Bundschuh 2008).

2.2 Fluids

2.2.1 Types of Water

Waters forming geothermal fluids may be derived from a variety of sources; the following are descriptions adapted from Ellis and Mahon, 1977 and Nicholson, 1993:

- Meteoric water - surface water that has travelled to depths of several kilometres through permeable horizons and fractures.
- Connate or formation water ('Fossil' waters) - water buried with host sediments which has been out of contact with the atmosphere for geologically long periods.
- Juvenile water ('new') – water derived from primary rock magma, not previously part of the hydrosphere.
- Metamorphic water – specially modified connate water derived from hydrous minerals during their recrystallization to less hydrous minerals during metamorphism.
- Magmatic water – Water derived from magma that may not necessarily be juvenile water, because magma may incorporate deep circulating meteoric water or water from sediments.

2.2.2 Geothermal Fluids

Compositions of fluids in active geothermal areas depend on magmatic contributions, duration of fluid/rock interaction, subsurface temperatures, processes occurring within a reservoir and mineralogies of the rock that fluids flow through (Browne & Rodgers 2006). Most geothermal fluids can be classified into four main types;

- **Chloride (Alkali Chloride) -** The primary fluid within geothermal reservoirs is chloride which has a near neutral pH (5-9). It ascends through the reservoir as a single phase fluid until it reaches a depth at which it boils and the CO_2 and H_2S gases dissolved within it partition to the vapour phase and continue to ascend with the fluid (Browne & Rodgers 2006). At the surface these waters commonly occur in areas with active geysers and boiling springs; the dissolved salts in these waters are dominated by sodium and potassium chlorides (Ellis & Mahon 1977). Alteration associated with these waters is argillic – propylitic and silica sinters commonly surround the discharge features at the surface (Nicholson 1993).

- **Acid Sulphate –** Are superficial fluids low in chloride created by condensation of geothermal gases below about 400 ^{o}C into surface waters. Hydrogen sulphide in the steam is subsequently oxidised to sulphate. Acid sulphate waters are generally found on the margins of geothermal fields, away from the main upflow area, over boiling zones, topographic levels higher than the water table and in perched water tables. Typical surface features of acid sulphate waters include cloudy (turbid) pools, mud pools and sometimes springs. The hot acidic nature of the waters allows them to dissolve rock forming large caves and collapse craters (eg. Waiotapu and Orakei Korako) often plunging into the ground at an oblique angle rather than vertically (Nicholson 1993).

  Acid sulphate fluids react rapidly with host rocks and leach them, producing an advanced argillic alteration. Cristobalite, kaolinite and halloysite are diagnostic minerals of this type of alteration. Surface deposits are rare around springs; alunite and other sulphates may be found.

- **Bicarbonate –** Bicarbonate waters are the product of gas and steam condensation (CO_2 and H_2S) into poorly oxygenated sub-surface groundwaters. CO_2-rich fluids and neutral bicarbonate-sulphate water are included within the bicarbonate group. Bicarbonate waters are typically found on the margins of volcanic geothermal areas and can occur in umbrella shaped perched aquifers overlying the geothermal system. Common surface features are 'soda springs' and warm to hot springs with a near neutral pH. Argillic alteration with clays (montmorillonite and kaolin) is common with these fluids and some calcite and silicification may occur. Surface deposits of $CaCO_3$ (travertine) are common around bicarbonate springs and may indicate subsurface temperatures < 150 ^{o}C. Rare aragonite may form if surface discharge cooling is rapid (Nicholson 1993).

- **Dilute Chloride-(HCO_3) Waters –** Formed by the dilution of chloride fluids by either bicarbonate water or ground water during lateral flow. These waters commonly occur as the discharge from warm to hot springs in low temperature systems, and are mostly restricted to the margins of major outflow structures and upflow zones in high temperature systems. A near neutral pH (6-8) is common and chloride is the major anion. Some chloride fluid alteration may be present but is commonly variable. Sometimes development of silica sinters or travertine around springs may occur but this is uncommon. Chloride waters that have only been diluted by groundwater may still be used for geothermometry, even if geothermometry is not possible the spatial distribution of the springs is an important tool to help with understanding the system (Nicholson 1993).

2.2.3 Common Solutes

In geothermal systems deep reservoir chloride fluids have similar dissolved constituents. The concentration of constituents varies greatly in different systems due to variations in gas content, heat source, permeability, rock type, fluid source or mixing and the age of the thermal system. The common species include:

- **Neutral:** SiO_2, As, B, NH_3, Noble Gases
- **Anions:** Cl, SO_4, HCO_3, Br, I, F
- **Cations:** Na, K, Mg, Li, Rb, Cs, Ca, Mn, Al, Fe

The following is a summary of the behaviour of the most commonly abundant of these common species:

Neutral Species

Silica (SiO_2)

Concentrations of silica in geothermal fluids are controlled by the solubility of different silica minerals; typical concentrations of silica in geothermal fluids are 100-300 mg/l. The different species of silica have been extensively studied with the solubility of each species being examined thoroughly. Silica occurs in various polymorphs or forms (amorphous silica, opal, quartz, cristobalite and chalcedony) which all have slight variations in solubility. Quartz and amorphous silica are of most interest in geothermal systems as their behaviour determines the dissolution and precipitation of silica. Chalcedony is important in some systems (Iceland) and in unusual situations where fluid pathways interact with rocks rich in cristobalite or volcanic glass. The extremely soluble silica polymorphs control the concentrations of silica within the liquid until they are dissolved (Nicholson 1993).

Arsenic (As)

Arsenic occurs as As(III) (its reduced state) in geothermal reservoir fluids and hot springs (Ballantyne & Moore 1988). Once all the sulphate available in a hot spring is oxidised As (V) will

occur alongside As (III) already present in the fluid, but is by far the smaller component. In hot spring discharges in New Zealand, the arsenic content is typically 97-100% As (III) (Nicholson 1993).

Boron (B)

Boron is an important solute in geothermal studies as the ratio of Cl/B is used to indicate a common reservoir source for fluids. Differences in this ratio occur due to changes in lithology and the adsorption of B onto clays during lateral flow (hence caution is required when applying the ratio because waters from the same reservoir may show differences). Concentrations of 10-50 mg/l are common in well and spring discharges; springs tend to have the lower concentrations. In volcanic regions andesitic host rocks show higher boron levels than other volcanics (Nicholson 1993). Higher concentrations of boron (~800-1000 mg/l) can be found in organic rich sedimentary rocks.

Ammonia (NH_3 – NH_4^+)

As a gas (NH_3) or solute (NH_4^+, ammonia ion) ammonia is a minor but commonly occuring constituent of geothermal fluids. High concentrations are found in deep fluids derived from sedimentary horizons. High levels of NH_3 can also be produced by steam heating of water as gas condenses out of the vapour phase. High NH_4/B ratios can indicate the amount of steam heating occurring in near surface fluids (the ratio increases with increased steam heating) (Nicholson 1993).

Noble Gases (Ar, He, Kr, Ne, Xe)

Noble gases are contributed to geothermal systems through meteoric water recharge. The amount of these gases dissolved into fluids depends on the salinity, ambient temperature and air pressure (altitude). Argon, xenon and krypton are highly dependent on temperature and the solubility of noble gases decreases with total dissolved salts. However the majority of geothermal systems contain mostly dilute fluids so this effect can be ignored, unless sea waters are associated with the geothermal system (Nicholson 1993).

Anions

Chloride (Cl)

Chloride is the most common and conservative element in geothermal waters, making it an important solute in the interpretation of water chemistry. It is used in ratios with other elements to eliminate boiling or dilution effects and to determine common reservoir sources (eg: Cl/B, Cl/F, Cl/As and Cl/HCO_3). High chloride concentrations in spring waters suggest a direct link to the deep reservoir with minimal mixing effects or conductive cooling. Chloride concentrations may range from <10 to >100,000 mg/l (Nicholson 1993), most well waters in TVZ have concentrations of around 1000 to 2000 mg/l.

Sulphate (SO_4)

Concentrations of sulphate are generally low in deep geothermal fluids (<50 mg/kg) but increase with increasing oxidation of hydrogen sulphide. Steam condensation into near surface waters can cause high concentrations of sulphate (Nicholson 1993).

Bicarbonate (HCO_3)

The total dissolved and individual carbonate concentration (HCO_3, H_2CO_3, $CO_{2\text{-}aq}$ and CO_3^{2-}) is determined by the partial pressure of carbon dioxide in the deep fluid (P_{CO_2}) and the pH of the solution. During boiling carbon dioxide is lost raising the pH by consuming protons through reactions. At pH 6-10 bicarbonate is the dominant species and at lower pH values carbonic acid (H_2CO_3) is dominant.

The concentration of HCO_3 is influenced by permeability and lateral flow as it is formed by reactions between host rocks and dissolved carbon dioxide. Fluids in boiling springs at the surface fed directly from depth tend to have the lowest HCO_3 concentrations because of this. The flow of a fluid away from the main upflow allows more opportunity for water-rock interactions to occur increasing the production of HCO_3. This allows the ratio of HCO_3/SO_4 to be used as an indicator of flow direction (Nicholson 1993).

Fluoride (F)

Fluoride usually occurs in low concentrations in high temperature fluids. Higher concentrations of fluoride are found in rhyolitic volcanic regions than in sedimentary host lithologies (Mahon 1964). Its concentration is determined by the retrograde solubility of fluorite (CaF_2) and is influenced by water-rock interactions where it can occur as a trace ion in micas. In rare cases high P_{CO_2} in deep fluids may remove the available Ca during calcite deposition leaving excess F. Abnormally high levels of fluoride may occur when volcanic gases (HF) are condensed into meteoric waters and accompany high levels of Cl and SO_4 (Nicholson 1993).

Cations

Sodium and Potassium (Na, K)

Concentrations of Na and K are controlled by mineral-fluid equilibria, which form the basis for the Na/K geothermometer. The major cation in geothermal systems is sodium with concentrations of ~200-2000 mg/l. Potassium is present at lower levels than sodium; concentrations are generally a tenth of the concentration of sodium, but it is still a major cation. The Na/K ratio is important in areas of high temperature, as a lower ratio represents higher temperatures. Lower ratios (~<15) usually occur in water that reaches the surface rapidly through upflow structures (faults, fractures, joints) or areas of high permeability. Waters that are subject to conductive cooling, lateral flow or near surface reactions tend to have high Na/K ratios (Nicholson 1993).

Magnesium (Mg)

High temperature geothermal fluids generally have very low levels of magnesium (0.01-0.1 mg/l) as it becomes incorporated into secondary alteration minerals like chlorite, illite and montmorillonite. Higher Mg levels may indicate the Interaction of hot fluids with near surface Mg-rich groundwater or reactions with local rocks leaching Mg from them.

Lithium, Rubidium, Cesium (Li, Rb, Cs)

Grouped as the 'rare alkalis', these elements are regarded as conservative species in geothermal systems and can be used to identify waters from common sources when used with Cl and B. They often decrease in concentration with lateral migration and with increasing migration to the surface. These elements are also easily incorporated into secondary alteration minerals. The greatest concentrations of these elements are found in areas with rhyolitic or andesitic host rocks (1-10 mg/l). Areas with basaltic rocks show much lower concentrations (~ <0.1 mg/l).

Lithium generally has concentrations of ~ <20 mg/l and is taken up in quartz, chlorite and probably clays during near surface reactions, increasing the B/Li ratio with increasing lateral flow.

Rubidium has concentrations of ~ <2 mg/l and becomes concentrated into illite and adularia to a lesser extent. It can also be adsorbed into xenolites and clays.

Cesium has concentrations of ~ <2 mg/l and is concentrated into zeolite minerals like wairakite.

Calcium (Ca)

Calcium concentrations are generally low in geothermal systems (<~ 50 mg/l) but increase with salinity and acidity. Minerals of retrograde solubility (eg. calcite, anhydrite and fluorite) and Ca rich aluminosilicates tend to control the calcium concentrations in fluids. The level of Ca in fluids can also be influenced by the factors that influence the solubility of these minerals; CO_2 as calcite often precipitates as a response to the loss of CO_2 during boiling. Upflow zones can be indicated by the Na/Ca ratio, higher values represent a more direct link to the reservoir.

Manganese (Mn^{2+}, Mn^{4+})

Concentrations of manganese rarely exceed 0.01 mg/l in geothermal systems. Modern manganese oxide deposits have been reported in Japan and the USA where waters contain manganese concentrations are higher than 5 mg/l.

Aluminium (Al)

Concentrations of aluminium in reservoir fluids are mostly <2 mg/l; in chloride waters at the surface it is often not detectable. Aluminium is generally considered an immobile species, but the accumulation of the metal in sinters and co-precipitation of aluminium with silica means this is a false assumption. Acid waters are in contrast with chloride waters having several hundred mg/l of aluminium in concentration through rock leaching.

Iron (Fe^{2+}, Fe^{3+})

Iron concentrations in chloride fluids is almost always low (0.001-1.0 mg/l), although it increases with salinity and acidity. In systems > 180 ^{o}C deep fluids are in equilibrium with pyrite. High levels of iron in chloride surface features indicate near surface leaching of iron by acidic waters mixed with chloride fluids.

2.3 Processes Affecting Fluid Composition

The composition of geothermal fluid is affected by physical and chemical processes occurring within a given geothermal reservoir during its accent to the surface. The dominant physical process is boiling, with mixing and conductive cooling also being important processes. Chemical processes are dominated by mineral-fluid interactions including deposition and dissolution (Nicholson 1993).

2.3.1 Chemical Processes

Mineral-fluid Equilibria

Two main groups of dissolved constituents found in deep chloride reservoir fluids can be separated by their different solubility behaviours.

Common Rock Species – these constituents have solubilities controlled by temperature dependant fluid-equilibria and will only become part of the fluid when the host minerals have been altered. These constituents include SiO_2, Ca, Mg, Na and K.

Soluble Group Species – these constituents readily pass into solution even before alteration of the surrounding rocks has occurred. Most of the species can be involved in near surface interactions especially with clays; however Cl tends to remain in solution and is considered a conservative species. Soluble species include Cl, B, Br, Cs and As.

Mineral-fluid equilibria is one of the important processes that determines the chemistry of fluids discharged, the reactions that take place are due to changes in pressure, temperature, salinity and host rocks within the geothermal system/reservoir. There are two main types:

- **Solubility Reactions –** Determine the amount of a certain species that enters and then remains in solution before precipitation occurs. Quartz, calcite and anhydrite are the solubilities which play a major role in controlling the composition of geothermal fluids. Temperature is the main control on mineral solubility in geothermal systems, but changes in salinity, pressure or pH may have effects. The solubility of minerals in geothermal systems generally behaves in one of three ways:
    1. Solubility increases with increasing temperature (alkali metal chlorides)
    2. Solubility increases with temperature but only to a point at which the mineral solubility then decreases with further rise in temperature (silica)
    3. Solubility decreases with temperature, termed <u>retrograde solubility.</u> (gypsum, calcite, anhydrite)

SiO_2 and Ca are two of the main causes of scaling in wells; silica and calcite equilibria govern the amount of each in solution making it an important piece of information for geothermal systems (Nicholson 1993).

- **Ion-Exchange Reactions –** involve the transfer of ions between two or more aluminosilicate minerals and control the ratios of cations in solution (including H+); pH

in solution may be increased by a silicate mineral assemblage due to this transfer. Geothermal alteration assemblages are formed by reactions including:

- Albite – K-Feldspar
- K-Feldspar – K-Mica + quartz
- Wairakite – Ca-Montmorilonite + quartz
- Pyrite – Pyrrhotite

2.3.2 Physical Processes

Mixing (dilution) with other waters

The process of mixing or dilution (mixing of high saline waters with waters of lower salinity) occurs when deep geothermal fluids mix with cold groundwater before discharging at the surface. When interpreting well or spring chemistries the recognition of mixed fluids and criteria that indicates mixed fluids is important (Nicholson 1993). Criteria for identifying this mixing were developed by Fournier (1979) and Arnorsson (1985) and include:

- Fluids with high Mg concentrations
- Fluids with a low pH relative to water salinity (pH 6-7 for waters with Cl<100 mg/l)
- Fluids undersaturated in calcite
- Fluids with high concentrations of silica relative to their discharge temperature.

The most common type of fluid mixing is that of deep fluids mixing with cold meteoric water; in rare cases deep fluids may mix with other shallow reservoir waters or steam-heated condensates. In more rare cases plots of Cl Vs SiO_2 and Cl Vs SO_4 can indicate mixing is occurring (Nicholson 1993).

Boiling (Adiabatic) Cooling

As geothermal fluids rise upwards hydrostatic pressure is reduced allowing boiling to occur, therefore with a high flow rate and reduced pressure (adiabatic) cooling may occur. At the point of boiling gases and volatiles within the fluids partition out forming the vapour (steam) phase which moves separately from the liquid phase. The loss of mass during the separation causes the

constituents dissolved within the liquid to become more concentrated which can cause a dramatic change in the chemistry of the fluid. For example the loss of CO_2 from the fluid during the boiling process causes a rise in the pH, increase in silica solubility and an initial fall in calcite solubility (Nicholson 1993).

Springs discharging waters cooled by boiling are the most useful for mixing-models and geothermometry because the fluids have not had enough time to have significant interaction with the surrounding rock. Therefore the discharge closely reflects the chemistry of the reservoir fluid, after correcting the chemistry for steam loss (Nicholson 1993).

Conductive Cooling

Fluids that ascend to the surface slowly may spend sufficient time in contact with the surrounding cool host rocks to cool down by conduction. In this case no steam will have been lost during the ascent so the concentration of chloride discharged from the spring will be similar to that of the reservoir. Rock-water interactions during the ascent mean that concentrations of the other major solutes in the fluid alter due to reactions with primary mineral and secondary alteration minerals. This is caused by the slow ascent of the fluid towards the surface. Springs discharging conductively cooled waters are unsuitable for geothermometry (Nicholson 1993).

2.3.4 Solute Geothermometers

Geothermometers are valuable tools for evaluating new geothermal fields and monitoring the hydrology of producing fields, as they allow the temperature of the reservoir fluids to be estimated (Nicholson 1993). Solute geothermometers are applied to fluids using temperature dependant mineral-fluid equilibria; their application relies on five key assumptions developed by Ellis, 1979; Fournier, 1977; Fournier et al., 1974; White, 1970 these are:

1. The concentration of species or elements used in the geothermometer is controlled only by a temperature-dependent mineral-fluid reaction.
2. An abundance of minerals and/or dissolved species is available in the rock-fluid system for the reaction to occur readily.

3. Equilibrium from the reaction is attained in the reservoir
4. No re-equilibrium occurs after the fluid leaves the reservoir due to rapid flow to the surface (no near surface reactions).
5. Mixing or dilution of the deep fluids does not occur (this situation can be accounted for if the amount of dilution is able to be evaluated).

Silica Geothermometers

Silica geothermometers are based on the relationship of silica solubility vs temperature. Once the silica content in a geothermal water sample is obtained and considering all of the above criteria, reservoir temperature estimates can be made. Equations for the straight line of the temperature range 20 – 250 ^{o}C have been developed which estimate the reservoir temperature (Chandrasekharam & Bundschuh 2008). The limit of 250 ^{o}C is due to silica dissolving and precipitating rapidly at higher temperatures, not allowing the concentration of silica in solution to remain constant as fluids are discharged at the surface (Nicholson 1993).

- Quartz Geothermometer (no steam loss):

$$T\ (^{o}C) = (1309/5.19 - \log S) - 273.15$$

- Quartz Geothermometer (maximum steam loss):

$$T\ (^{o}C) = (1552/5.75 - \log S) - 273.15$$

- Chalcedony Geothermometer

$$T\ (^{o}C) = (1032/4.69 - \log S) - 273.15$$

(Where S = total silica concentrated in fluid)

Cation Geothermometers

Cation geothermometers are based on ion exchange reactions using temperature dependent equilibrium constants (Chandrasekharam & Bundschuh 2008). Due to the long residence time of geothermal fluids and constant high temperatures in geothermal reservoirs water-rock reactions attain equilibrium. At high temperatures these temperature dependant fluid equilibrium

reactions are common; an example of this is the reaction involving Albite (Na feldspar) and geothermal fluids rich in K^+ ions. The following is a summary from Chandrasekharam and Bundschuh (2008) showing the details of this reaction and how it applies to geothermometry:

$$NaAlSi_3O_8 + K^+ \leftrightarrow KAlSi_3O_8 + Na^+$$

(Albite) (K-Keldspar)

$$\mathbf{K_{eq} = (KAlSi_3O_8)\ (Na^+)/(NaAlSi_3O_8)\ (K^+)}$$

(K_{eq} = Temperature dependant equilibrium constant)

When the activity of solids is considered to be in unity the equation above reduces to:

$$K_{eq} = (Na^+)/(K^+)$$

The equilibrium constant can be related to temperature in terms of the van't Hoff equation:

$$K_{eq} = C_0 + (\Delta H^0/2.303\ RT)$$

Where C_0 is a constant of integration, ΔH^0 is the enthalpy of the reaction, R is the gas constant and T is temperature in degrees Kelvin.

As most geothermal systems have temperatures below 260 ^oC and their ΔH^0 does not vary much between 0 and 300 ^oC, the equilibrium constant (K_{eq}) can be substituted for the ratios of actions of various ions to estimate reservoir temperatures from derivations of the equation below:

$$[Na^+]/[K^+] = C_0 + (\Delta H^0/2.303\ RT)$$

However it is difficult to assess these types of reactions (exchange of Na by K, reaction between albite and hydrogen ions) in natural geothermal systems, so there are several variations in the Na/K geothermometer from various authors. Below is an example of a Na/K geothermometer from Fournier (1983):

$$T\ (^oC) = 1217/1.483 + \log(Na/K) - 273.15$$

(Where Na and K are expressed in mg/l)

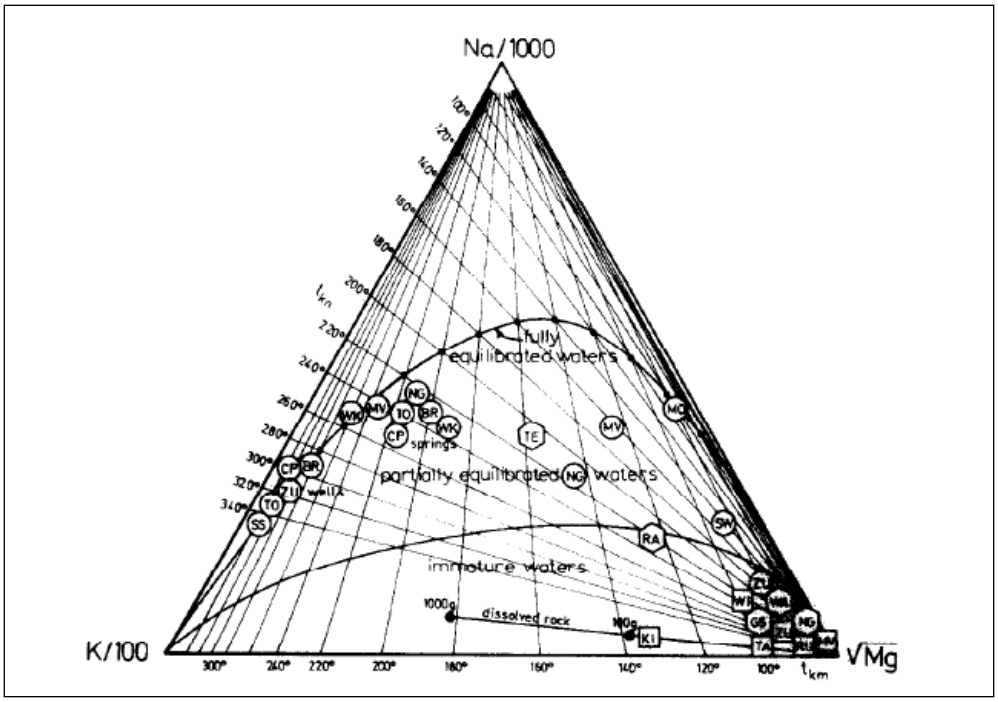

Figure 2.2: The Na-K-Mg geothermometer diagram. The fast equilibrating K-Mg geothermometer is represented by lines joining the Na apex and the K-Mg base. Lines joining the Mg apex with the K-Na base represent the slow equilibrating Na-K geothermometer (Giggenbach 1988).

The inherent problem with the Na/K geothermometer is that the reaction between K-Na equilibrates at high temperatures. Mixed fluids (fluids near the surface in which Na and K are not necessarily in equilibrium) are unsuitable for Na/K geothermometry as near surface fluids are of lower temperatures. To resolve this issue Giggenbach (1988) developed the Na-K-Mg geothermometer, which uses the reaction involving K and Mg which equilibrates at lower temperatures, because reactions involving K and Na do not adjust quickly to conditions at shallower depths. Giggenbach (1988) combined the Na/K and K/√Mg on a triangular diagram (Figure 2.2) and the concentrations of Na-K-Mg in the geothermal fluid are plotted to gain temperatures from both the geothermometers at the same time (Chandrasekharam & Bundschuh 2008).

The full equilibrium line drawn on the diagram is based on the assumption of steam loss from the geothermal fluid during its ascent. The concentrations of Na^+, K^+ and Mg^{2+} in the geothermal fluid plotted on this diagram are normalised to percentages from their initial measurement (mg/l).

2.4 Gases

2.4.1 Overview

CO_2, H_2S, NH_3, N_2, H_2 and CH_4 are the gases (together with steam) that are commonly present in geothermal discharges from wells and naturally occurring features (Nicholson 1993). These gases are commonly referred to as 'non-condensable gases'. These gases form during the thermal breakdown of volatile-rich components in reservoir rocks, contributions from degassing magma bodies, reactions of circulating fluids with reservoir rocks and air-saturated meteoric water contributions (Goff & Janik 2000). The concentration of these gases is inversely related to the percentage of steam flashed from water, and therefore to the separation pressure of the steam when collected from its discharge point (Ellis & Mahon 1977). Geothermal steam is created by the boiling of fluids at depth; the vapour phase produced generally migrates to the surface vertically. The residual fluid often migrates laterally away from the boiling zone eventually reaching the surface, which may be kilometres away from the upflow zone (Nicholson 1993). In these cases knowledge of different discharge chemistries across the field can give insight into the structure of the system, which can give more information than distant associated hot springs.

2.4.2 Geothermal Gases

Geothermal gases can be split into two main groups

1. Reactive Gases – These provide information on sub-surface temperatures and other conditions and take part in chemical equilibria (eg. CO_2, H_2O, NH_3, H_2S, CH_4, N_2, H_2).
2. Inert Gases – These be used to provide information on the gas source and act in a similar style to chloride as they do not take part in chemical reactions (eg. Hydrocarbons other than methane and the noble gases).

The most abundant gas in geothermal systems is CO_2 produced through thermal alteration of carbonate rocks and minerals, the degradation of organic manner within sedimentary rocks, near surface reactions, the boiling of meteoric waters and some may be derived from a magmatic origin. It is an important gas in geothermal systems as it in one way or another influences water

chemistry, pH, density, boiling point relationships, deposition of secondary minerals and boiling depth point relationships.

The other common gasses used in assessing the source for geothermal systems include hydrogen sulphide, methane, argon, helium and nitrogen.

2.4.3 Physical Process Indicators

Chemical changes in steam flows in a given geothermal field can be instrumental in determining sub-surface processes when used in combination with diagnostic solute ratios. The following outlines indicators of chemical changes in steam flows where steam continually evolves from its original source a hot water flow.

The following is an outline from Nicholson, 1993 describing how steam is used to asses important processes in geothermal fields.

Flow Direction

Gas concentrations lower as steam travels further away from the reservoir and the ratios of CO_2/H_2S, CO_2/H_2 and CO_2/ NH_3 increase. Gases are lost from fluids at depth during boiling and the further the fluid travels, more near surface boiling occurs, lowering the gas content in the steam. This allows the flow direction of fluids within a geothermal field to be tracked.

Source of Gases

Ratios of He, Ar, N_2, HCl, SO_2 and HF can be used to determine the source of the gases. Common sources are radiogenic gases, as the He/Ar ratio is much higher in geothermal systems than in normal atmospheric conditions, with the helium content in the fluids increasing with increased residence time. Meteoric sources are detected with the molar ratios of $H_2/Ar = 38$ and $He/Ar = < 0.001$. Magmatic steam from active volcanoes is recognised with high HF, HCl and SO_2 concentrations; however in geothermal systems that may be less obvious and high N_2 concentrations and N_2/Ar of ~ 800-2000. To simplify the identification of different gas sources

Giggenbach (1980) created the N_2, He, Ar ternary diagram which allows the dominant source for gases to be easily recognised (Figure 2.3)

Locations of Permeable upflow zones

Fumaroles with low ratios of CO_2/NH_3, CO_2/H_2S and CO_2/H_2 and high gas concentrations are fed by steam which has the most direct linkage to the deep reservoir. These sites generally sit above the major heat source in a geothermal reservoir and can assist in drilling for geothermal exploration.

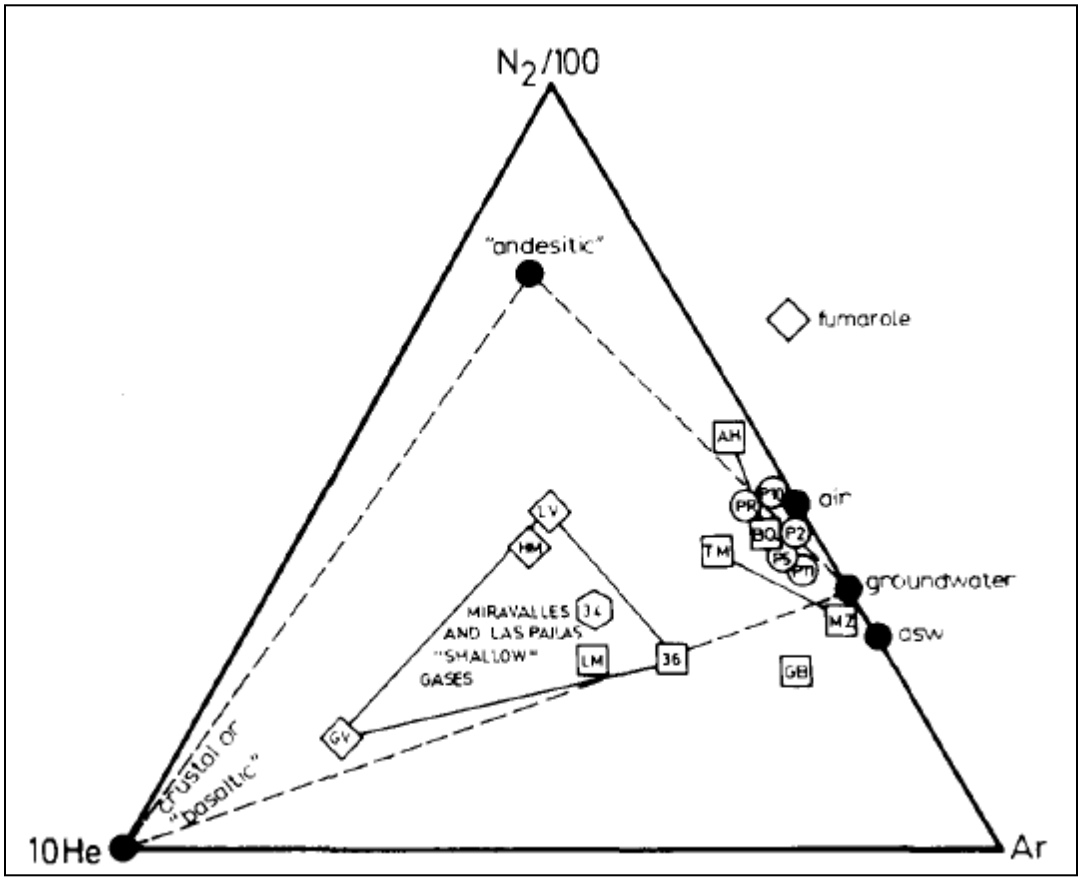

Figure 2.3: The N-He-Ar ternary plot, used to determine whether a geothermal gas source is crustal (High He), meteoric (high Ar) or magmatic/andesitic (High N). This plot shows gas chemistry for the Guanacaste geothermal region in Costa Rica (Giggenbach & Soto 1992).

Distance travelled from major upflow zones

Gases dissolved in reservoir fluids will prefer to enter the vapour phase when possible. During boiling the initial few percent of steam formed contains the highest amounts of dissolved gases (steam formed at this point has higher gas contents). The liquid left behind is depleted in these gases and later stages of steam separation will continue to lower the concentration of gases. Low gas contents, high enthalpies and low CO_2/H_2S ratios indicate continuous or several stages of steam loss prior to discharge at the surface which is associated with increased lateral migration from the major upflow zone.

2.4.4 Gas Discharge Features

There is a wide range of gas/steam discharge features associated with thermally active areas including:

Fumaroles – An opening in the ground where steam from the subsurface is emitted to the atmosphere. Compositions of deep fluids and gases cannot be obtained without well discharge data so initial investigations of geothermal fields use the gas chemistry of fumaroles to determine the flow structures within a field. Larger fumaroles with a high discharge provide the most reliable data on the composition of sub surface steam, as the large flow rate is assumed to indicate rapid migration of fluids from depth to the surface. This also means there is less time for any rock/steam and condensation near surface reactions to occur (Nicholson, 1993).

Steaming Ground – Areas where steam (with gases) discharges into the atmosphere through the ground due to underground boiling of a geothermal water reservoir. The steam rises to the surface independent of the liquid phase. Areas of steaming ground are typically dominated by argillic alteration, temperatures at boiling point just centimetres below the surface; physical features like mud pots, acid springs and hydrothermal eruption craters are common.

Kaipohan – Are areas of cold diffuse geothermal gas emission commonly surrounded by argillic alteration and dead vegetation. Kaipohan are different from steaming ground because the

ground is cold and only the gas emitted from the ground is evolved. The steam content as part of the original discharge has condensed at depth forming a perched aquifer. To form Kaipohan a low permeability formation and/or sheer, typically andesitic terrain combined with a high gas flux and low water table is needed (Nicholson, 1993).

Solfataras – Term used to describe either a fumarole discharging sulphur dioxide and/or hydrogen sulphide, or areas of steam discharge that contain both fumaroles and steaming ground.

Hot pools – Gas discharges directly from the vent of hot pools, making collection relatively easy. However even in deep pools some atmospheric gas contamination can occur.

Well Discharges – Further constrain the interpretations made from fumarole chemistry as they give gas/steam relationships at the initial stage of boiling, which allows steam/water ratios and the gas content of a reservoir to be calculated. This also allows better constraints of upflow areas and flow directions to be made (Nicholson 1993).

2.4.5 Processes Affecting Steam Composition

Several different factors may contribute to the composition of steam discharge. These include (Nicholson 1993):

- The chemistry of the reservoir fluid boiled to produce the steam
- Gas content of the reservoir fluid
- Pressure and temperature of the geothermal reservoir
- The solubility of a gas in the liquid phase
- The proportion of the mass of original reservoir fluid that converts to steam.
- The stage at which steam is separated (later separated steam contains a lower proportion of gas than early separated steam).
- Reactions in the steam phase as it ascends (eg. oxidation, rock-steam interaction, condensation

2.5 Stable Isotopes

Stable Isotopes are non-radioactive (stable) isotopes. An isotope is an atom of an element defined by the number of neutrons in its nucleus. Some isotopes decay radioactively because there is not a balance of protons and neutrons. Light isotopes are the most abundant (^{16}O and ^{12}C are good examples), which makes them useful proxies and tracers because:

- Light isotopes have a relatively low atomic mass
- The relative difference between heavy and light isotopes is large
- They form chemical bonds with a high degree of covalency (the heavier isotope is preferentially 'held' by stronger bonds (covalent).

Oxygen and hydrogen isotopes are the most abundant in the earth's crust and hydrosphere respectively. Oxygen's three stable isotopes ^{16}O, ^{17}O and ^{18}O make up 99.74 %, 0.05 % and 0.21 % of the earth's crust respectively. Hydrogen's two stable isotopes ^{1}H and ^{2}H (or D – Deuterium) make up 99.98 % and 0.02% of the earth's hydrosphere (Chandrasekharam & Bundschuh 2008).

2.5.1 δ – Values

In isotope chemistry, values are noted as delta (δ) values. To calculate δ values the isotopic composition of the material in question is reported as an equation (using ^{18}O as an example):

$$\delta^{18}O = [(^{18}O/^{16}O_{sample}) - (^{18}O/^{16}O_{standard}) / (^{18}O/^{16}O_{standard})]$$

Where standard isotope values for ^{16}O are the same as the ^{16}O value in standard mean ocean water (SMOW), developed by Craig (1961). Meteoric waters (precipitation) have negative δ values relative to SMOW (this does not mean the δ ratio for meteoric water is negative). These values are then plotted against the meteoric water line (MWL), which may be the global meteoric water line (GMWL) and/or local meteoric water line (LMWL). The GMWL was developed by Craig (1961) who collected 400 precipitation samples from all over the world determining a relationship for deuterium and oxygen-18 concentrations in natural waters. The relationship is defined by the equation $\delta^{2}H = 8.13\ \delta^{18}O + 10.8$ which defines the straight line relationship for the

data**.** A LMWL can be determined from individual rain events at a study location. A LMWL for New Zealand was developed so that waters in any part of the country could be compared with each other. The equation for the New Zealand MWL is $\delta^2H = 8.13\ \delta^{18}O + 13$ (Stewart & Taylor 1981), which is very similar to the GMWL which will be used for comparison in this study. Any positive shift in oxygen from this line in geothermal systems will suggest an exchange of oxygen due to mixing with magmatic water, rock-water interactions or steam loss (Figure 2.4); (Chandrasekharam & Bundschuh 2008).

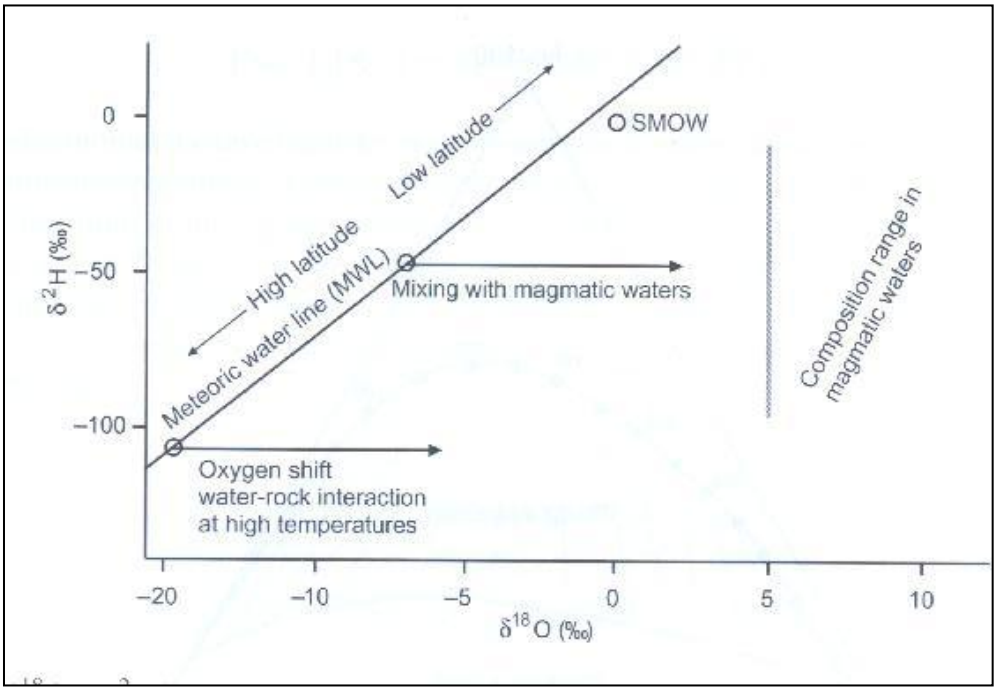

Figure 2.4: $\delta^{18}O$ vs δ^2H/D diagram showing the effect of interaction with magmatic waters or water rock interactions at high temperatures (Chandrasekharam & Bundschuh 2008).

2.5.2 Fractionations

Isotopes that are more susceptible to fractionation are those elements that are most abundant on earth (H, N, C, O and S)

Three main types of isotopic fractionation occur that affect the isotopic composition of a given substance (Faure 1977);

1. **Equilibrium Fractionation** – an isotopic exchange reaction that occurs between two different phases of a compound at a rate that allows equilibrium to be maintained (eg. the conversion of water vapour to liquid precipitation). Although this process is in equilibrium the rate at which the exchanges occur is different, creating enrichment in the heavier isotope (eg $^{1}X + {}^{2}Y \leftrightarrow {}^{2}X + {}^{1}Y$). Equilibrium fractionation can also be influenced by vibrational energy and temperature (no isotopic fractionation at very high temperatures).

2. **Isotopic Fractionation** – occurs because the bond energy of each isotope is slightly different as heavier isotopes have stronger bonds and slower reaction rates. The heavy and light isotopes partition differently between two compounds or phases. The difference between the heavy and light isotopes is proportional to the mass difference between them. This means light isotopes are more likely to exhibit isotopic fractionation than heavy Isotopes. An example of this is the fractionation of ^{12}C and ^{13}C (relatively light) which have an 8 % mass difference and undergo isotopic fractionation. Whereas ^{87}Sr and ^{86}Sr are heavier and only have a 1.1% mass difference, therefore they do not exhibit a detectable mass fractionation.

3. **Kinetic Fractionation** – equilibrium is not attained in kinetic fractionation as it is unidirectional. The best example of this is in surface waters where the lighter isotopes react faster and become concentrated in the product of the fractionation (i.e the surface water becomes enriched in ^{18}O because as evaporation occurs because the lighter isotope (^{16}O) is easily transferred to water vapour (clouds)).

2.5.3 Application to Geothermal Systems

Stable isotopes are important tracers in geothermal fluids as they allow determination of the origin of the fluids recharging the system. Oxygen (^{18}O) and Hydrogen/Deuterium (^{2}H or D) are the most important isotopes in a geothermal system, as they represent the lithosphere and the hydrosphere respectively. The isotopic composition of fluids combined with the major ions can provide information on the sub-surface processes occurring in geothermal systems. Most geothermal systems are recharged by local meteoric waters and will become enriched in oxygen as they interact with waters derived from a magmatic source or reservoir rocks. A shift in oxygen and deuterium can occur due to three main processes; steam separation, mixing with magmatic waters and water-rock interactions.

Steam Separation

A high rate of equilibrium between steam and liquid is attained when single stage steam separation occurs at shallow depths. This separation causes a shift in the $\delta^{18}O$ and δ D values of geothermal water and steam, with water values moving to the right of the MWL and the separated steam moving to the left. At separation > 220 ^{o}C the $\delta^{18}O$ values are enriched and δ D values decreased for waters, at 220 ^{o}C there is enrichment of $\delta^{18}O$ and no change in the δ D (no fractionation occurs in D) and < 220 ^{o}C in there is enrichment in both $\delta^{18}O$ and δ D. Steam on the other hand shows a decrease in both $\delta^{18}O$ and δ D above 220 ^{o}C, no change in δ D and a decrease in $\delta^{18}O$ at 220 ^{o}C and a decrease in $\delta^{18}O$ and an enrichment in δ D below 220 ^{o}C.

To recalculate water samples taken from well fluids separated at 100 ^{o}C to reservoir composition the steam fraction lost from the original fluid and the isotope fractionation factor need to be considered. To do this a simple mass balance equation is derived from the isotope fractionation (temperature dependent) equation (using oxygen-18 as an example) (Chandrasekharam & Bundschuh 2008):

$$\delta^{18}O \text{ (liquid)} - \delta^{18}O \text{ (vapour)} = 10^3 \ln \alpha$$

(Where α represents the isotope fractionation factor which is 5.24 at 100 ^{o}C (Friedman & O'Neill 1977))

So by rearranging the equation above the isotopic composition of reservoir water can be calculated from a geothermal brine sample by using the following equation:

$$\delta\,^{18}O\,(reservoir) = (1-X) * \delta\,^{18}O\,(liquid) + X * (\delta\,^{18}O\,(liquid) - 5.24)$$

(Where 'X' is the steam fraction measured from the original fluid)

Magmatic Water Mixing

In tectonically active areas like subduction zones (eg. TVZ), deep circulating, meteoric waters in geothermal systems may mix with magmatic-derived water. Enrichment in $\delta^{18}O$ is seen when meteoric waters mix with magmatic waters causing them to plot to the right of the MWL. The $\delta^{18}O$ of waters derived from basaltic or andesitic magmas range from 5 – 10 ‰ (Henley et al. 1985). The δ D varies from -10 to -30 ‰ for andesitic magmas and from -60 to -90 for basaltic magmas, meaning waters may or may not become enriched in δ D depending on their geographic location (Chandrasekharam & Bundschuh 2008) (Figure 2.5).

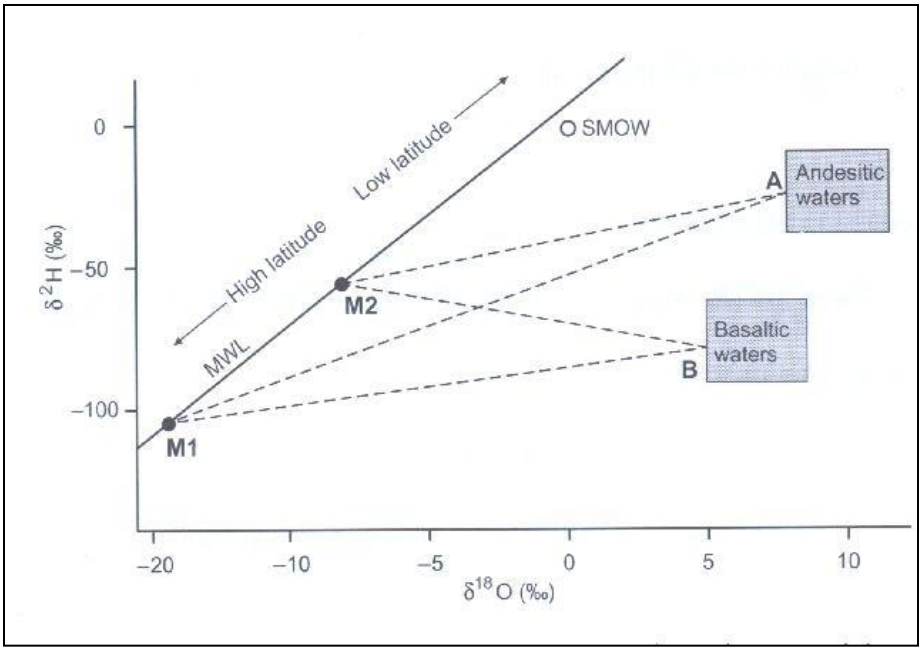

Figure 2.5: Geothermal-magmatic water mixing relationships. Oxygen and deuterium concentrations in geothermal waters become more enriched when mixed with magmatic waters (Chandrasekharam & Bundschuh 2008).

The distance a sample plots away from the MWL represents the amount of mixing with magmatic water that has occurred (the amount of magmatic contribution to the geothermal water). Giggenbach (1995) added magmatic component lines onto the plot to determine the amount of magmatic fluids actually being incorporated into meteoric water. Every 1 ‰ shift to the right of the MWL representing a 10% magmatic inclusion in the geothermal water (Figure 2.6)

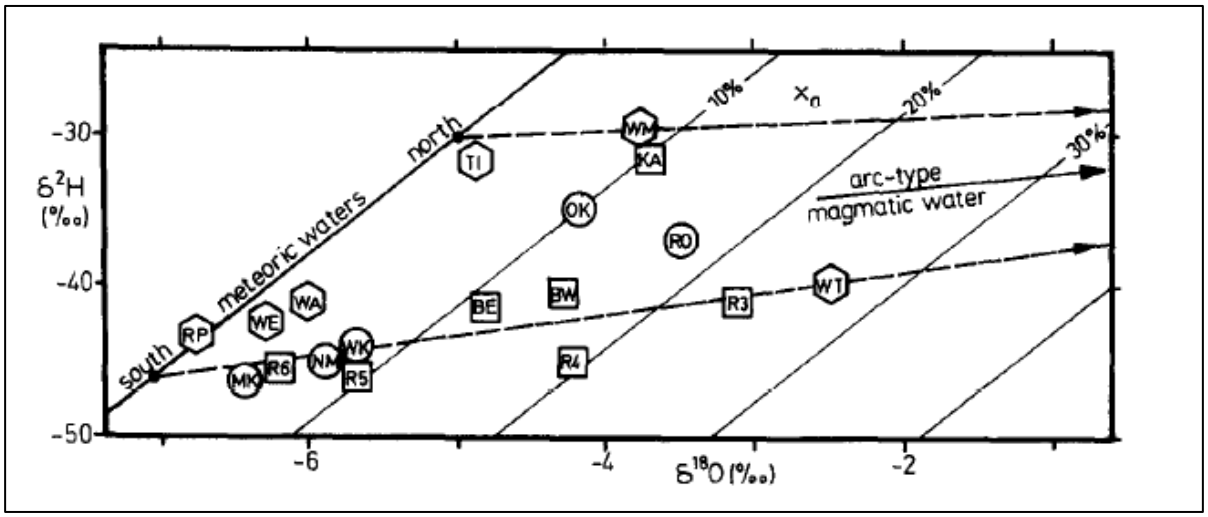

Figure 2.6: The isotopic composition of geothermal waters in TVZ. Each line moving to the right of the MWL represents a 10% contribution from magmatic fluids (Giggenbach 1995).

Water-Rock Interactions

All silicate minerals, no matter what rock type, contain $\delta^{18}O$ values between 5 and 10 ‰ (Faure 1977). Any oxygen exchanges between rock and geothermal waters forces the oxygen values in the rocks to be depleted hence plotting to the left on the $\delta^{18}O$ vs δ D diagram (the corresponding enrichment in geothermal waters can also be observed). The exchange of oxygen between geothermal waters and rock occurs ≥ 220 ^{o}C, where the percentage of oxygen depleted from the rock is equal to enrichment of oxygen in the geothermal water (Chandrasekharam & Bundschuh 2008)

Chapter 3: Ngatamariki

3.1 Location and Extent

The Ngatamariki Geothermal Field is located in the central TVZ approximately 20 km north of Taupo, in the central North Island of New Zealand. The field is approximately 8 km from the eastern margin of the Maroa Volcanic Centre (MVC) and sits on the edge of the Whakamaru caldera, 7 km south of the Orakei Korako field (Figure 3.1). The field covers an area of 12 km^2 as delineated by MT survey measurements (Urzua 2008), with the Waikato River marking the northern boundary and Orakonui Stream forming the western boundary; where the majority of thermal features are located. Information on the area was first provided by Grange (1937).

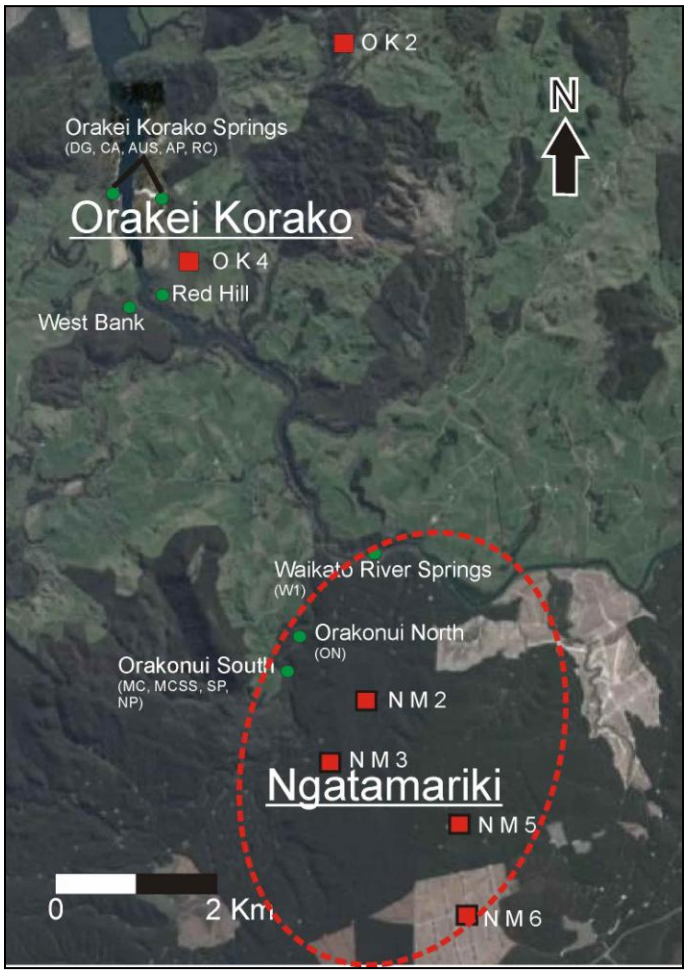

Figure 3.1: Location of the Ngatamariki and Orakei Korako Geothermal Field's and locations of thermal features. Springs are represented by green dots; wells are represented by red squares and the red dashed line represents the approximate extent of the Ngatamariki geothermal field as delineated by electromagnetic and MT surveys (Risk et al. 2003; Urzua 2008) (Satellite image sourced from Google Earth, 2009) .

3.2 Geology

3.2.1 Regional Geology and Structure

The main rock types at Ngatamariki are rhyolite or rhyolite eruptive products, which are mainly soft ignimbrites and pumice breccias (Bennie 1983), believed to be derived from the Whakamaru caldera and MVC (Urzua 2008) (Figure 3.5). The boundary of the Whakamaru caldera is based on the distribution of the Whakamaru group ignimbrites which were deposited between 340 and 320 ka (Houghton et al. 1995). The MVC has been dated at a younger age than the Whakamaru caldera. The majority of Maroas volume is made up of dome lavas erupted from the Maroa East and West Complexes over a short 29 kyr period beginning at 251 +/- 17 Ka (Leonard 2003). The centre is comprised of five pyroclastic deposits (Korotai, Atiamuri, Pukeahua, Putauaki and Orakonui) and rhyolite domes which are confined locally and of a small volume (Leonard 2003). Ngatamariki sits just outside the eastern margin of the Ngakuru Graben marked by the Paeroa fault, a normal fault with a series of smaller south west trending faults.

3.2.2 Surface Geology

The surface geology at Ngatamariki was initially mapped by Lloyd (1972) during work he was doing around the periphery of Orakei Korako. Subsequently Brotheridge (1995) described the cover deposits at Ngatamariki which mainly consist of sedimentary and volcanic products. The following is a summary of the surface stratigraphy in the Ngatamariki area from Lloyd (1972) and Brotherdge (1995);

- **Hydrothermal eruption breccias –** are located at South Orakonui and surround the pools and hot springs. The breccias are composed of fresh

Figure 3.2: Hydrothermal eruption breccia at Orakonui South forming the western wall of the main crater (May, 2009).

and hydrothermally altered tuffs, pumices and lithics. They lie above the Taupo Pumice and are the product of hydrothermal eruptions in 1948 and April 2005 from the large crater at Orakonui South.

- **Taupo Pumice alluvium -** is the unit that forms the river terraces and infill's the small stream tributaries in the area. It is recognized as the product of pyroclastic flows and airfall eruptions from the 186 AD eruption from Lake Taupo (Wilson et al. 2009). Large extensive cliff sections of > 10 m thickness are seen in road cuttings in the Ngatamariki and Orakei Korako areas and the Orakonui Stream valley.

Figure 3.3: Taupo Pumice in a small quarry on farmland at Ngatamariki located to the east of the main crater at Orakonui South. The black pieces in the pumice are carbonised trees (charcoal) (February 2009).

- **Hinuera Formation -** is characterized by bedded gravels to bedded sands, derived from previous volcanic deposits (rhyolitic volcanic and sediments) and the Huka Formation. The formation is considered an aggradational deposit resulting from the last glaciations (Lloyd 1972). The formation outcrops to the west of Ngatamariki.
- **Orakonui Formation -** comprised of soft pumice breccias and ignimbrites which surrounds the Orakonui Stream. It is the product of pyroclastic flow eruptions from the MVC and probably the Wairakei Breccia which underlies it near Wairakei.

- **Parekauau Andesite –** occurs as an andesite dike exposed in a road cutting along Tutukau Road. The dike was first mapped by Grindley (1960) and intrudes the Huka Group and Haparangi Rhyolite. The full extent of the dike has not been constrained but drill holes came across andesite in wells NM-2 and NM-3 below 950 m (Wood 1985), although it is unlikely that they are related.
- **Huka Group –** comprised of the Huka Falls Formation and Waiora Formation. The Huka Falls Formation is a series of sandstones, mudstones and siltstones derived from local ignimbrites and other volcanics; which act as an aquitard for the geothermal field at Wairakei. The Waiora Formation underlies this and is dominantly thick pumice breccia creating the main aquifer unit at the Wairakei field. The Huka Falls Formation outcrops west of Ngatamariki and was seen in the base of the escarpment near the main crater at Orakonui South. The Huka Falls formation can be seen in the river valley as you travel downstream from Ngatamariki to Orakei Korako.

Haparangi Rhyolite – the name given to rhyolite flows and domes Pleistocene in age by Grange (1937). A large rhyolite dome (680m.a.s.l) called Whakapapataringa is located on the western margin of the field. The dome was extruded along north-north-west trending fractures along the western margin of the field with scattered boulders of devitrified flow banded rhyolite on the Somerville's farmland also on the western side of the field.

Figure 3.4: Haparangi Rhyolite on the south eastern end of Whakapapataringa on the Somerville's farmland at Ngatamariki (February 2009).

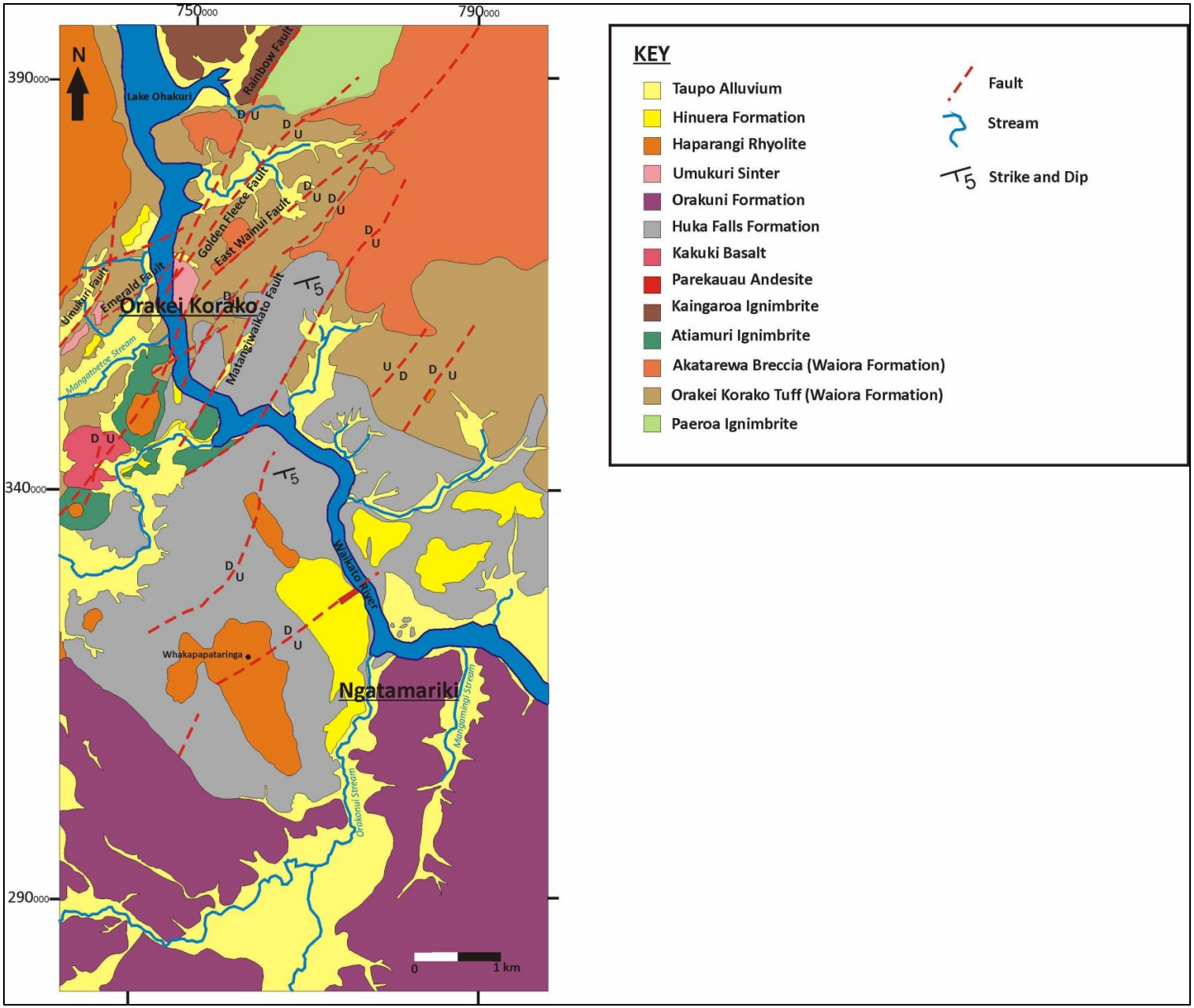

Figure 3.5: Geological Map of the Ngatamariki – Orakei Korako area (after Lloyd, 1972).

3.2.3 Detailed Deep Stratigraphy

The stratigraphy of the wells drilled by the crown is well documented by Dr C.P, Wood in 1985 and 1986 in four unpublished reports detailing stratigraphy, hydrothermal alteration and permeability. The nature of wells NM5-7 is documented by GNS in reports by Ramirez & Rae (2009). The following outlines the basic stratigraphy from the seven wells. Detailed logs of stratigraphy and alteration are given in Appendix A.

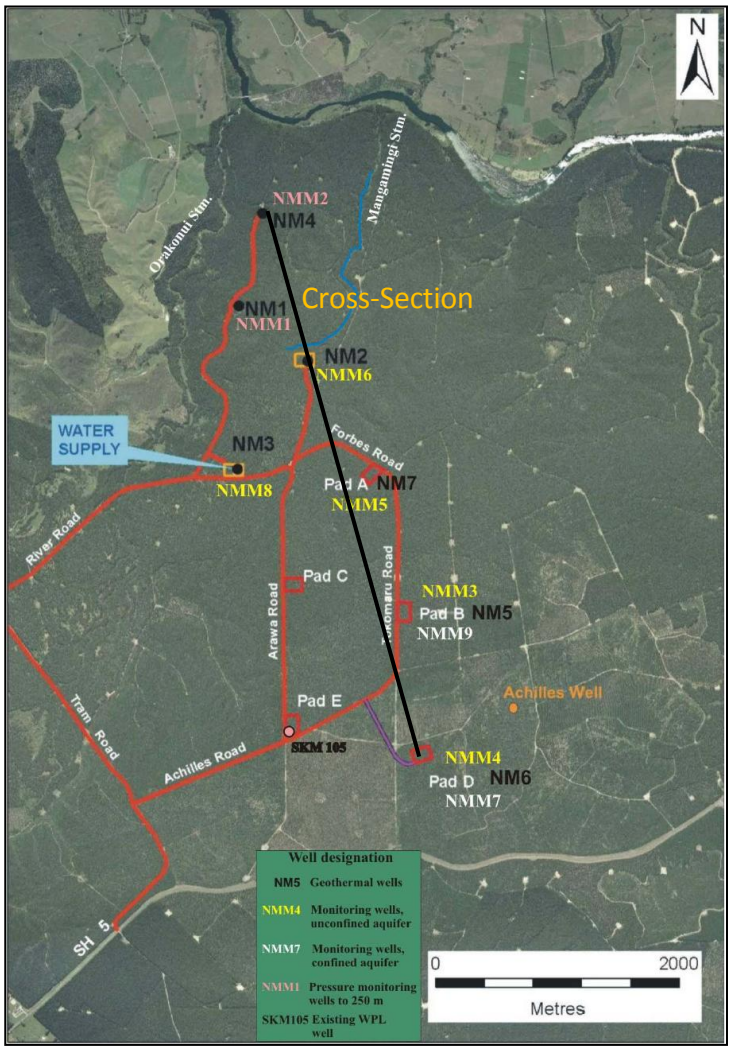

Figure 3.6: Location of exploration and monitoring wells at Ngatamariki and the line of cross section for the geological model (Rae et al. 2009).

- **NM1 –** NM1 was drilled to a depth of 1308 m (950 m.b.s.l) and passed through a series of sediments, gravels, rhyolites, breccias and ignimbrites (Brotheridge 1995). The top of the rhyolite unit appears to be brecciated (Wood 1985) where it comes in contact with the overlying sedimentary unit, suggesting that it may be a shallow lateral flow zone which feeds the hot springs on the west of the field (Hedenquist 1986). Alteration mineralogies in the units corresponded well with the measured temperatures down hole. A major thermal inversion occurs about 600 m below the surface, the flow of cool groundwater down a fault is thought to be the cause of this (Wood 1985).

- **NM2 –** NM2 is located about 730 m south east of NM1 and was drilled to a depth of 2410 m (2060 m.b.s.l). The grade of alteration in generally higher is NM2 than NM1 and the units in the top half of the well correlate to the ones seen in NM1 (Wood 1985). Below this a large andesite unit occurs in NM2 which is not existent in NM1.

- **NM3 –** NM3 was drilled of a depth of 2200 m (1850 m.b.s.l). Like NM2 andesite was encountered in the bottom of the well, the shallow lithologies are also similar to NM1 and NM2 with silicified black mudstone and dacite occurring at intermediate depths. At 300m depth a shallow outflow zone occurs along the brecciated surface of the rhyolite (Hedenquist 1986), and alteration styles in NM3 are similar to those seen in NM1 (Wood 1985).

- **NM4 –** NM4 was drilled to 2749 m depth (2400 m.b.s.l) and was the first well drilled in New Zealand to encounter a pluton. The well bottoms in diorite which has an associated halo of phyllic alteration formed before the present geothermal regime (Wood 1986; Browne et al. 1992). Shallow lithologies in NM4 are similar to those seen in the other wells, but a fault down thrown significantly to the north between NM1 and NM4 is inferred to account for a 325 m displacement of a quartz rich ignimbrite unit in the two wells (Wood 1986). Hydrothermal alteration is low rank above 1000 m and shallow lateral flow above the rhyolite is assumed (Brotheridge 1995).

- **NM5 –** NM5 was drilled to a depth of 2997 m (2606 m.b.s.l), 2 km south-south east of NM2 and NM3 in October through December 2008. The shallow lithologies in NM5 are similar to those in the other wells. High amounts of hydrothermal alteration occur below 425 m depth above the Waiora Formation and between the Wairakei Ignimbrite and underlying rhyolite breccia (765-845 m depth). The deepest high intensity alteration occurs between 1205 and 1295 m depth, where illite and kaolinite alteration is seen between the Tahorakuri Formation and an underlying rhyolite breccia. It appears that at this depth there have been fluids with fluctuating temperatures and pH running along the contact between the two units allowing kaolinite to form (Ramirez & Rae 2009).
- **NM6 –** NM6 was drilled to a depth of 3398 m depth (3015.5 m.b.s.l) between 13th January and 13th March 2009. The shallow lithologies in NM6 are similar to those seen in the other wells but NM6 is the only Ngatamariki well known to intersect the greywacke basement. Hydrothermal alteration at ~3400 m depth suggests that at some point the system was above 300 ^{o}C. The high temperature alteration minerals (anhydrite, bladed calcite) are overprinted by lower temperature minerals (illite, epidote, adularia and wairakite) which suggest reservoir temperatures of 240-300 ^{o}C. These temperatures are the same as the ones obtained from fluid inclusion heating measurements suggesting that these temperatures are more indicative of the current reservoir conditions (Rae et al. 2009)
- **NM7 –** NM7 was drilled to a depth of 2963 m depth (2575.5 m.b.s.l) between the 22nd of May and 3rd of July 2009 and lies ~1 km north of NM5 and ~1 km east of NM3. The lithologies in NM7 are similar to those in the other 6 wells but are downthrown with respect to NM3 which lies just to the east. Quartz fluid inclusion temperatures suggest that reservoir temperatures are > 210 ^{o}C (Ramirez et al. 2009).

The following (Figure 3.7) is the geological model inferred from the 7 drill holes described above.

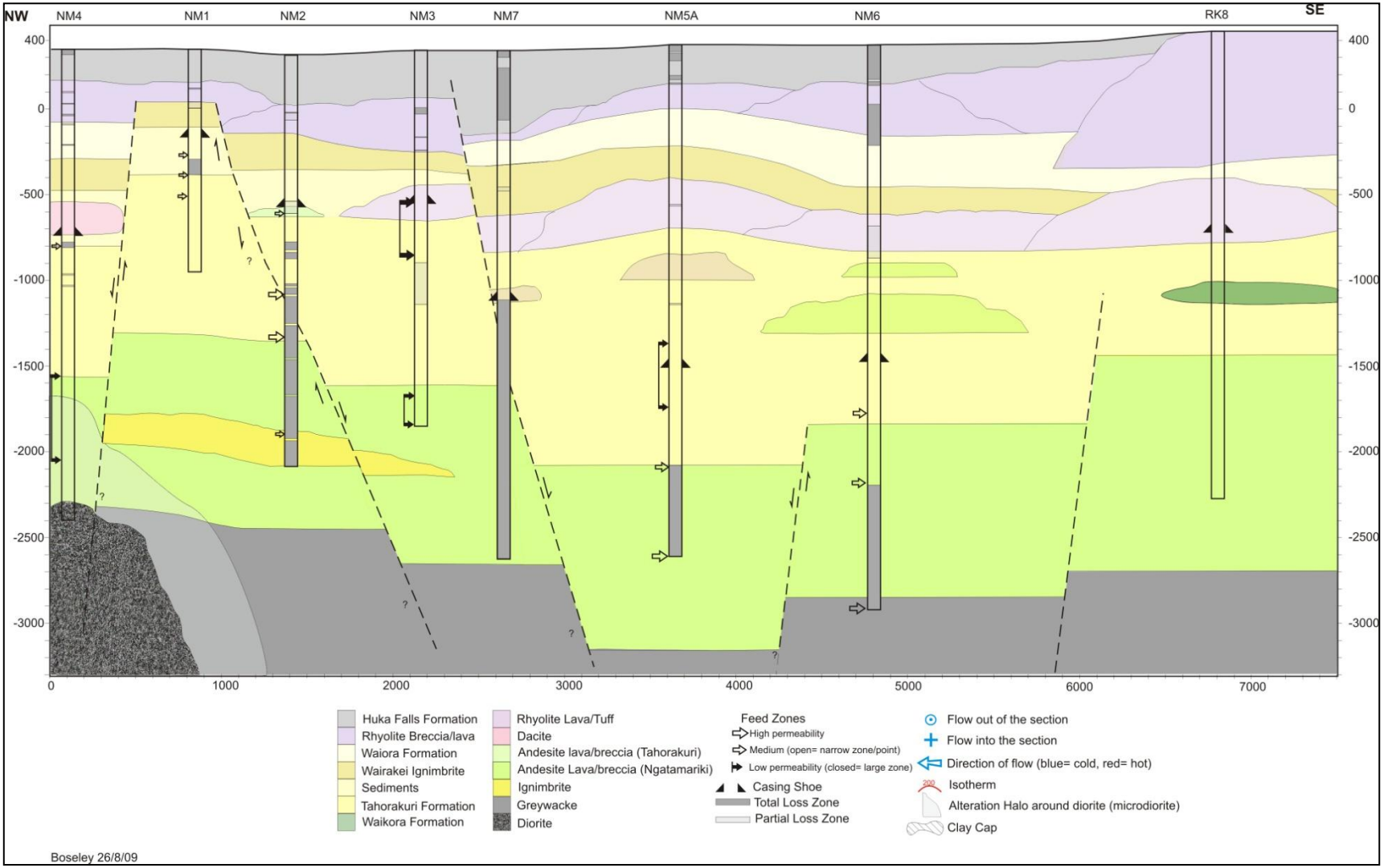

Figure 3.7: Sub-surface geological model inferred from the exploration wells at Ngatamariki (courtesy of Mighty River Power).

An important lithology across TVZ is the Whakamaru Group Ignimbrites. The Wairakei Ignimbrite represents this group at Ngatamariki and is intersected in all of the wells in the field. The Whakamaru Group was first named informally by Wilson et.al, (1986) and refers to a wide spread group of ignimbrites covering 13, 000 km^2 with a volume of over 1000 km^3 and includes the Whakamaru, Manunui, Rangitaiki, Te Whaiti, Wairakei and Paeroa Range Group Ignimbrites (Figure 3.8). The ignimbrites were grouped because of their similar geochemistry and timing of eruption (330-340 ka) (Brown et al. 1998).

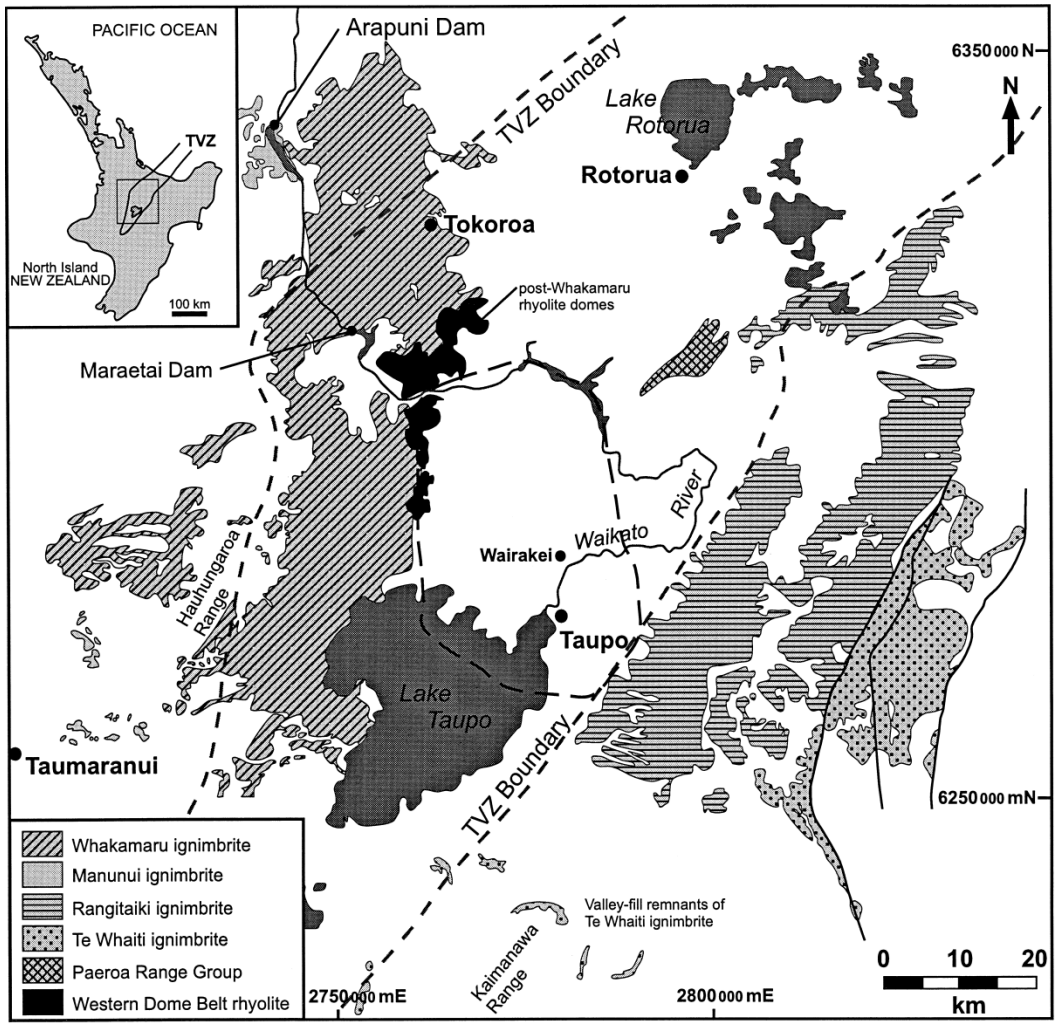

Figure 3.8: Distribution of Whakamaru Group Ignimbrites. The dashed line enclosing an area north of Taupo represents the Whakamaru Caldera (Wilson et al. 1986; Brown et al. 1998)

3.3 Thermal Areas

Thermal areas at Ngatamariki are mainly restricted to the western boundary of the field aligned along the Orakonui Stream. Other small springs are located along the Waikato River on the northern boundary of the field but these are often flooded. The springs along the Orakonui Stream occur in two main areas Orakonui North and South (Figure 3.9). The following details the nature of the thermal areas in 2009 during fieldwork and compares this to previous studies. All field notes are included in Appendix B.

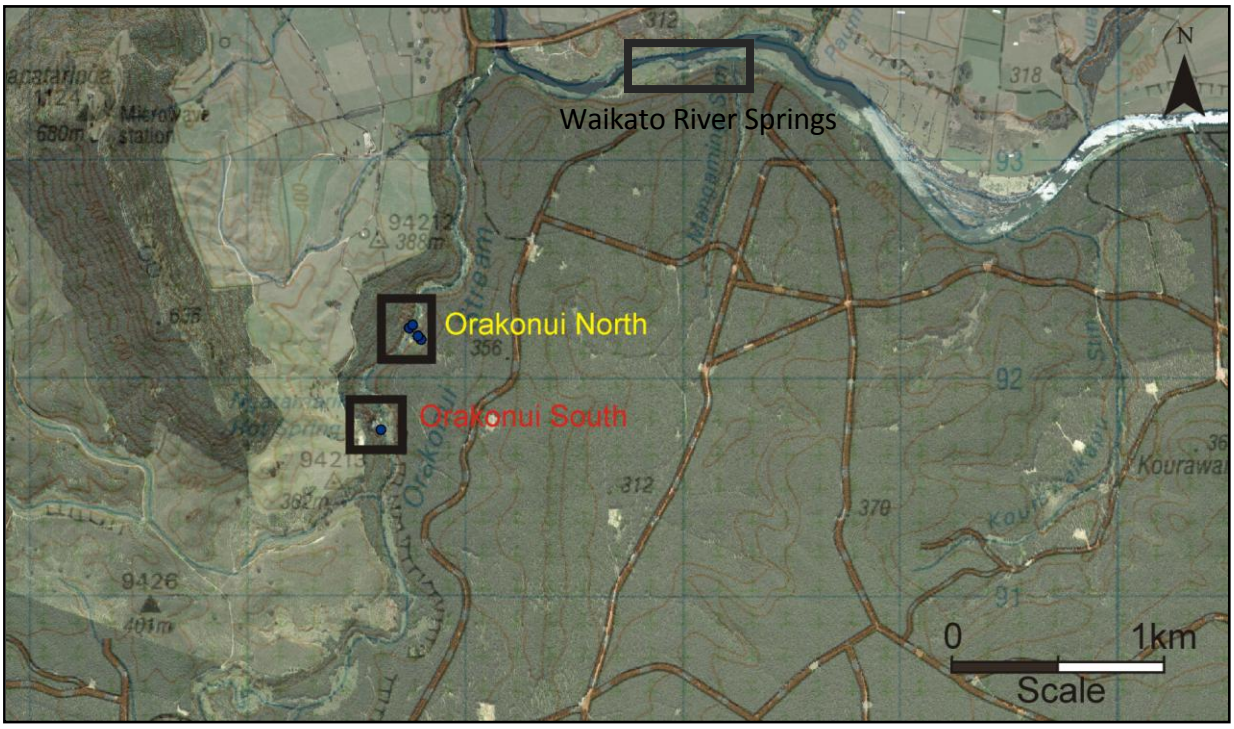

Figure 3.9: Location of areas of thermal activity at Ngatamariki (Air photo courtesy of Mighty River Power).

3.3.1 Orakonui North

The thermal area at Orakonui North is characterized by three main silica sinters on the eastern bank and a series of smaller hot alkaline chloride springs and seeping aquifers on the western bank (Figure 3.10).

Figure 3.10: Location of hot springs and sinter aprons at Orakonui North (Air photo courtesy of Mighty River Power).

East Bank

On the eastern bank a very small amount of sinter is being deposited from the springs, mostly overgrown by vegetation.

The middle sinter (figure 3.12 B) is approximately 20 x 10 m and has two active springs located at the top of the sinter fan. Both springs are alkali-chloride composition and have temperatures between 64 and 83 ^{o}C. The spring at the top of the sinter area (Devils Mouth) is 1 x 0.4 m in size

and has sintered margins (figure 3.11 C). It appears to have been one of the springs previously feeding a sinter fan that is now inactive. The other spring 15 m to the north (Middle Sinter Pool) is smaller in size but much deeper and bubbles intermittently at 64 ^{o}C (figure 3.11 A).

The northern sinter (figure 3.12 D) is split into two areas overgrown by native bush and has no active springs. Warm geothermal fluids however seep out of the sinter and flow across the sinter fan in small channels down into the Orakonui Stream.

The southern sinter (figure 3.12 A) is the largest of the three areas of sinter and has a very small pool close to the centre from which a small amount of fluid runs down the platform into the Orakonui Stream.

Below the southern sinter just above the stream level is a large hot spring and associated boiling mud pot (Father and Son). The spring is very hot (94.4 ^{o}C) and the boiling mud pot is 15 x 15 cm and has a temperature of 75.8 ^{o}C (figure 3.11 D).

Figure 3.11: Springs at Orakonui North A) Middle Sinter Pool spring (east bank). B) Clear Black spring (west bank). C) Devils Mouth spring (east bank, photo Karl Spinks) D) Father and Son spring (east bank). (For locations see figure 3.9, photos taken May 2009)

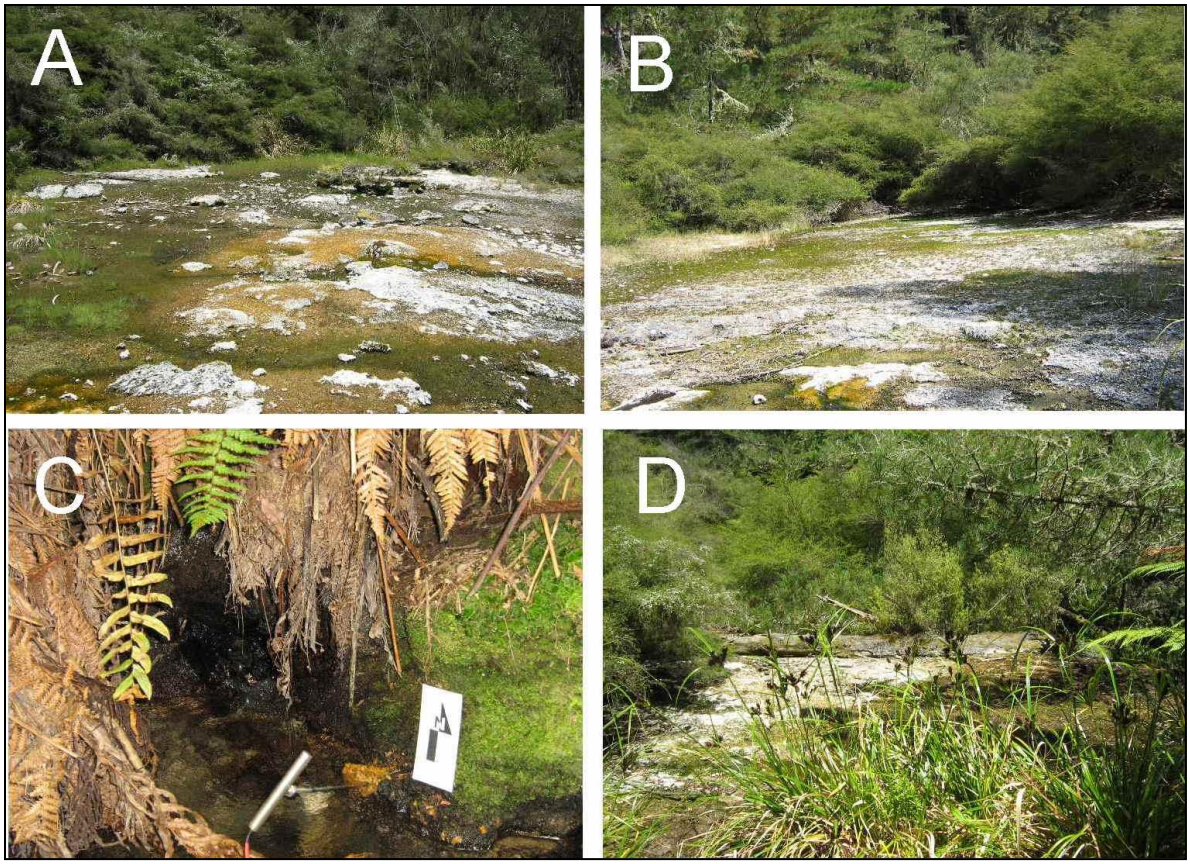

Figure 3.12: Sinter areas and seeping aquifer at Orakonui North. A) Southern sinter looking south; waters flow from left to right down into the Orakonui Stream. B) Middle sinter looking south; waters flow towards the north down into the Orakonui Stream C) Seeping aquifer south of Clear Black in the western bank of the Orakonui Stream. D) Northern sinter looking south west towards the Orakonui stream. (Locations see figure 3.10, photos taken May 2009).

West Bank

The springs located on the western bank (Clear Black and Little Clear Black) are very hot. Clear Black is the southernmost spring of the two and is about 40 cm x 25 cm in size (figure 3.11 B). Clear black was the hotter of the two at 94 ^{o}C and sits in a small pool containing hydrothermally altered bedrock. Little Clear Black is located about 10 m to the north and is smaller in size (20 x 10 cm) and lower in temperature. There is also a seeping aquifer in the bedrock to the south of these

springs where water is discharging directly into the Orakonui Stream through hydrothermally altered bedrock at about 35 ^{o}C (Figure 3.12 C).

Orakonui North Springs		
Western Bank Springs	**Temperature (^{o}C)**	**pH**
Clear Black	94	7.4
Little Clear Black	83.3	-
Eastern Bank Springs		
Father and Son	94.4	7.3
Devils Mouth	83	7.4
Middle Sinter Pool	64	-

Table 3.1: Spring temperature and pH levels at Orakonui North

3.3.2 Orakonui South

The Orakonui South thermal area is about 1.8 km south of the Waikato River and the dominant feature is a large 50 x 30 m pool occupying a hydrothermal eruption crater (Figures 3.13 and 3.14). About 50 m south and 30 m to the north of the crater two smaller 10 x 5 m clear pools exist (Figure 3.15). Another small spring had occurred alongside the Orakonui stream about 60 m north called the Pavlova Spring; however, during field work the spring was not evident.

The main crater had an ambient temperature of 54 ^{o}C and a pH of 8 Crater during February 2008 field work; Brotheridge et .al (1995) recorded a pool bottom temperature of 52.5 ^{o}C in 1994 at which time the pool was 2 m deep. The crater discharges into the Orakonui Stream via an outlet from the north eastern edge of the crater. Before the 2005 eruption the outlet had a discharge of ~ 4.5 l/s into the stream from the southern end of the crater (Bennie 1983).

Figure 3.13: View facing west of Main Crater December 2009. The outflow to the Orakonui Stream is located in the bottom right of the photo.

Figure 3.14: View facing south of Main Crater December 2009.

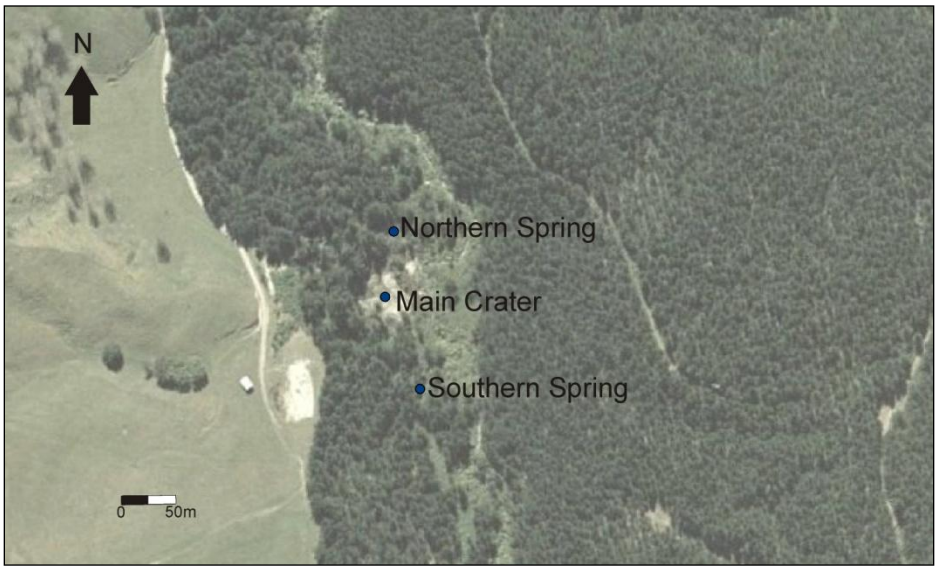

Figure 3.15: Location of major features at Orakonui South (Air photo courtesy of Mighty River Power).

A series of smaller springs also surround the Main Crater but they are very ephemeral and are mostly inaccessible, however, a spring 1.5 m in diameter (Main Crater Side Spring – MCSS) sits about 10 m from the outflow of the Main Crater on its eastern rim (Figure 3.16). The water within the spring is black and has a temperature of 49.5 ^{o}C. The water level in the spring is lower than it used to be which is obvious from its current low level and inactive outflow channel which runs into the main crater.

Figure 3.16: Main Crater side spring February 2009. Note black colour and the former outflow which runs towards the bottom right corner of the photograph.

The northern most pool has an average temperature of 30 ^{o}C and a pH of 7.2. The pool also seems to occupy an eruption crater but its morphology is covered by the surrounding vegetation. There is no surface discharge evident from the pool (Figure 3.17).

The southern pool is the hottest of the three springs at Orakonui South at 72.3 ^{o}C and has a pH of 7.5. The pool has a curved shape and is considerably hotter at the eastern bend where the man upflow of hot water occurs (Figure 3.17).

Figure 3.17: Northern pool (left) and the high temperature upflow of the southern pool (right) at Orakonui South in May 2009.

Orakonui South Springs		
Spring	**Temperature (^{o}C)**	**pH**
Main Crater	51.8	7.3
Northern Pool	30	7.6
Southern Pool	72.3	7.5
Main Crater Side Spring	49.5	6.4

Table 3.2: Spring temperatures and pH levels at Orakonui South (for locations see figure 20).

3.3.3 Waikato River Springs

The springs along the Waikato River mark the northern boundary of the geothermal field. Springs on the southern bank of the river (W1 and W3) discharge directly into river water in shallow mangroves through seeps (Figure 3.19). Water temperatures were between 60 and 80 ^{o}C during fieldwork in December 2009. On the northern bank there is one spring (W2) that discharges into the river through a small waterfall (Figure 3.18).

Figure 3.18: Location of the Waikato River Springs (GNS 2009).

Figure 3.19: Pictures of W1 seeps December 2009.

Waikato River Springs		
Spring	**Temperature (°C)**	**pH**
W1	~70	7.2
W2	~70	6.8

Table 3.3: Spring temperatures and pH levels of the Waikato River Springs.

3.3.4 History of Thermal Activity at Ngatamariki

Orakonui North

The Orakonui North area was dominated by a considerably larger area of sinter which is seen in the 1941 aerial photograph (figure 3.20) with the northern sinter still separate from the southern and middle sinters. The sinter apron was estimated to be less than 10 % of its original size by Brotheridge (1995); the apron is now completely obscured by surrounding vegetation. Healy (1974) describes the Orakonui North are as having a number of thermal springs ranging in

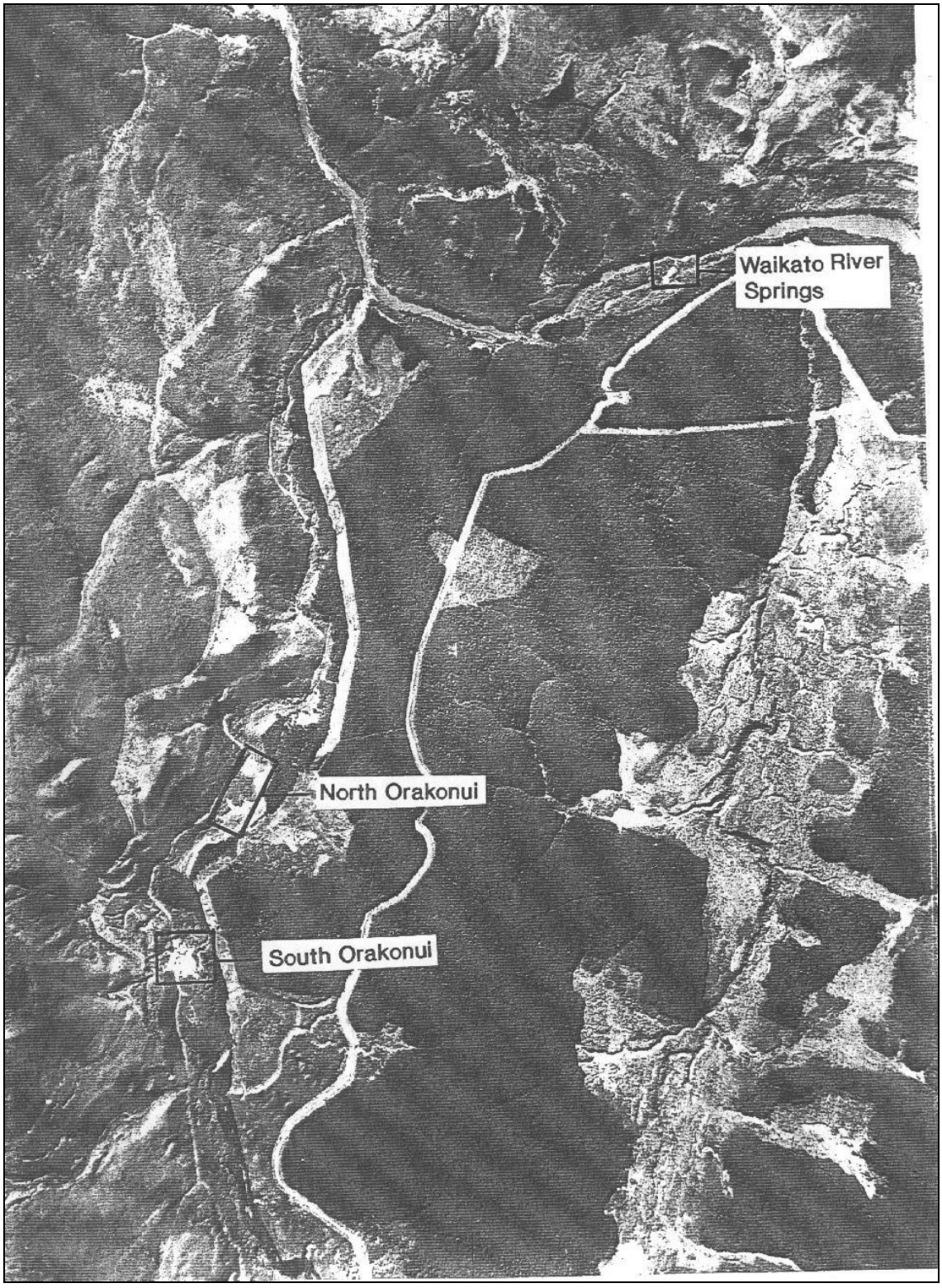

Figure 3.20: Aerial photograph taken 06/05/1941 showing the extent of the thermal areas at Orakonui North and South and the Waikato River Springs. Approximate scale 1:14,000. (Brotheridge 1995)

temperature from 65 to 96 ^{o}C. Bennie (1983) also measured temperatures for a group of springs in this area with temperatures ranging from 30.5 to 79.5 ^{o}C. Brotheridge (1995) subsequently described the area as being restricted to a few tiny springs ranging in temperature from 62 to 88 ^{o}C.

Orakonui South

The first records of thermal activity at Orakonui South are reports which detail an alkaline green pool and associated mud pots depositing sinter (Grange 1937). No pools can be identified from the 1941 aerial photos; they show large areas of barren ground and sinter at the same location as the main crater but larger in area. This suggests that the northern pool sits within a hydrothermal eruption crater that formed later.

Healy (1974) reported several springs including the largest one (presumably main crater) which had a temperature of 68 ^{o}C and a discharge or 14 l/s. He also noted that the northern pool was larger than it is at present and had a temperature of 29 ^{o}C.

Bennie (1983) also describes this pool; but with a temperature of 34.5 ^{o}C and discharge of 4.5 l/s and bubbling acid pools and sulphur deposits around steam vents. Bennie also recorded the northern pool as having a higher temperature of 81 ^{o}C and flowing via an outlet down to the Orakonui Stream, which deposited silica as it travelled to the stream. Bennie notes small pools 200 m to the south of the main crater.

Brotheridge (1995) describes all three of the pools mentioned above in 3.3.2. Main Crater was described as having a similar sized lake than present with a maximum depth of 2.85 m, mean temperature of 40 ^{o}C and surrounding feeder springs with temperatures from 58 to 90 ^{o}C. The northern pool was much deeper at about 8 m and had higher temperatures with bottom and surface temperatures of 79 and 60 ^{o}C, respectively. Although the pool was 8 m deep it had dropped below the level of the outflow channel and was not flowing into the Orakonui Stream as, is seen today.

Campbell et.al (2002) details the Orakonui South area in a very similar fashion to the present day, with the exception of the extent of the hydrothermal eruption breccia and the location of the outflow channel from the main crater after the 2005 eruption (Figure 3.21).

The Pavlova Spring mentioned in these previous studies is no longer present at Orakonui South.

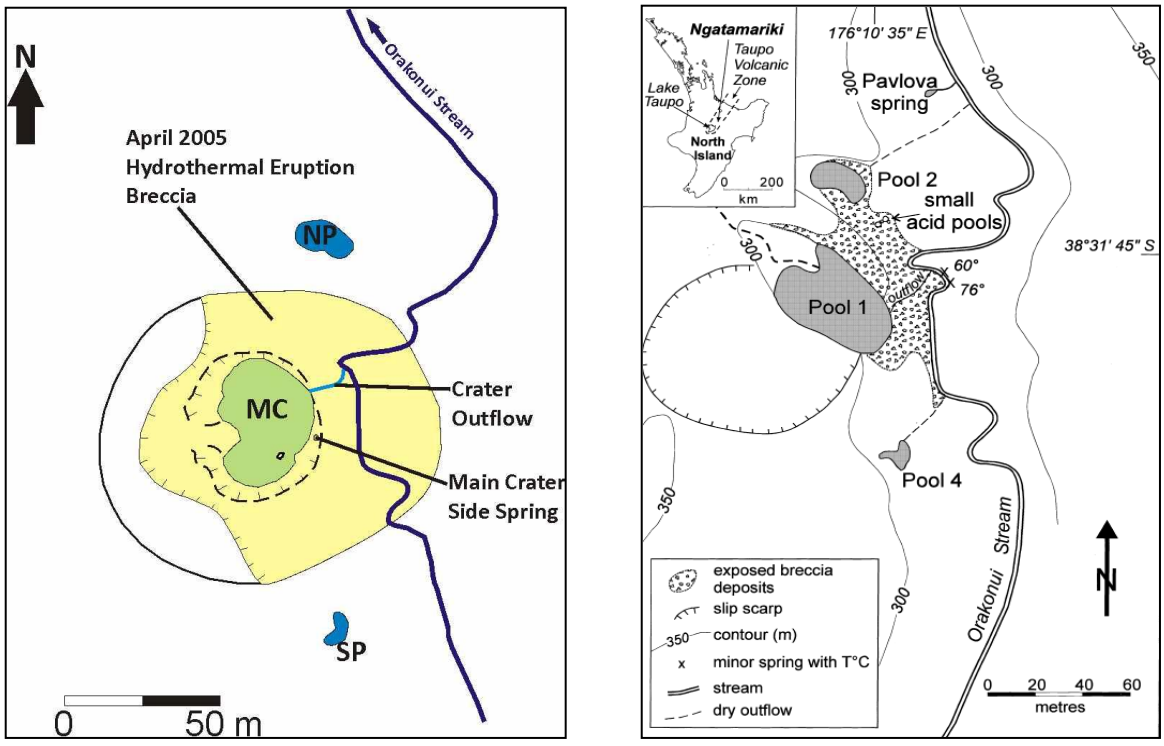

Figure 3.21: Location of features at Orakonui South. The diagram on the left shows the location of features as of December 2009 (MC-Main Crater, NP- Northern Pool, SP-Southern Pool). The diagram on the right shows the location of features in 2002 before the 2005 eruption (Campbell et al. 2002).

Hydrothermal Eruption History

In the documented history of the Ngatamariki thermal area the main pool (Main Crater) has erupted twice, once in 1948 and again in April 2005. The 1948 eruption created the crater that the pool sits in today. Prior to the eruption in 2004 the crater was largely dry. Campbell et al. (2002) report that by 1998 the crater was almost completely dry, but the surrounding springs were discharging into the dry crater (Figure 3.22).

The 1948 eruption created the crater that the thermal pool now sits in; the eruption had a maximum deposit thickness of 0.5 m and maximum clast size of 0.15 m (Browne & Lawless 2001). Witness accounts suggest the eruption column in the 2005 eruption reached 200 m high into the sky and the deposits still cover both sides of the Orakonui Stream (D Somerville, pers comm, February 5, 2009). Several explosions occurred; erupting a significantly large enough amount of material (maximum depth ~2 m and maximum clast size ~ 0.3 m) to dam the Orakonui Stream and change the location of the outflow channel for the main crater pool.

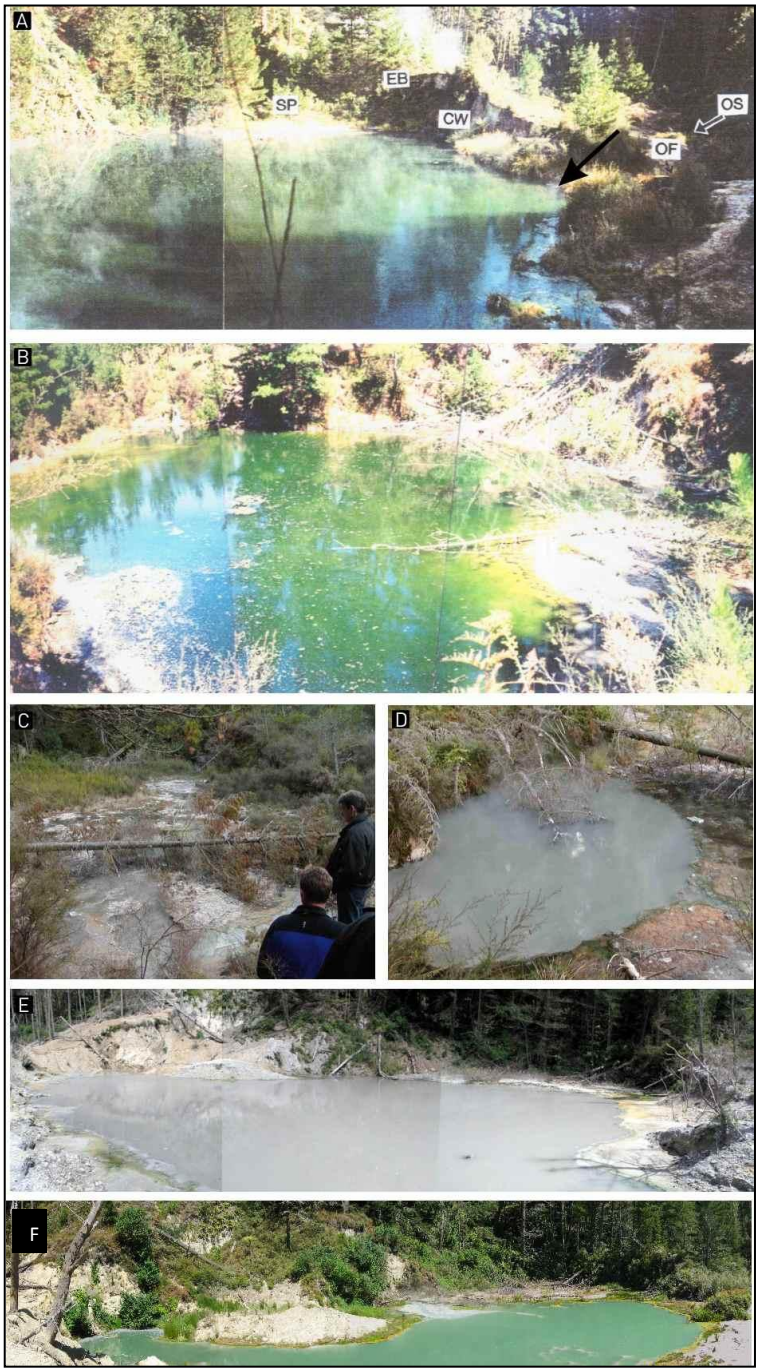

Figure 3.22: Photographs of the main crater at Orakonui South taken in A) 1985, B) 1994, C) and D) 2004 (note low level of lake prioir to eruption), E) 2006 and F) 2009. (Photos A-E courtesy of Karl Spinks)

The northern pool at Orakonui South also shows evidence that it may have at some point been subjected to an explosion event; as the steep walls of the pool suggest it maybe an eruption crater.

Waikato River Springs

Bennie (1983) was the first to recognise the Waikato River Springs on the northern boundary of the field; describing a spring surrounded by a large sinter platform on the southern bank of the river. From the 1941 aerial photograph a large patch of barren ground or sinter is visible in the area of the springs. After the flooding of Lake Ohakuri upon construction of the Ohakuri Dam in 1961 the area was destroyed and/or flooded.

Chapter 4: Orakei Korako

4.1 Location and Extent

The Orakei Korako geothermal field is located approximately 25 km north of Taupo (for location see figure 3.1). The currently active area covers approximately 1.8 km^2 on either side of the Waikato River (Figure 4.1), with evidence for more widespread geothermal activity, or migration of the centre of activity, seen from extinct geothermal features in the area. In January 1961 the level of the Waikato River was raised 18 m as a result of the damming of the river at Ohakuri for the hydroelectric power scheme. This raised the river level to approximately 290 m above sea level and formed Lake Ohakuri, drowning approximately 75% of the active geothermal features at Orakei Korako (Lloyd 1972). Lloyd had, however, undertaken an extensive study of the thermal area prior to the river level being raised and published this in 1972.

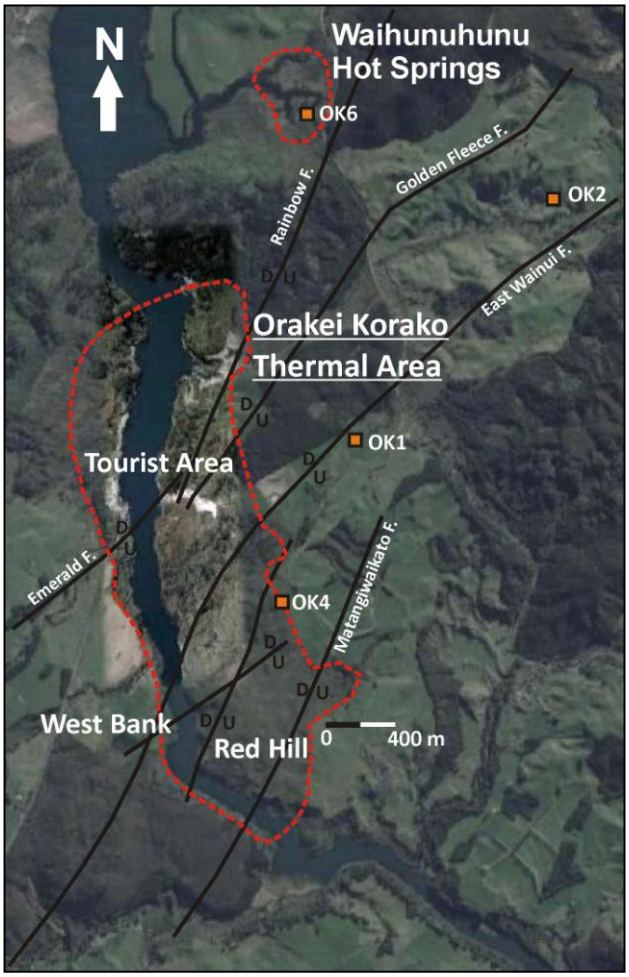

Figure 4.1: Extent of the Orakei Korako thermal area. The dashed red lines show the extent of the presently active areas. Black lines represent the faults that cut through the area and the exploration wells are represented by orange squares. (Modified from Lloyd (1972) and Hamlin (1999)) (Satellite image sourced from Google Earth, 2009).

4.2 Geology

4.2.1 Regional Geology and Structure

Orakei Korako is located on the eastern margin of the Maroa Volcanic Centre (MVC) (see section 3.2.1) and on the edge of the Whakamaru Caldera. Most of the pyroclastic material surrounding the area is derived from the MVC, which consists of several basaltic cones and twenty or more rhyolite domes between Atiamuri and Wairakei (Lloyd 1972) (Figure 3.5).

The Orakei Korako area is dominated by a series of south-west trending normal faults, splaying from the southern end of the Paeroa Fault (Golden Fleece, Rainbow, Emerald and East Wainui). These faults create the terraces across which sinter is being deposited presently (Figure 4.1). The Paeroa Fault forms a prominent scarp with a minimum vertical offset of 450 m to the northwest, indicated by topography (Bignall 1994).

4.2.2 Surface Geology

The stratigraphy at Orakei Korako was first described by Grange (1937), and has been subsequently described by Grindley (1960), Lloyd (1972), Bignall (1994) and Hamlin (1999). The following is an overview of the stratigraphy in the area as given by the reports mentioned above:

Surface deposits at Orakei Korako can be split into four groups; Pleistocene lake sediments, Quaternary igneous rocks and their associated breccias, Pleistocene – Recent alluvium and hot spring deposits and Recent pyroclastics and hydrothermal eruption breccias.

Umukuri Sinter – is the name given to siliceous sinter deposits at Orakei Korako, including deposits to the west of Lake Ohakuri as far as the Umukuri Stream; ranging from early Pleistocene to Recent in age and covering an area of approximately 1 km^2 (Lloyd 1972). The most probable explanation for this large distribution of sinter is that the silica precipitated as several discrete deposits, some possibly more than 20 m thick (Hamlin 1999).

Hydrothermal Eruption Breccias – are mixed in with other older pyroclastic deposits pre the 186 AD Taupo eruption (Wilson et al. 2009). Younger breccias are mainly restricted to the Red Hill

Crater and are the youngest deposits in the area. Recent eruptions have only ejected fragmented silica suggesting a relatively shallow origin for the eruptions. All materials from earlier eruptions were intensely hydrothermally altered Huka Group sediments from a deeper source.

Taupo Pumice Alluvium, Hinuera Formation and Orakonui Formation - see section 3.2.2.

Kakuki Basalt – is a small basaltic cone squeezed between two rhyolite domes; made up of flows and scoria just to the south of the tourist area at Orakei Korako. It is a high alumina, olivine-augite rich basalt thought to be the most primitive basalt in the TVZ (Cole 1972; Houghton et al. 1987; Gamble et al. 1990; Gamble et al. 1993). It can be seen today in a cutting on Orakeikorako Road. A large amount of this basalt is seen in the Matangiwaikato and East Wainui Faults (Lloyd 1972).

Tatua Basalt – is another olivine-augite rich basaltic cone made up of flows and scoria located about 5 km to the west of Orakei Korako near the former site of the Tatua Mill. Along the Waikato valley scoria correlated with the Tatua Basalt is inter-bedded with sandstones of the Huka Group (Lloyd 1972).

Parakauau Andesite – See section 3.2.2

Kaingaroa Ignimbrite – is confined to the northern section of the Orakei Korako field in the Te Weta Block. The Kaingaroa ignimbrite represents the only large scale ignimbrite from the Reporoa Caldera and is thought to be 0.23 Ma in age (Beresford & Cole 2000). It has two members: 1) an upper sheet of pinkish, devitrified, welded tuff containing re-crystallised fragments of previous igneous rocks and some small phenocrysts of plagioclase; 2) a lower sheet of poorly welded dark grey to black pumice tuff. To the west of the Te Kopia hydrothermal area it is poorly welded and inter-bedded with pumice tuff and tuffaceous mudstones of the upper Huka Group. Remnants of the Kaingaroa Ignimbrite also lie unconformably on Paeroa ignimbrite (Lloyd 1972).

Atiamuri Ignimbrite – is an orange to pink coloured soft ignimbrite and pumice breccia, containing prominent vesicular fragments of black glass up to 30 mm in size (Leonard 2003). The ignimbrite is located to the north west of Orakei Korako near Atiamuri and also just to the west of the tourist area at Orakei Korako, beneath a thin rhyolite sheet (Lloyd 1972).

Orakeikorako Tuff – is a poorly bedded pumice tuff that contains rhyolite, pumice and crystal fragments in a mircolitic texture. In the northern part of the main tourist area it forms conspicuous outcrops that are overlain with sinter, pyroclastic deposits and alluvium.

Huka Group and Haparangi Rhyolite - See section 3.2.2.

Paeroa Ignimbrite (Whakamaru Group) – is a grey quartzose ignimbrite, lithologically similar to the Te Kopia ignimbrite (Wilson et al. 1986). It is located in the northern part of the Orakei Korako area and forms the crest of the Paeroa Ridge in the upper part of the Paeroa Fault scarp (Bignall 1994).

Te Weta Ignimbrite (Whakamaru Group) – is a light grey to pink coloured crystal rich ignimbrite containing large pumice clasts. The Te Weta Ignimbrite is mineralogically similar to the Paeroa Ignimbrite however recognition of the unit is sometimes difficult due to variable pumice content further away from source. It outcrops in the middle of the highest part of the Paeroa Fault scarp (Bignall 1994).

Te Kopia Ignimbrite (Whakamaru Group) – is a hard, dark grey, crystal rich welded tuff that outcrops at the base of the Paeroa Fault scarp in the northern part of the field. The Te Kopia Ignimbrite occurs in all but one of the Orakei Korako wells and has been dated at an age of 0.35 Ma (Bignall 1994).

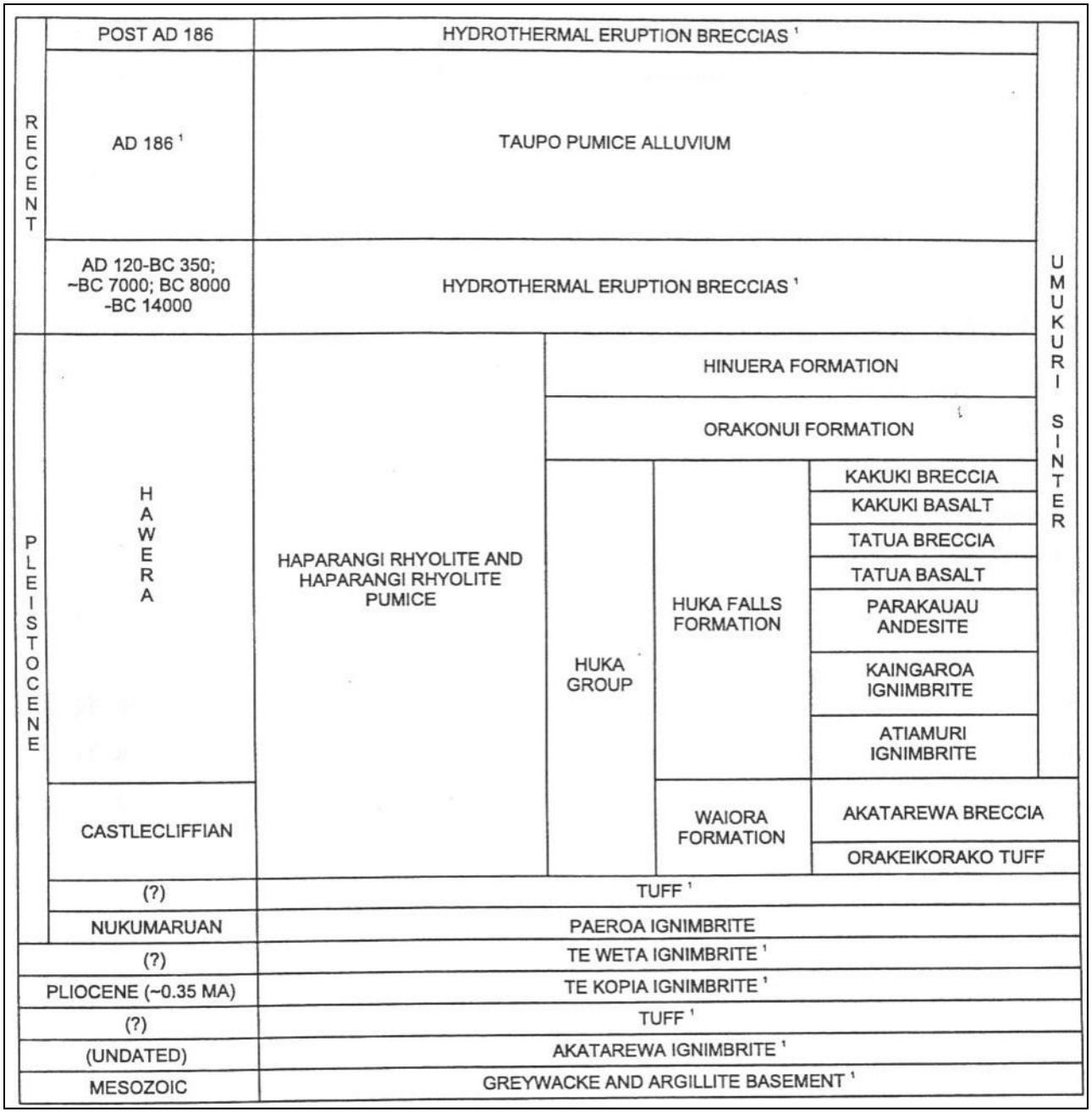

Figure 4.2: Stratigraphic sequence at Orakei Korako reported by Lloyd (1972) and Bignall (1994). [1]Lithological units referred to by Bignall (1994) (Hamlin 1999).

4.2.3 Deep Stratigraphy

Deep stratigraphy at Orakei Korako is known because during 1964 and 1965 four geothermal exploration wells (OK1, OK2, OK4 and OK6) were drilled by the crown to assess the areas potential for electrical power generation (figure 4.3). The following is a summary of the four wells from Grindley (1965), Lloyd (1974), Sheppard and Lyon (1984) and Bignall (1994). See figure 4.1 for locations of wells.

OK1 – OK1 is the deepest well in the field and was drilled 1405 m deep to the east of the tourist area. Highest temperatures were encountered at 914 m deep (221 ^{o}C) and in a fault zone intersected between 533 and 652 m deep (146 ^{o}C). The well was never tested. OK1 passed through sediments of the Huka Group and then through a series of ignimbrites and rhyolites before bottoming in the Akatarewa Ignimbrite.

Akatarewa Ignimbrite – part of the Tahorakuri Formation; is the oldest unit drilled into on the Orakei Korako Field but does not outcrop at the surface. It is a quartz-bearing ignimbrite that is grey-green in colour, indurated and coarse grained; with strong lenticular textures in OK1 and OK2 and more massive in OK6.

OK2 – OK2 is the eastern-most well and was drilled to 1155 m, fluid discharged from the well had an enthalpy of 960 kj/kg. Excessive drawdown due to low permeability caused failure of the discharge. The highest temperature for the field (265 ^{o}C) was measured at 1140 m deep and the highest chloride content (550 mg/L) was also found in this well. The estimate for the fluid temperature supplying the well was 225 ^{o}C. OK2 also passes through a series of ignimbrites and rhyolites including the Paeroa and Te Kopia ignimbrites and bottoms in the Akatarewa Ignimbrite.

OK4 – OK4 is the southern well in the field and was drilled to 1375 m. The maximum temperature encountered in the well was 235 to 240 ^{o}C at 427 m deep; a temperature of 230 ^{o}C was also

measured at 610 m deep and continued to descend to 186 ^{o}C at 853 m. The well was discharged for several days and waters were considered to be derived from a 234 ^{o}C source. OK4 intersects a large succession of Huka Group sediments (~800 m) and bottoms in rhyolite.

OK6 – OK6 is located among the Waihunuhunu springs in the northern part of the field. OK6 was drilled to 1220 m deep and had a maximum temperature of 259 ^{o}C at 1097 m. The well was discharged but then blocked after two hours and continued later at a diminished rate; water discharged from OK6 was thought to be derived from 214 ^{o}C fluids at depth. OK6 intersected a series of ignimbrites and rhyolites; with the most extensive being the Te Kopia ignimbrite which is approximately 400 m thick. Tuffs are also intersected in the well which bottoms in the Akatarewa Ignimbrite.

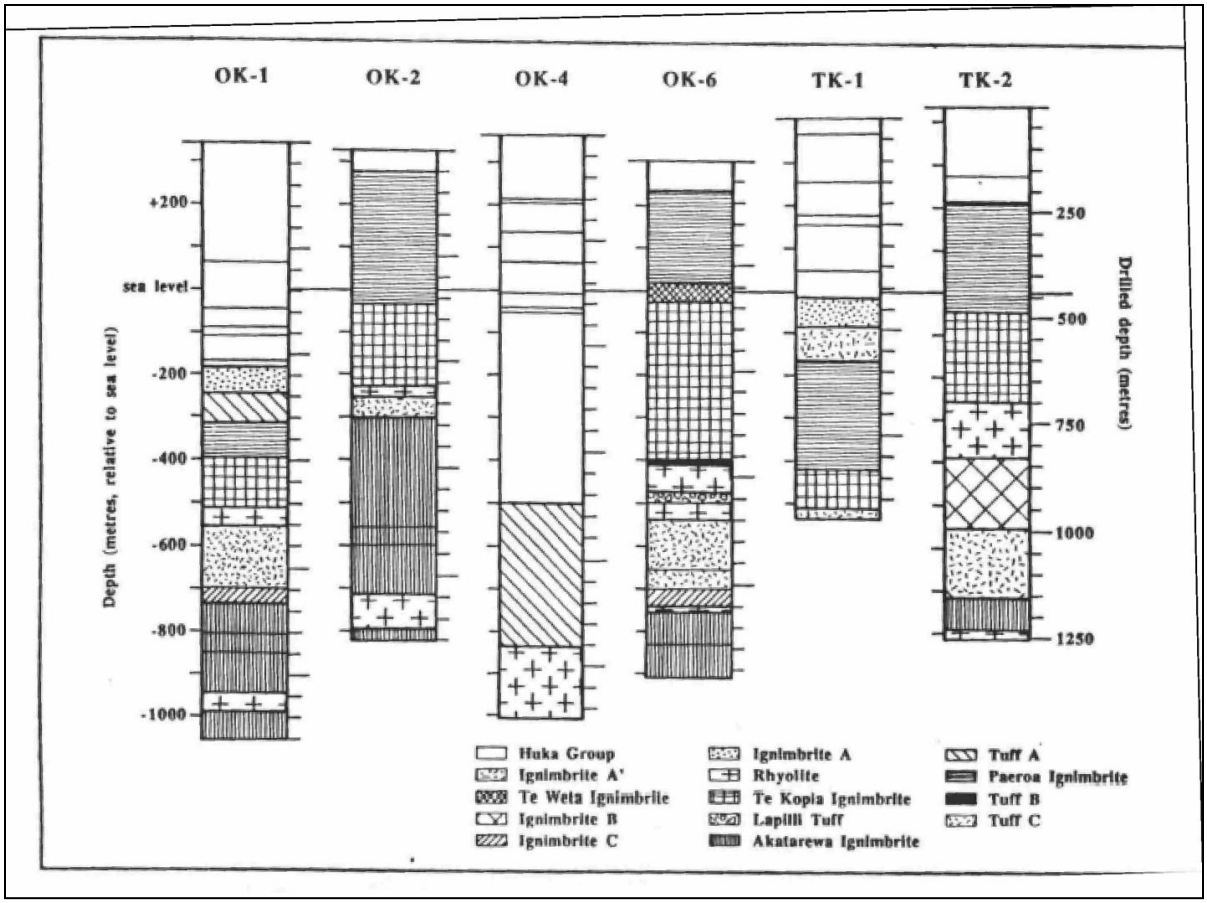

Figure 4.3: Stratigraphic logs for the Orakei Korako and Te Kopia wells (Bignall 1994).

4.3 Present Thermal Activity

The Orakei Korako thermal area can be divided into three main areas; the tourist area, the Waihunuhunu springs and Red Hill/West Bank. This study is concerned with the tourist area, Red hill/West Bank area and south towards Ngatamariki.

4.3.1 Tourist Area

The tourist area is located in the centre of the field and has the most thermal features. The features are located on the eastern and western banks of Lake Ohakuri. The following outlines the nature of these features in 2009/10. It appears that little major change has occurred since Hamlin's studies in 1999. A map of all the features in the area is located in Appendix C.

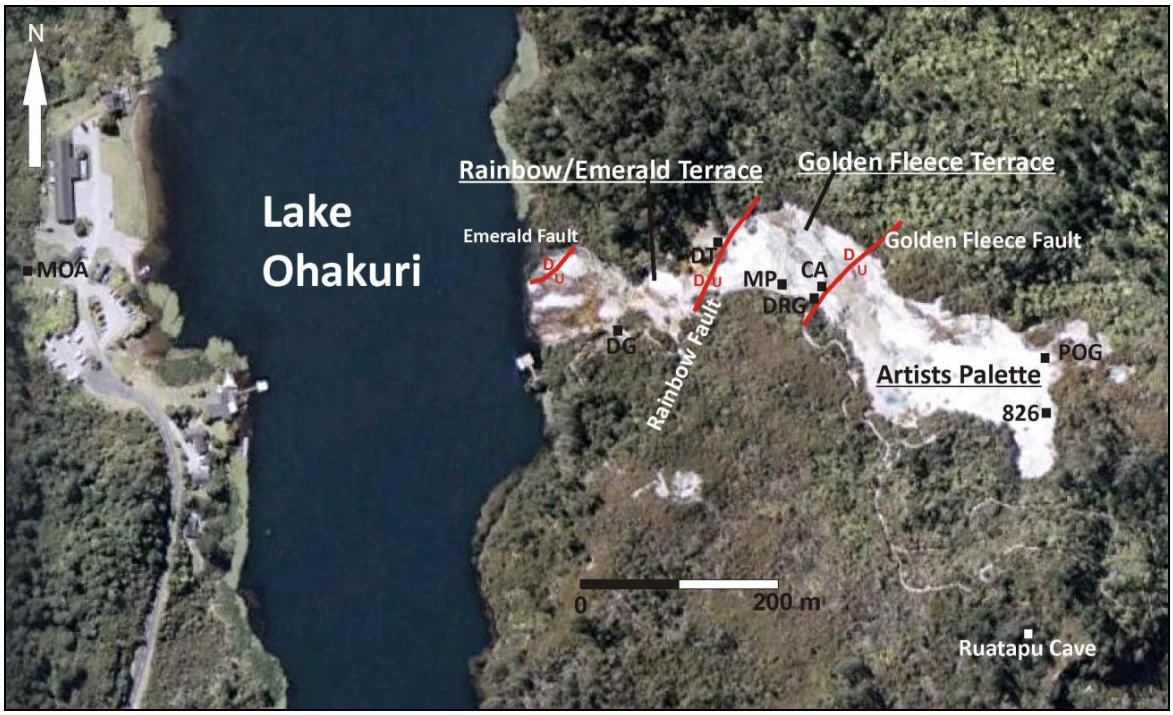

Figure 4.4: Location of springs mentioned or sampled at the tourist area. For a complete list of springs and their locations see Appendix C. MOA = Map of Australia, DG = Diamond Geyser, DT = Devils Throat, MP = Manganese Pool, DRG Dreadnought Geyser, CA = The Cauldron, 826 = Artists Palette Spring 826 and POG = Pyramid of Geysers (modified from Hamlin 1999) (Satellite image sourced from Google Earth, 2009).

Eastern Bank

The eastern bank is dominated by silica terraces created by diluted alkali chloride waters from hot pools and geysers travelling across the scarps of the Rainbow, Emerald and Golden Fleece Faults. The faults are south-west trending normal faults which cut through the area creating the terraces. Temperatures of the hot pools and geysers range from 87 ^{o}C to 75 ^{o}C mostly with near neutral pH. Ruatapu Cave is also located in this area above the sinter terraces and has anomalous acidic water chemistry (pH 2.5) when compared with the rest of the field. Two hydrothermal eruption craters are located beside Ruatapu Cave.

The temperature and pH of four springs covering all of the terraces on the eastern bank were attained during this study. They were the Diamond Geyser, The Cauldron, Artists Palette pool 826 and Ruatapu Cave (Figure 4.4, 4.5). The Diamond Geyser is located at the bottom of the scarp of the Rainbow Fault and has a pool 1.5 x 1.5 m in diameter. The geyser erupts irregularly and eruptions

last from a few minutes to a few hours (Lloyd 1972). During Fieldwork in 2009 the Geyser was only seen erupting once for a short period. The water in the Diamond Geyser pool had a temperature of 83.4 ^{o}C and a pH of 7.4. The Cauldron is located below the Golden Fleece fault scarp 5 m to the north-east of the Dreadnought Geyser. The Cauldron pool was about 2 m deep on all occasions it was visited in 2009 and had a temperature of 86.7 ^{o}C and a pH of 7.24. The Artists Palette spring 826 is located about 10 m to the south of the Pyramid of Geysers. The spring was about 0.5 m in diameter and had a temperature of 75.1 ^{o}C and a pH of 5.9 which is much more acidic than the rest of the springs in the field. The last feature sampled was Ruatapu Cave which is the eastern most feature on the east bank and is surrounded by two hydrothermal eruption craters. Two pools are located in Ruatapu Cave; the main pool is called Waiwhakaata and is a permanent feature in the cave. Waiwhakaata is a clear warm, acidic pool that is perched about 15 m above the Artists Palette (Lloyd 1972); in 2009 the pool had a temperature of 35 ^{o}C and a pH of 2.67 and was about 12 x 8 m in size and ~1.5 m deep. This is of interest because the

springs below on the Artists Palette all discharge alkali chloride waters. A subsidiary chamber called Rahu Rahu is located 5 m above Waiwhakaata which has two ephemeral pools, which when active release steam into the cave creating a humid atmosphere within the cave (Browne & Rodgers 2006).

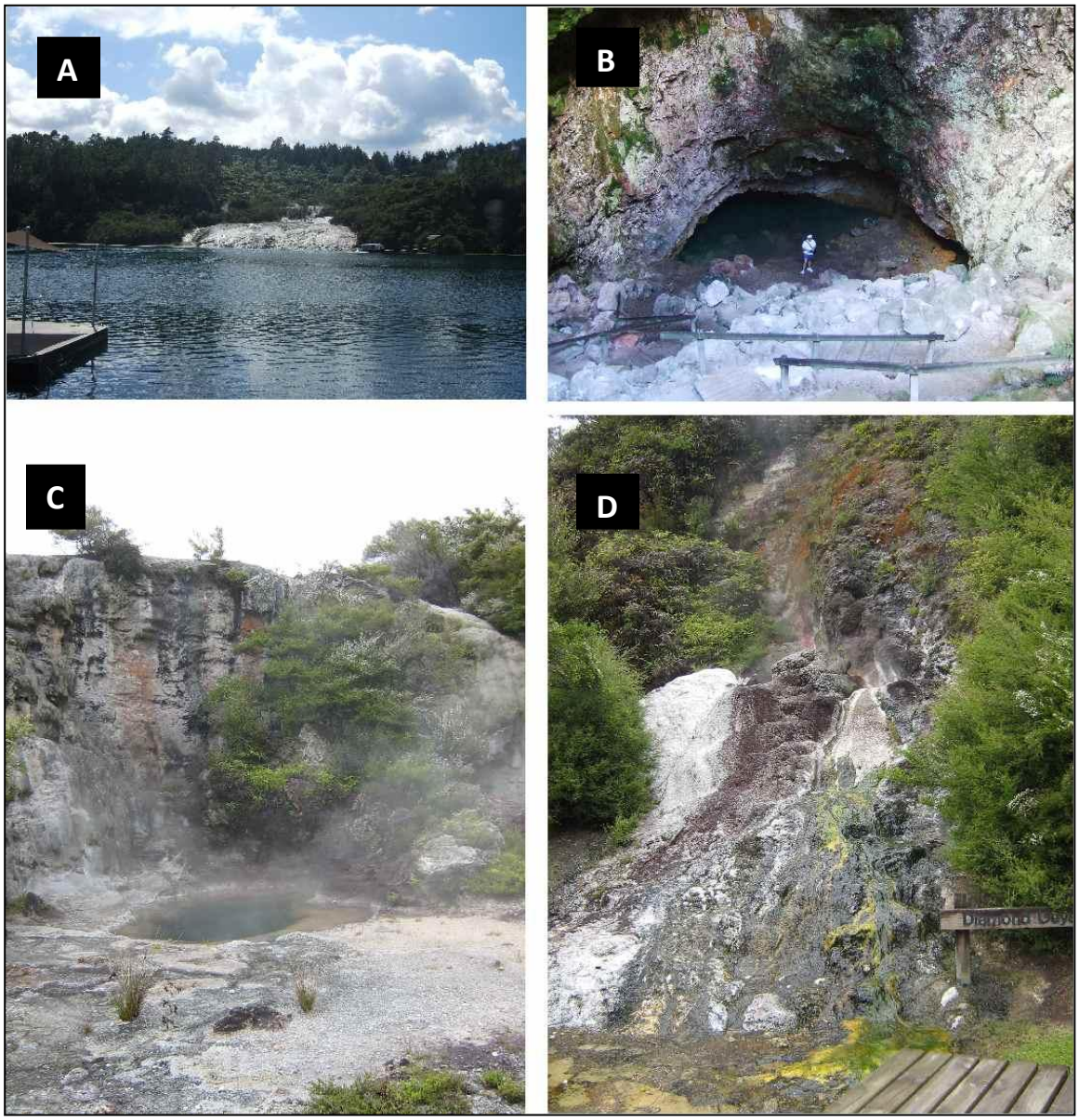

Figure 4.5: Thermal features at the Tourist Area A) Veiw looking from west to east across lake Ohakuri at the thermal area (February 2009). B) Ruatapu Cave with Waiwhakaata visible in the bottom of the cave (February 2009). C) The Cauldron hot spring at the base of the Golden Fleece Fault scarp (December 2009). D) The Diamond Geyser beneath the scarp of the Rainbow Fault (December 2009).

Western Bank

On the western bank of the tourist area a few small geothermal springs/pools are present including the Map of Australia, Green Pool, Brown Pool, Bracken Pool and Utility Pool (Hamlin 1999). All these springs are alkali-chloride waters with temperatures between 90 ^{o}C and 80 ^{o}C and have a near neutral pH. The Map of Australia (Figure 4.4) was sampled during fieldwork in May 2009; it had a temperature of 80.5 ^{o}C and a pH of 8.19 and was about 10 x 5 m in size and about 4 m deep. Further springs also occur at higher elevation behind these springs.

4.3.2 Red Hill/West Bank Springs

Red Hill

The Red Hill area is located approximately 1.5 km south of the tourist area on the eastern bank of Lake Ohakuri. The area is dominated by steaming ground that covers the hill and scattered small springs, probably created by a series of north east trending faults that intersect the area creating paths for hot water (Mahon 1972). The largest hot spring feature is the Hot Waterfall Geyser documented by Hamlin (1999); the geyser sits approximately 50 m up on the river bank behind the Tutukau Baths which sit below a waterfall created by the outflow from the geyser. The geyser only erupts in small frequent spurts radialy 5 m from the vent in the surrounding native bush. Water in the pool is at boiling point and has a pH of 9.46.

Figure 4.6: Thermal Features at Red Hill**.** Hot Waterfall Geyser (left) about 50 m above the river bank at Red Hill and the hot waterfall that supplies the Tutukau Baths with hot water from the discharge of the geyser (December 2009).

West Bank

There is minimal activity on the western bank of Lake Ohakuri opposite Red Hill. However there is a small geyser pool at NZMG E2784533, N6297083, it is possibly spring 984 from Lloyd (1972) but there is no mention of the nature of the spring in Hamlin (1999). For the purpose of this study the spring will be called West Bank Geyser (WBG). WBG sits about 1.5 m above the level of the Waikato River and has a small outflow channel that runs into the lake. Vegetation is dead or nonexistent on the bank above the 1.5 x 1.5 m pool suggesting the occurrence of irregular eruptions. Sediment in the lake around the spring is at boiling point and burns feet through the soles of hiking boots. Water in the pool is at boiling point and has a pH of 8.

Figure 4.7: Location of sampled springs at Red Hill and West Bank (HWG = Hot Waterfall Geyser and WBG = West Bank Geyser)(Satellite Image sourced from Google Earth, 2009).

Figure 4.8: West Bank Geyser on the West Bank Area at Orakei Korako.

4.3.3 Waihunuhunu Hot Springs

The Waihunuhunu hot springs are located in the northern part of the Orakei Korako field and were not sampled or visited during reconnaissance for this project. They are associated with the Whakaheke fault and were mostly submerged during the flooding of Lake Ohakuri. However the springs that had the highest discharge before the flooding still remain today discharging into one of the eastern arms of the lake. Exploration well OK6 is located within this area.

4.3.4 History of Thermal Activity at Orakei Korako

The history of thermal activity at Orakei Korako is well documented from 1859 onwards. Firstly by Hochstetter (1864) whose account of the area was mainly confined to the western bank of the Waikato River and counted 76 pools on both banks which included geysers and steam clouds. He also recognised silica sinter which was being deposited from geysers. Activity in the area was next documented by Grange (1937) who also describes the occurrence of sinter and geysers on both banks of the Waikato River. Keam (1955) was the next to report on the area publishing a tourist guide called "Volcanic Wonderland". He noted that the Artists Palette was occasionally dry and had a continuously active geyser in the centre. Lloyd (1972) is the most comprehensive account as it covers the area before the flooding of Lake Ohakuri in 1961 when approximately 75% of the thermal features were submerged, and the effects of the flooding on the area immediately after. His study includes detailed observations of sinter terraces and thermal activity in the area as well as extensive geological, hydrological and chemical studies of the area. In his account he indicates that there were 18 alkali-chloride springs and 9 mud pots on the western bank ranging in temperature from 40 ^{o}C to 91 ^{o}C. The pools mentioned in this study on the western bank of the tourist area probably correlate to the larger lower temperature pools mentioned by Lloyd. The area below the current location of the tourist centre was dominated by a series of large intermittent geysers sitting on a sinter platform 100 x 60 m wide. These geysers could erupt to

heights of over 36 m high but the last recorded eruption of the Rahurahu geyser in 1985 or 86 was only 18 m high. His report also details the locations and nature of all the springs and thermal activity on both banks of the Waikato River. Subsequently Sheppard and Lyon (1984), Bignall (1994) and Hamlin (1999) have also documented the area.

Chapter 5: Geochemistry at Ngatamariki

5.1 Methods of Water Collection and Analysis

5.1.1 Water Collection Methods

Water samples were taken from places deemed to be representative of the area interest. These were generally the middle of the spring or area of highest upflow, or from the area of greatest flow within a stream or in production wells from the weir box by the well discharge. Samples were first collected into a 10 L bucket which had been rinsed several times with the water being sampled. The sample was then put into one 500 ml bulk unfiltered PET, bottle directly from source, where appropriate, or from the bucket. Two smaller bottles (bottles obtained from GNS Wairakei) were then rinsed and filled, one filtered with a 0.45 μm filter from the sample bucket or source, where appropriate, the other using the same process without filtering (to be acidified later at the GNS Wairakei research centre lab prior to analysis). A 10 ml glass bottle from University of Canterbury's Stable Isotope Lab was also filled for analysis of ^{18}O and D. All sample bottles were rinsed several times with the water being sampled, and the sample lid closed under water to minimise interaction with the atmosphere; filtered bottles were filled to the top of the bottle for the same reason.

5.1.2 Rock Collection Method

Two rock samples were taken from locations in the 2005 hydrothermal eruption deposits around the Orakonui Stream to determine their mineralogy by X-Ray diffraction analysis (XRD). The aim of was to determine the depth of the source for the 2005 eruption.

5.1.3 Major Ion Chemistry

Analysis of major ion was carried out in the geochemistry laboratory at GNS Wairakei (analyst Dr Bruce Mountain). The following gives brief descriptions of the methods involved in determining

the concentration of the various aqueous ions. A full list of the methods used and detection limits is located in Appendix D.

HCO_3^- Titration Method (HCO_3-) – Samples are titrated with a standard acid to pH 8.3 (P titre) and pH 4.5 (T titre) and the total and/or permanent alkalinity is calculated. Results are recorded as equivalents of calcium carbonate or recalculated as carbonate, bicarbonate and hydroxide.

ICP-OES (B, Ca^{2}+, Li+, Mg^{2}+, K+, SiO_2, Na+) – Inductively Coupled Plasma – Optical Emission Spectrometer. After preservation with 10% nitric acid some non-metals and a wide range of metals can be analysed using ICP-OES. The solution is aspirated into an argon plasma and emit characteristic light or energy due to electron transitions as they pass through unique energy levels. The emitted light is focused onto a diffraction grating and separated into components, where photomultipliers measure the light intensity at different wavelengths, where the intensity is directly proportional to concentration.

Ion Chromatography (Br-, Cl-, F-, SO_4^{2}-) – Ion chromatography measures ionic species by separating them based on their reaction with a resin. The ionic species are then separated by species type and size before being passed through a pressurized chromographic column where the ions are absorbed by the constituents in the column. An extraction liquid is then run through the column and the absorbed ions separate from the column where the time taken for the species to separate determines its concentration (Bruckner 2009).

Flame Emission Spectrometry (Cs+, Rb+) – Involves the transformation of the initial solution being analysed into a vapour by flame containing free atoms or molecular compounds of the analyte. The optical signal of the analyte (carrying the information on the concentration and kind of analyte) that arises from the vapour is then detected by a spectrometer. The amplification and read-out of the electrical signal of the analyte then gives a concentration in mg/l (Jackson & Mahmood 1994).

Methylene Blue Method (H_2S) – Uses the reaction of sulphides in a water sample with dimethyl-p-phenylenediamine in the presence of ferric chloride to produce methylene blue. The method

measures the total acid soluble sulphides and concentrations are reported in mg/l. The method was first developed by Fischer (1883).

5.1.4 Stable Isotopes (^{18}O and $D/^{2}H$)

Epstein and Mayeda (1953) outline the standard procedure for the analysis of the Oxygen-18 and Deuterium composition of water. University of Canterbury's Thermo Scientific TC/EA (Thermo-Combustion Elemental Analyser) uses the methods developed by Sharp et,al. (2001) to analyse the ^{18}O and D composition of waters. The method involves the equilibration of CO_2 with 1-1.5 µl of water in a 1 ml? glass vile. Samples are then entrained in a helium carrier gas and pass through a glassy carbon packed furnace heated to 1450 ^{o}C. The sample is then admitted through an open split to an isotope ratio mass spectrometer where the composition of the water is analysed.

Quality of measurements is maintained by having two tertiary laboratory water standards (V-SMOW and V-SLAP) that are calibrated to international primary standards. Well samples were corrected to reservoir composition by using the steam fraction calculations located in section 2.5.3. Steam fractions, well pressures and measured enthalpies for wells analysed in this study are located in Appendix E.

5.1.5 X-Ray Diffraction Analysis (XRD)

XRD is used to identify unknown crystalline materials. The analysis is based on Bragg's equation relating the angle of incidence of the x-ray beam, the distance between the crystals atomic layers and the wavelength of the incident x-ray beam. The x-rays penetrate through the mineral lattice exiting the lattice of the crystals and diffracting the rays to a receiver. The principle assumes that each mineral has a different lattice spacing allowing the difference in diffraction of the rays to allow the determination of the mineral type.

Using University of Canterbury's Phillips PW1820/1710 X-ray Diffractometer system XRD analysis was carried out on hydrothermally altered material from the April 2005 eruption at Ngatamariki.

5.2 Geochemistry of Spring and Well Waters at Ngatamariki

This section summarises the results from chemical and isotopic analysis of waters from Ngatamariki springs and wells. A full list of results from analyses made as part of this thesis and from previous studies is listed in Appendix F.

5.2.1 Major Ion Concentrations

Water compositions in springs of Orakonui North and South show high chloride, sodium, silica and bicarbonate concentrations. However the chloride concentrations are low when compared with geothermal waters at Broadlands, Waiotapu and Wairakei. Springs at Waikite, Mokai and Orakei Korako have similar dilute chloride signatures (Brotheridge 1995). All the springs at Ngatamariki have a near neutral pH and are located on the margins of the field.

Figure 5.1: Locations of sampled springs and wells in this study. Spring areas are represented by green dots and production wells are represented by red squares. (CB = Clear Black, MSP = Middle Sinter Pool, FS = Father and Son, MC = Main Crater, MCSS = Main Crater Side Spring, SP = Southern Pool, NP = Northern Pool, DM = Devils Mouth). For more detailed maps of the areas see section 3.3 and for locations of monitoring wells see figure 3.5 (Satellite image sourced from Google Earth, 2009).

The spring waters at Ngatamariki can be classified as diluted chloride-bicarbonate waters low in sulphate which is clearly shown in the Cl-HCO_3-SO_4 ternary diagram below (Figure 5.2).

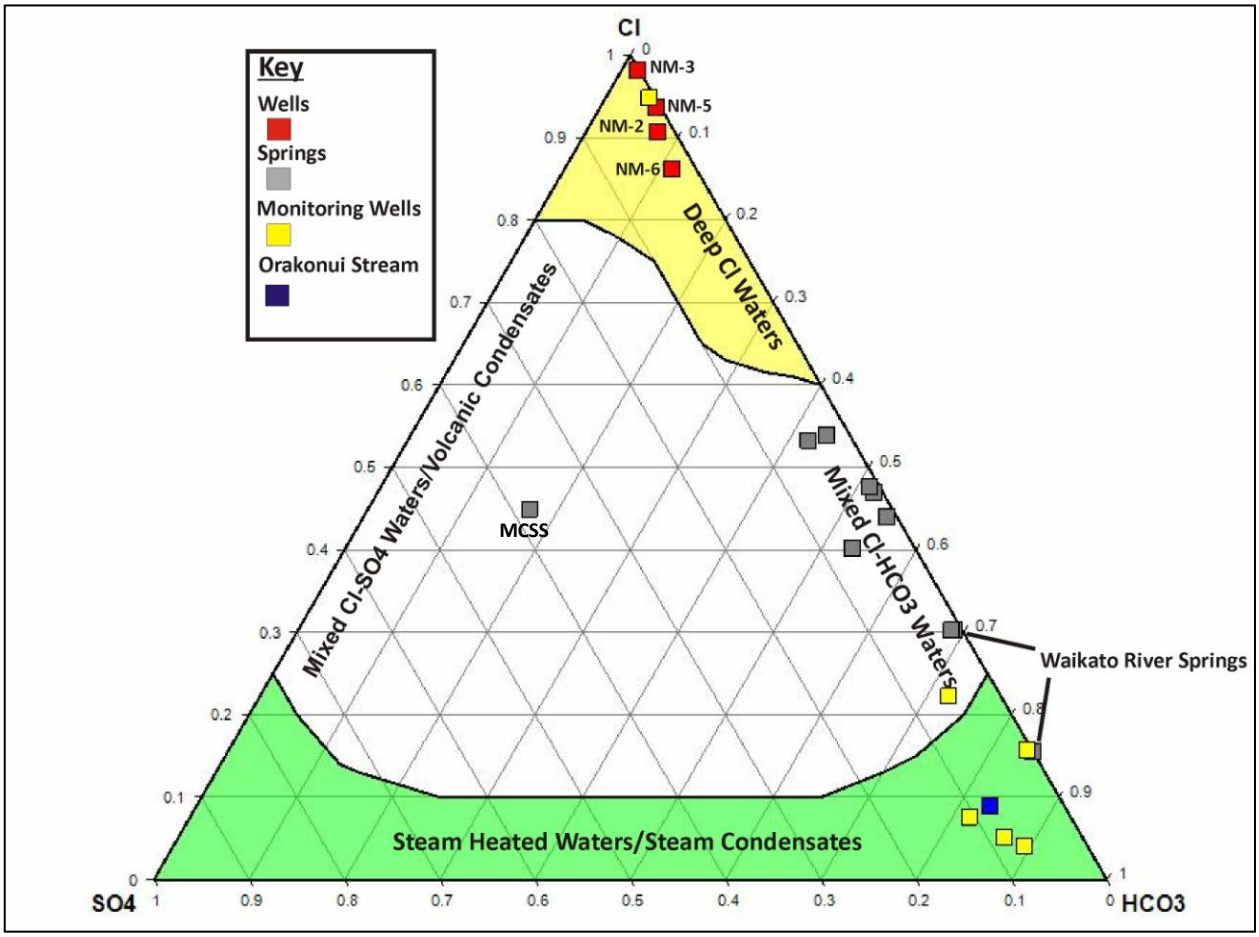

Figure 5.2: Cl-HCO_3-SO_4 ternary plot of spring, well and stream water at Ngatamariki (diagram adapted from Nicholson, 1993)

The exception is the Main Crater Side Spring which has higher sulphate concentrations suggesting it is some type of fumarole condensate. Chloride concentrations in spring waters range from 647 mg/l in the Orakonui South Southern Pool to 57 mg/l in the W2 spring along the Waikato River. Production Well (Well) waters are dominantly chloride with very minor influences from either bicarbonate or sulphate. Monitoring well waters are dominantly bicarbonate waters typical of

local groundwater; with some mixing with Cl waters. The Orakonui Stream water is also dominantly bicarbonate and represents local meteoric water chemistry.

Total dissolved solids (TDS) has a positive correlation with chloride (assumed conservative) (Figure 5.3) allowing three distinct groups of waters to be defined at Ngatamariki.

1. Deep (well) waters with the highest amount of TDS and chloride concentrations
2. Surface (springs) and near surface with intermediate TDS and chloride compositions
3. Local groundwater (stream and monitoring wells) which exhibits typically low TDS and chloride compositions.

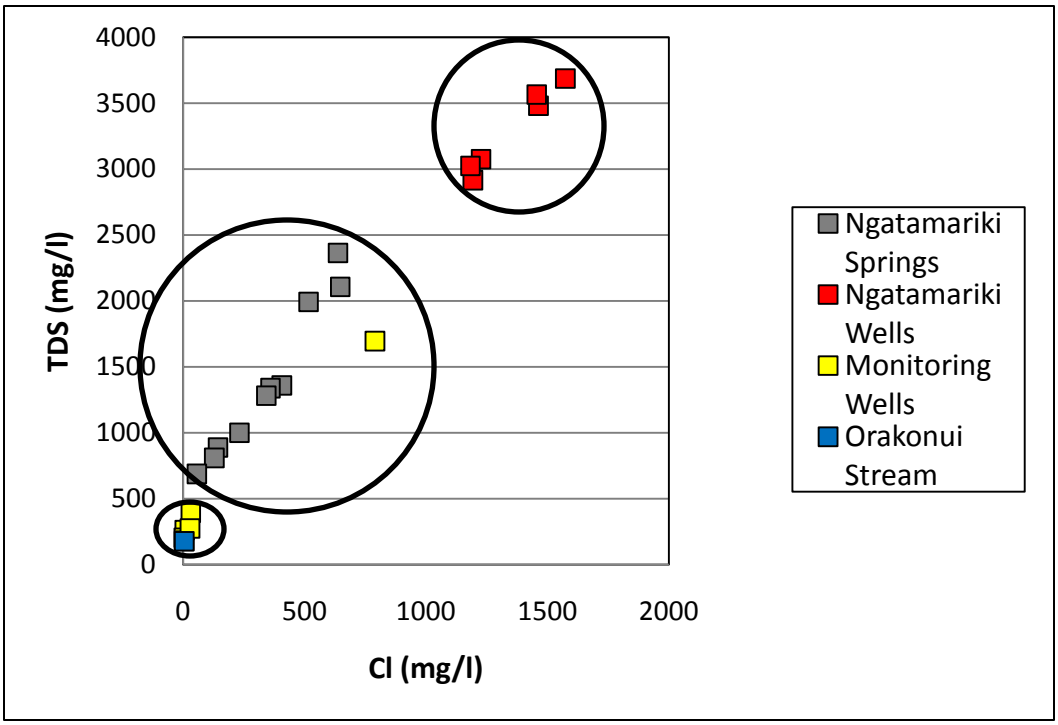

Figure 5.3: TDS vs chloride for well, spring and stream water at Ngatamariki. Three distinct groups are shown by circles around the clusters of data.

Ratios of chloride, boron and fluoride have been used to track common sources in a reservoir (see section 2.2.3). A strong positive correlation is seen between chloride and both boron and fluoride, indicating a common source for the whole field (Figure 5.4).

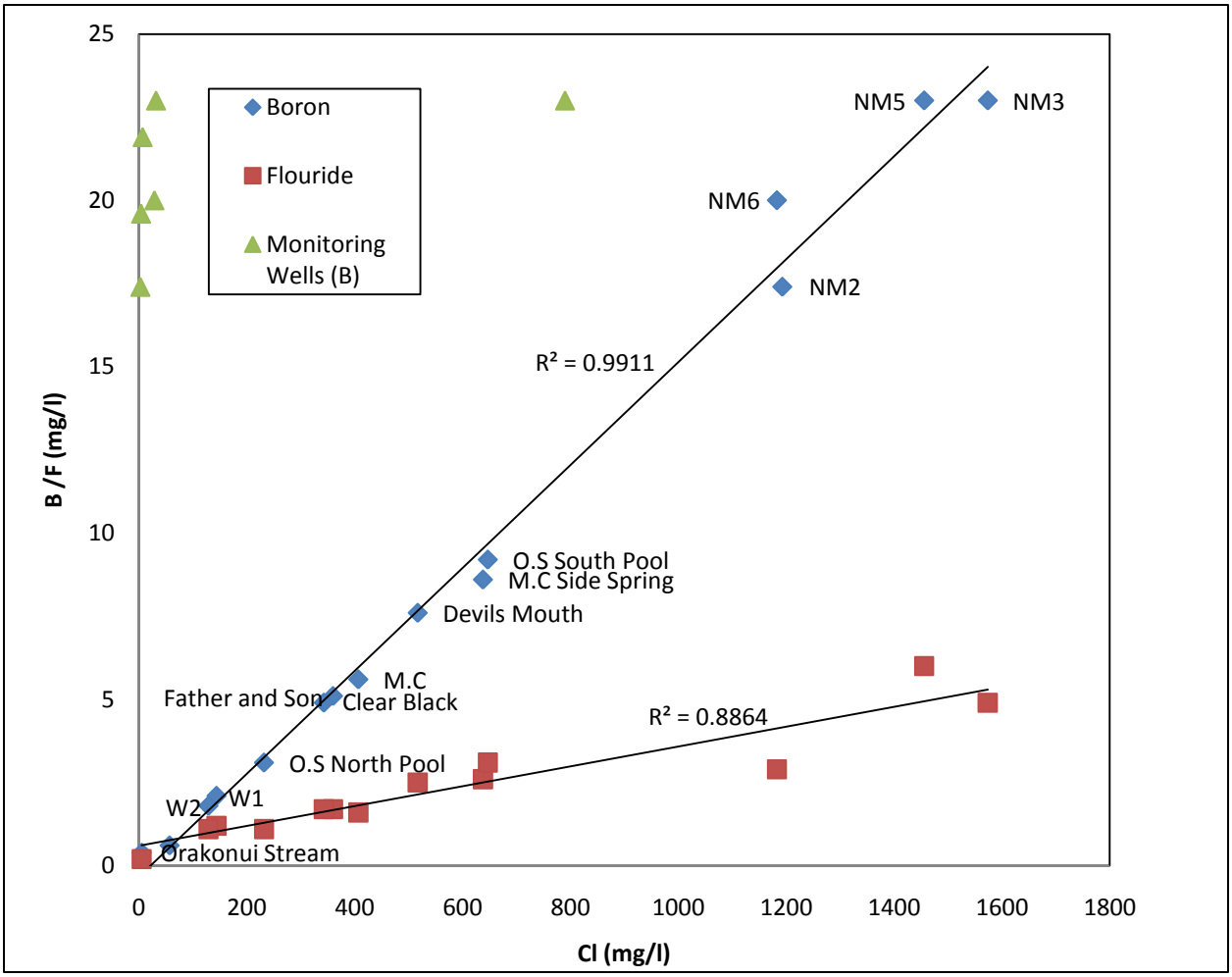

Figure 5.4: Cl/B and Cl/F ratios for Ngatamariki well, monitoring well, spring and stream waters.

The Ngatamariki monitoring wells show different Cl/B ratios from the rest of the field with very low chloride and high boron concentrations; suggesting that the local groundwater aquifer is completely independent of the thermal system.

Lithium is also an important constituent in geothermal systems as it allows the rate at which fluids travel towards the surface to be determined. Fluids travelling rapidly to the surface will have higher Li concentrations because they do not have time to become incorporated into low rank alteration products (clays and zeolites). The Cl-Li-B ternary plot below (Figure 5.5) shows that waters at Ngatamariki are relatively low in lithium and boron and all group tightly in an area at about 50 % relative Cl. The monitoring-well water chemistry is different to the rest of the field; with almost 100 % relative B, again suggesting that it is independent from the rest of the field.

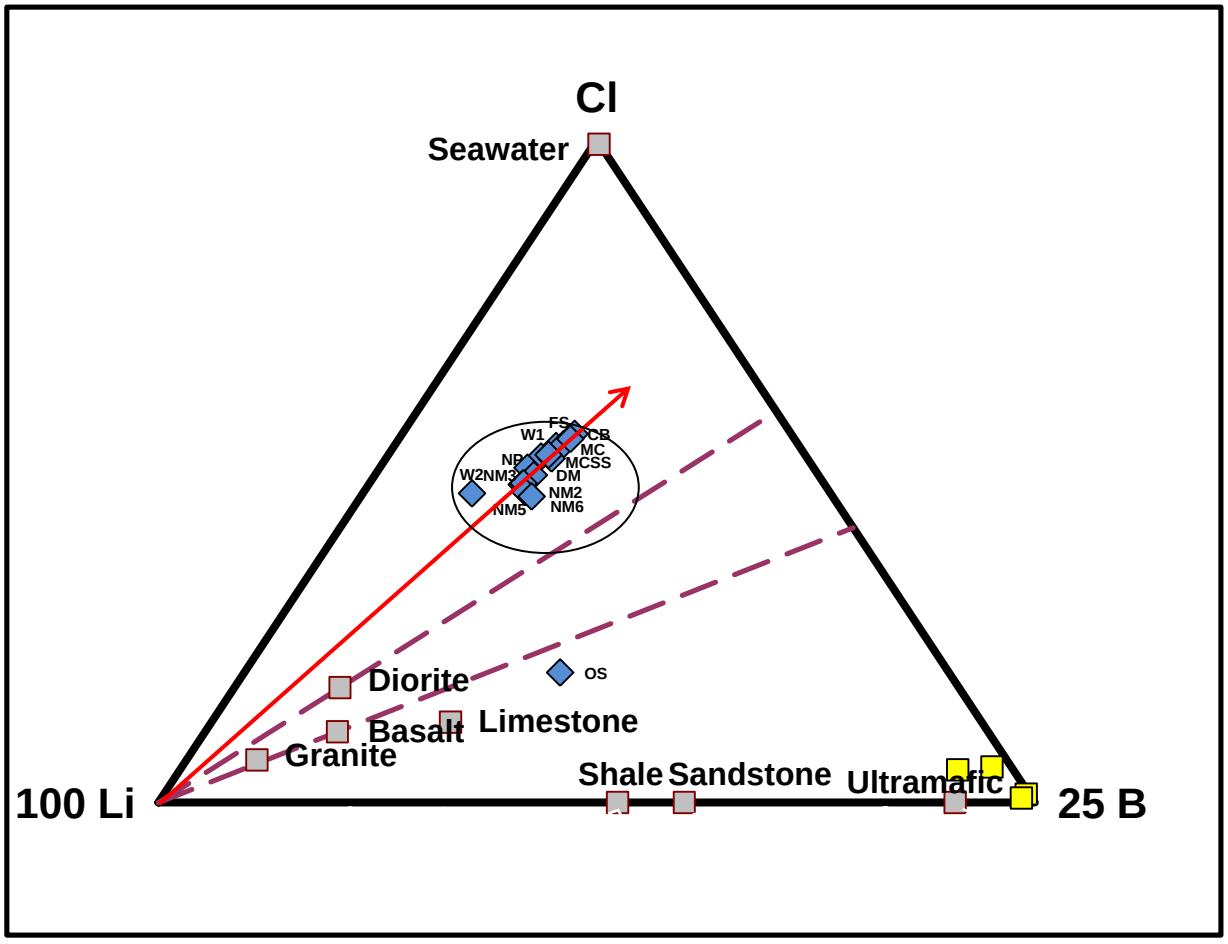

Figure 5.5: Cl-Li-B ternary plot for waters at Ngatamariki. Spring, well and stream waters are represented by blue diamonds; monitoring wells are represented by yellow squares.

5.2.2 Solute Geothermometers

The chemical equilibrium of water and rock is the basis for solute geothermometers; the following outlines the geothermal reservoir temperatures attained from using the chemistry results from geothermal waters. Detailed theory behind solute geothermometers is outlined in section 2.3.4 and geothermometer equations used are located in Appendix G.

Feature	Chalcedony	Quartz no steam loss	Quartz max steam loss	Na-K-Ca	Na-K-Ca Mg corr
M.C	156	178	166	181	164
M.C Side Spring	157	179	167	161	158
O.S South Pool	175	195	179	175	175
O.S North Pool	128	154	146	159	131
Clear Black	149	172	161	164	152
Father and Son	151	173	162	166	148
Devils Mouth	160	182	169	166	166
W1	157	179	167	199	117
W2	148	171	161	185	102
NM2	288	311	252	281	281
NM3	329	399	275	295	295
NM5	327	395	275	286	286
NM6	282	302	249	271	271

Table 5.1: Geothermometer results for waters at Ngatamariki, temperatures are in ^{o}C.

Results from the Na-K-Ca and Na-K-Ca (Mg corrected) correlate well with maximum interpreted temperatures from NM2 (286 ^{o}C at 1200-1350 m); as do the results for the springs which

correlate well to the interpreted temperatures of the intermediate aquifer at 300 m (150-180 ^{o}C) suggesting that the intermediate aquifer is the source of springs at the surface (Urzua 2008). The interpreted maximum temperature for NM5 is >240 ^{o}C (Ramirez & Rae 2009) which is close to the calculated temperatures for the Na-K-Ca, Na-K-Ca (Mg corrected) and quartz maximum steam loss (QMSL) geothermometers which range from 275 to 286 ^{o}C. However the quartz geothermometers have an upper limit of 250 ^{o}C, which excludes their results (see section 2.3.4). NM6 has interpreted reservoir temperatures of between 240 and 300 ^{o}C (Rae et al. 2009), this correlates well with the results from the Na-K-Ca, Na-K-Ca (Mg corrected) and QMSL geothermometers which sit between 249 and 271 ^{o}C. NM7 has a maximum interpreted reservoir temperatures of >210 ^{o}C (Ramirez et al. 2009), chemistry for this well is not included in this study.

Na-K-Mg Diagram

Figure 5.6 is an adaptation of Giggenbach's (1988) Na-K-Mg ternary plot which is described in section 2.3.4. Half of the Ngatamariki spring waters fall into the area of partial equilibration on the diagram indicating re-equilibration by dilution or mixing between 160 and 180 ^{o}C. With the exception of the Devils Mouth and Orakonui South Southern Pool which both plot on or above the full equilibrium line. All the Ngatamariki wells plot on the full equilibrium line suggesting reservoir temperatures of 280 – 320 ^{o}C for the field. The Waikato River springs show higher Mg contents than the monitoring wells and Orakonui Stream which suggests no geothermal influence on both.

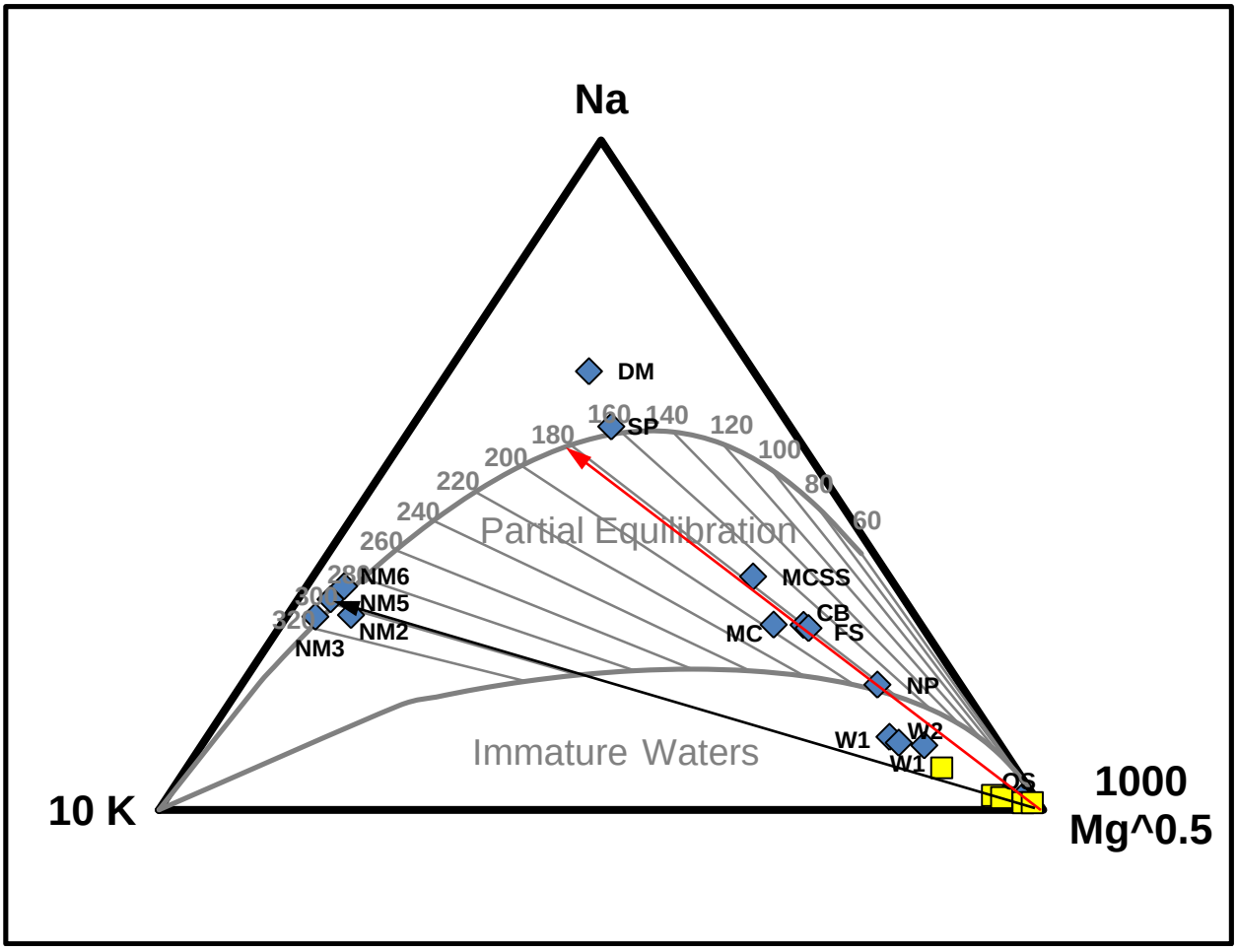

Figure 5.6: Na-K-Mg Geothermometer for waters at Ngatamariki. (after Giggenbach (1988)). Yellow squares represent the monitoring wells and blue diamonds represent all other waters.

5.2.3 Dilution Trends

Using the chemistry of surface springs and well discharges at Ngatamariki a chloride - enthalpy mixing diagram has been constructed (Figure 5.7). The inferred 'reservoir' equilibration temperatures have been estimated by assuming quartz saturation controls the silica content of sampled fluids. The quartz 'no steam' loss geothermometer was used to calculate temperatures for the springs and quartz maximum stream loss was used to calculate the temperatures for well waters.

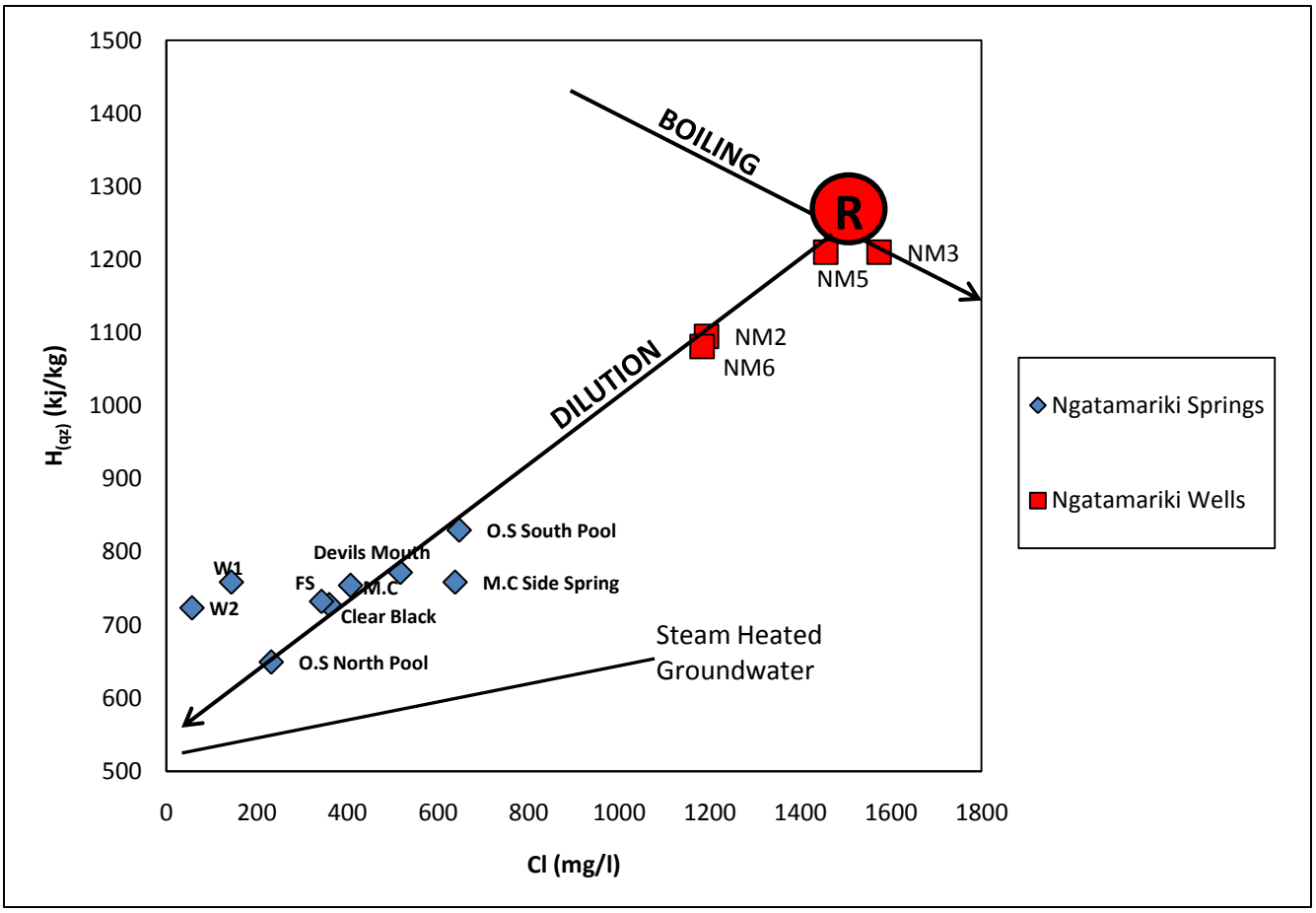

Figure 5.7: Enthalpy – chloride mixing diagram for 'reservoir' compositions of springs and wells. The red circle with the 'R' in the middle represents the inferred reservoir fluid (H = ~1300, Cl =1500).

An obvious dilution trend is seen between the inferred reservoir fluid and the spring chemistry. This suggests there is mixing with a cooler diluent with a temperature of around 140-145 ^{o}C (likely a steam heated groundwater). This is the same as the temperature of the diluent described by Brotheridge (1995) for Ngatamariki and is similar to that described at Waiotapu which has a dilutent of 160 ^{o}C (Hedenquist & Browne 1989). The maximum well temperature calculated from the silica no steam loss geothermometers is 275 ^{o}C in both NM3 and NM5 (Table 5.1) and chloride concentrations range from 1200 – 1500 mg/l. This is quite similar to the Broadlands – Ohaaki field (1000 – 1200 mg/l) but lower than the Mokai and Wairakei Fields (maximum 2000 mg/l at 300 ^{o}C) (Brotheridge 1995).

5.2.4 Stable Isotopic Compositions

Stable Isotopic analysis of ^{18}O and D in geothermal waters can help to determine the origin of fluids in a geothermal system and the interactions that occur as the fluids rise towards the surface. The results from stable isotopic analysis of Ngatamariki spring and well waters at the University of Canterbury are plotted below (Figure 5.8).

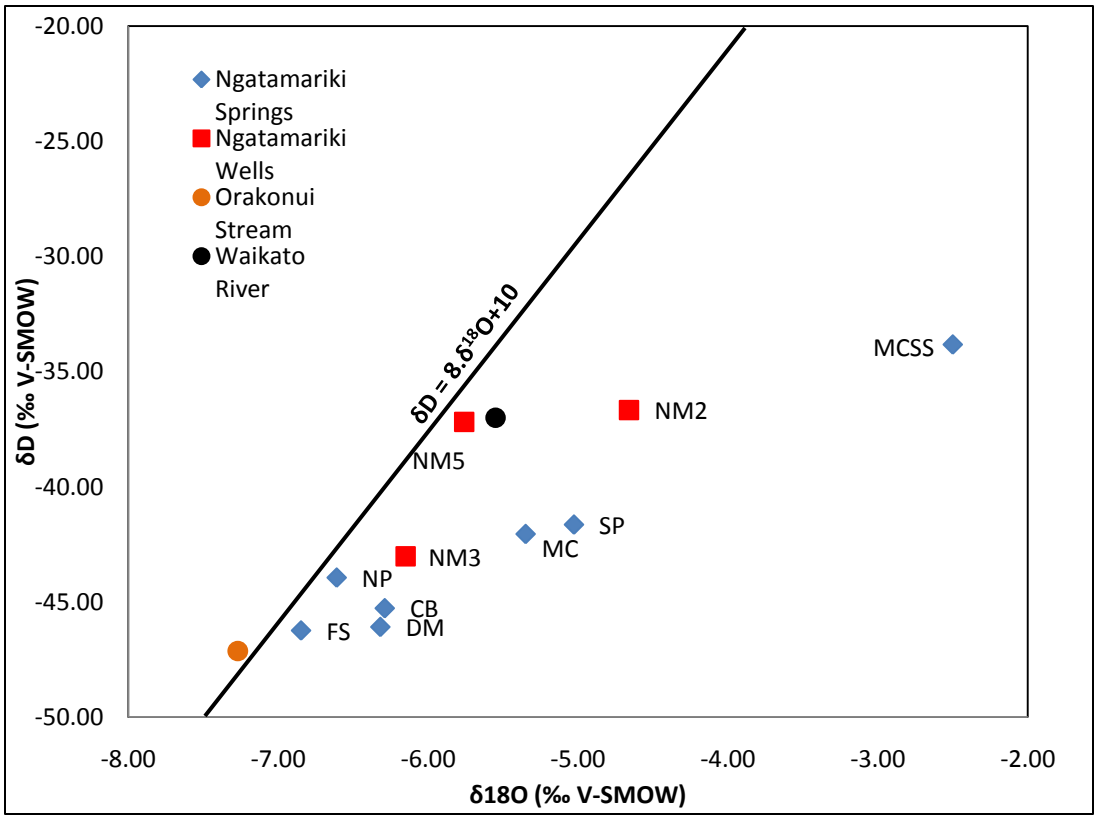

Figure 5.8: $\delta^{18}O$ vs δD for waters at Ngatamariki.

The springs and wells show a positive linear tend from the local meteoric water source which is the Orakonui Stream. This suggests that there is mixing with a different fluid at depth, causing a change in the isotopic composition of water between the surface and at depth ($\delta^{18}O$ = -5.6, δD = -41 at depth; $\delta^{18}O$ = -6.1, δD = -44 at the surface). It also suggests there may be interaction with silicate minerals from hydrothermally altered rocks causing this shift in composition. The Waikato River sample represents local cold water in the area.

5.2.5 XRD analysis

XRD analysis was carried out on hydrothermally altered material from the April 2005 eruption at Orakonui South. Two samples were taken, one less altered (Orakonui South unaltered – OSU) and one considered to be heavily altered (Orakonui South altered – OSA).

Sample	Minerals Present (%)	Molecular Composition
OSU	Quartz (20) Montmorillonite (5) Mordenite (40) Jarosite (35)	SiO_2 $(Na,Ca)_{0.33}(Al,Mg)_2(Si_4O_{10})(OH)_2{\cdot}nH_2O$ $(Ca,Na_2,K_2)Al_2Si_{10}O_{24}{\cdot}7H_2O$ $KFe^{(III)}_3(OH)_6(SO_4)_2$
OSA	Quartz (20) Montmorillonite (20) Mordenite (60)	SiO_2 $(Na,Ca)_{0.33}(Al,Mg)_2(Si_4O_{10})(OH)_2{\cdot}nH_2O$ $(Ca,Na_2,K_2)Al_2Si_{10}O_{24}{\cdot}7H_2O$

Table 4.2: XRD results from hydrothermally altered material at Ngatamariki. Diffraction patterns for both samples are located in Appendix H.

The dominant mineral in both samples is mordenite which is a zeolite commonly found in volcanic deposits. Both samples also contain 20 % quartz and montmorillonite a clay formed by hydrothermal alteration. The OSU sample also contains jarosite which forms due to the oxidation of iron sulphides.

Chapter 6: Geochemistry at Orakei Korako

This section summarises results from chemical and isotopic analysis of the Orakei Korako spring waters from this study and well waters from prior studies. Methods of collection and analysis are located in chapter 5; a full list of results is located in appendix F and locations of samples from previous studies are located in appendix I.

6.1 Geochemistry of Spring and Well Waters

6.1.1 Major Ion Concentrations

Fluid compositions in springs at the Tourist Area and Red Hill/West Bank areas show high chloride, sodium, silica and bicarbonate concentrations. The chloride concentrations at Orakei Korako are lower than that of geothermal waters at Wairakei, Broadlands and Waiotapu, but similar to those seen at Mokai, Ngatamariki and Waikite (Brotheridge 1995). All springs at Orakei Korako have a near neutral pH and are located in a long stretch alongside the Waikato River/Lake Ohakuri.

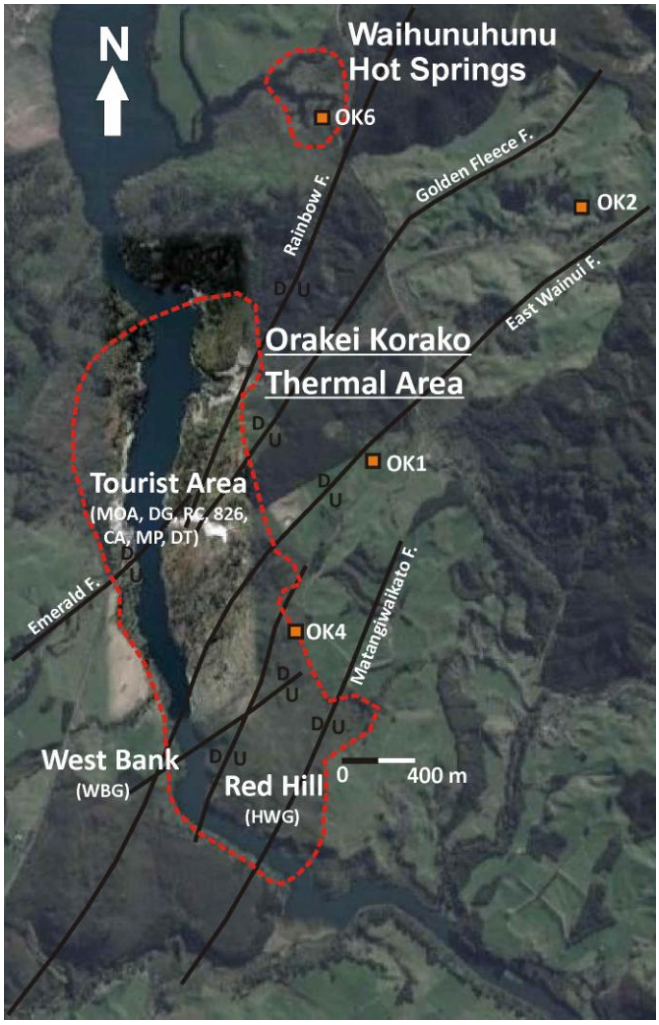

Figure 6.1: Location of springs sampled during this study and wells sampled by Mahon (1964). (MOA = Map of Australia, DG = Diamond Geyser, RC = Ruatapu Cave, 826 = Artists Palette Spring 826, CA = The Cauldron, MP = Manganese Pool, DT = Devils Throat, WBG = West Bank Geyser, HWG = Hot Waterfall Geyser). For more detailed descriptions of the sampling sites see sections 4.2 and 4.3 (Satellite image sourced from Google Earth, 2009).

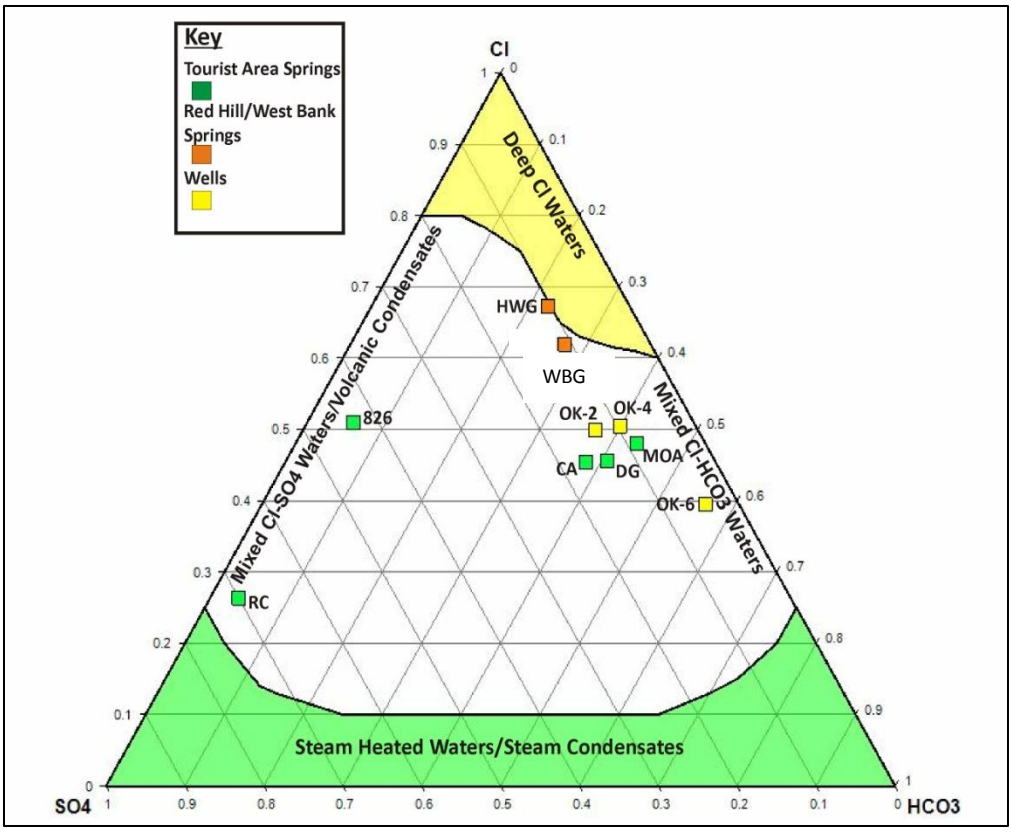

Figure 6.2: Cl-HCO_3-SO_4 ternary plot of spring and well waters in the Orakei Korako area.

Spring waters at the tourist area are diluted chloride-bicarbonate waters with low sulphate concentrations (Figure 6.2). The exceptions are Ruatapu Cave and Artists Palette spring 826, which both plot as volcanic condensates. This is expected because of the nature of Ruatapu cave with a pH of 2.5 and being in a cave. Spring 826 is however located on the Artists Palette amongst other typical alkali-chloride springs which suggests a connection with the Ruatapu Cave waters (Figure 6.2). Chloride contents of these waters range from 333 mg/l in the Map of Australia to 147 mg/l in Ruatapu Cave, which is generally lower than Ngatamariki.

Spring waters at Red Hill and West Bank show the least amount of dilution of any of the springs sampled in this study, suggesting that they are not interacting as much with local groundwater and have a direct conduit to the surface. Chloride contents in these waters are between 300 and 350 mg/l which are lower than springs at Ngatamariki.

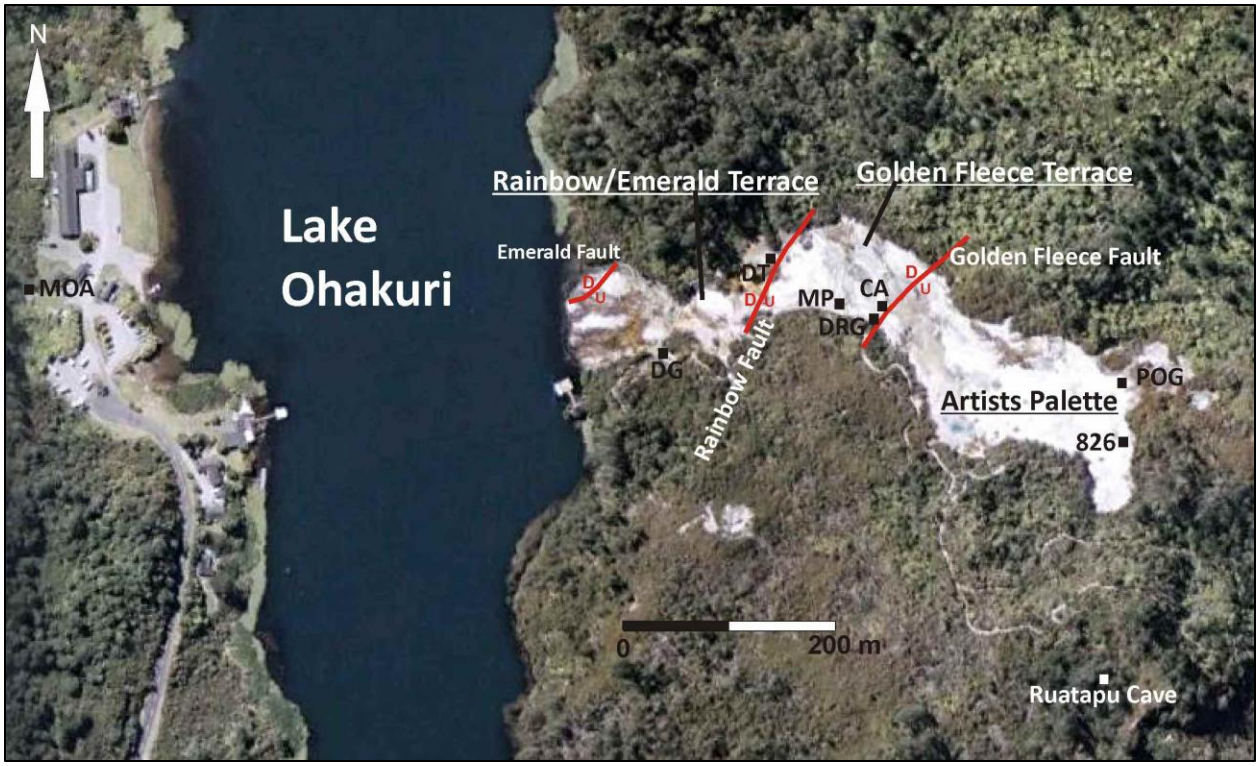

Figure 6.3: Locations of sampling sites at the Tourist Area, Orakei Korako (Satellite Image sourced from Google Earth, 2009).

Well waters at Orakei Korako are diluted chloride-bicarbonate waters which is anomalous in terms of geothermal systems in TVZ. The highest chloride concentrations (546 mg/l) are seen in well OK2 which is very small when compared with the Ngatamariki wells which all have chloride concentrations above 1100 mg/l.

TDS has a positive correlation with chloride in waters at Orakei Korako; but unlike Ngatamariki there are no distinct groups where different concentrations of TDS and chloride are able to distinguish between different water types in the field (figure 6.4). This suggests that local groundwater and thermal waters are mixed at depth.

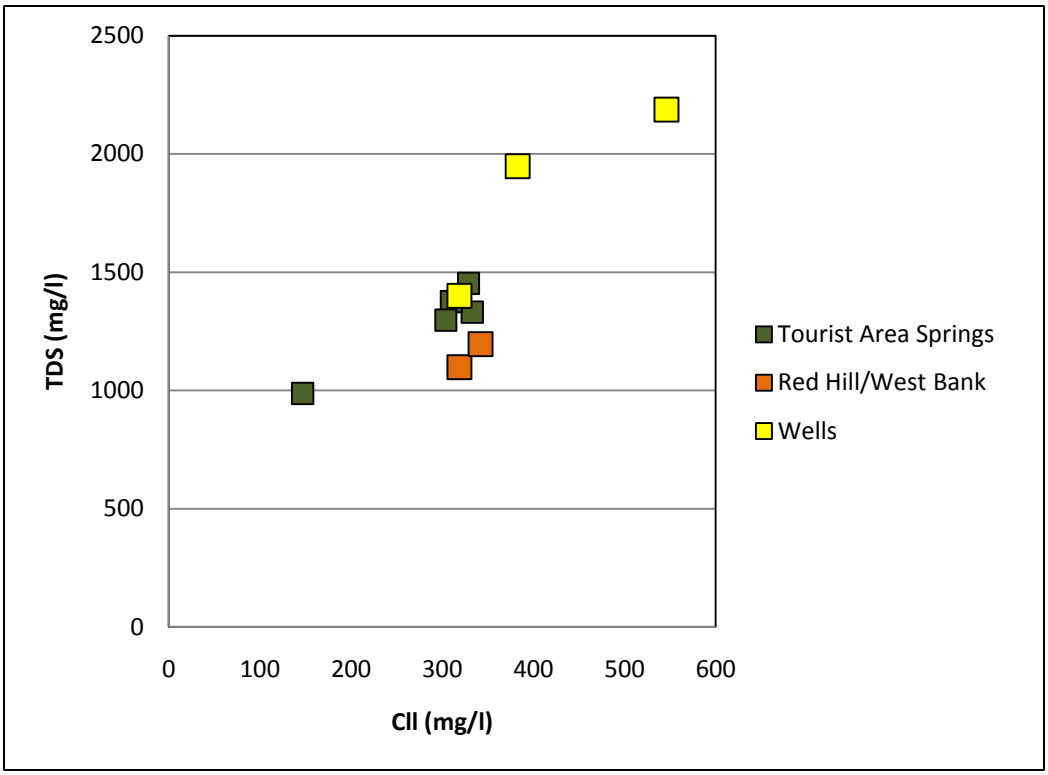

Figure 6.4: TDS vs chloride for well and spring waters at Orakei Korako.

Cl/B ratios for the Orakei Korako waters show a weakly positive relationship suggesting that there may be a common source for the field. Cl/HCO_3 ratios show a very weak relationship but they are not strong enough to suggest that there is no contamination from waters outside of the geothermal system (Figure 6.5). Cl/F ratios at Orakei Korako show no relationship unlike the waters at Ngatamariki which show strong positive relationships for the Cl/B and C/F ratios.

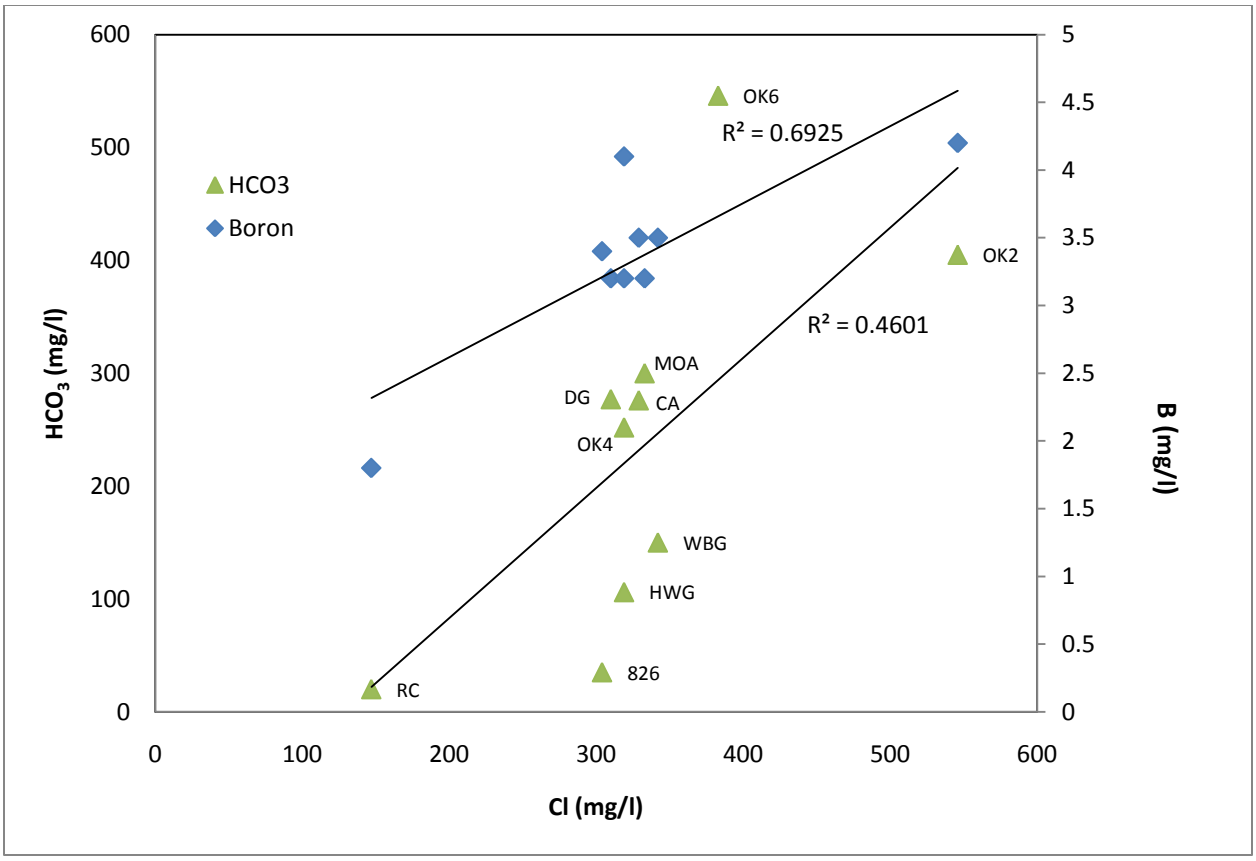

Figure 6.5: Cl/B and Cl/HCO_3 ratios for waters at Orakei Korako.

The Cl-Li-B ternary plot (Figure 6.6) for waters at Orakei Korako shows that well and spring waters are closely related forming a group between about 50 % relative lithium and chloride. The waters are relatively very low in boron (~10 %). This suggests that the thermal system at Orakei Korako is mixed at depth as the chemistry of surface features and wells is very similar.

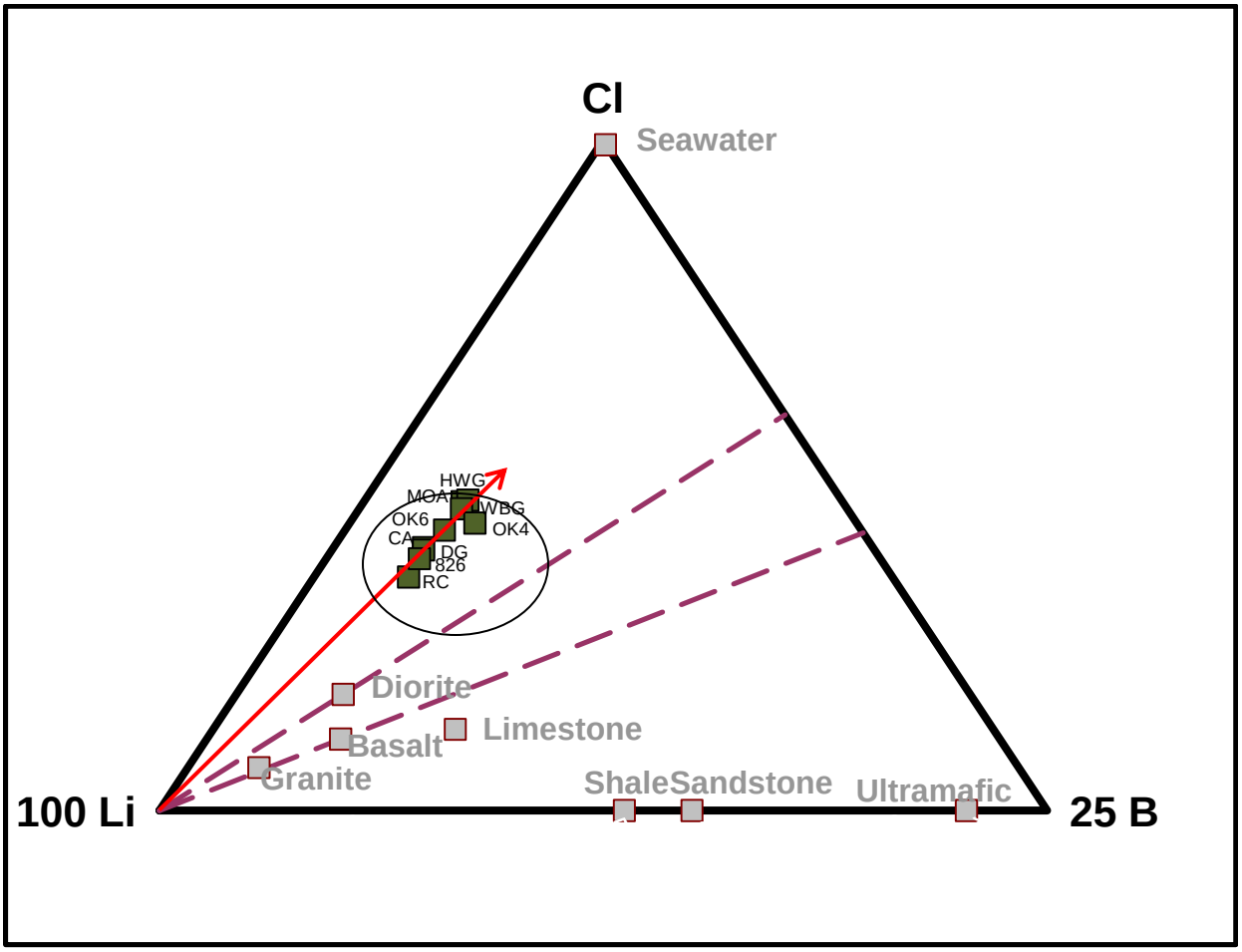

Figure 6.6: Cl-Li-B ternary plot of waters at Orakei Korako. Well and spring waters are represented by green squares.

6.1.2 Solute Geothermometers

Results from the Na-K-Ca (mg corrected) geothermometer for Orakei Korako wells are ignored because the waters were not analysed for magnesium (Table 6.1). Results from the Na-K-Ca geothermometer correlate well with the estimated reservoir temperature for OK2 of 225 ^{o}C (Sheppard & Lyon 1984) at 233 ^{o}C. Good correlations are also seen with OK4 and OK6 which had interpreted reservoir temperatures of 234 and 214 ^{o}C (Sheppard & Lyon 1984) respectively and Na-K-Ca results of 229 and 223 ^{o}C respectively. These temperatures are low compared with other geothermal systems in TVZ and lower than those seen at Ngatamariki.

Feature	Chalcedony	Quartz no steam loss	Quartz max steam loss	Na-K-Ca	Na-K-Ca Mg corr
Map of Australia	183	202	185	194	194
Diamond Geyser	197	214	195	231	231
The Cauldron	199	216	196	248	248
Ruatapu Cave	181	200	183	54	54
Artists Palette (Spring 826)	204	220	199	251	251
Hot Waterfall Geyser	186	204	187	231	230
West Bank Geyser	193	210	192	164	164
OK2	241	253	223	233	233
OK4	224	237	212	229	229
OK6	241	253	223	223	223

Table 6.1: Geothermometer results for waters at Orakei Korako. Temperatures are in ^{o}C.

Na-K-Mg Diagram

The Orakei Korako well waters cannot be plotted on the Na-K-Mg Diagram because they were not analysed for magnesium by Mahon (1964). The majority of the Orakei Korako area springs fall into the area of partial equilibration on the diagram suggesting re-equilibration by dilution or mixing between 170 and 280 ^{o}C (Figure 6.7). The exceptions are the Map of Australia (MOA) and Hot Waterfall Geyser (HWG) samples that plot close to the full equilibrium line. The broad range in reservoir temperatures for springs in the field may correspond to deep mixing processes in some parts of the field being more prevalent than in others, where fluids may rise directly from depth to the surface. Ruatapu Cave is the obvious exception to the rest of the springs because the waters are acid-sulphate cave waters, plotting in the far right of the diagram, suggesting that it is independent from the rest of the field.

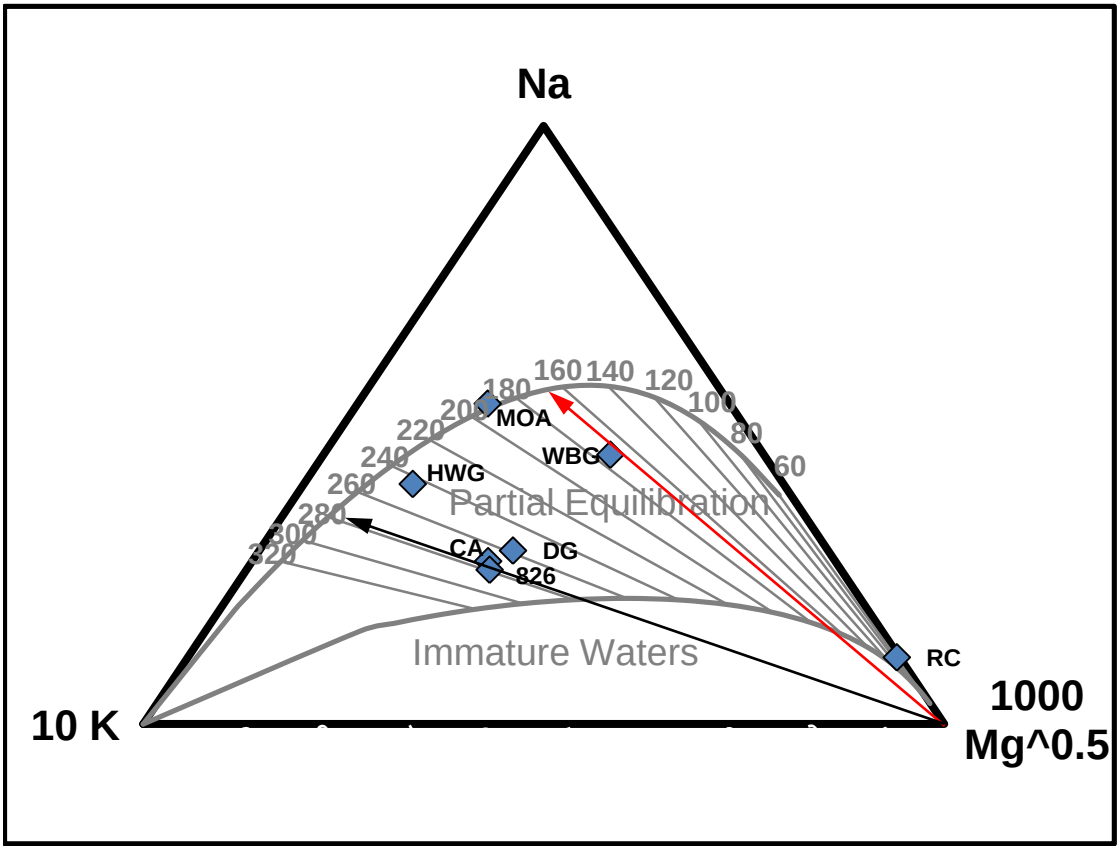

Figure 6.7: Na-K-Mg geothermometer for spring water samples from Orakei Korako. The two arrows outline the approximate range of re-equilibration temperatures for springs in the area. (After Giggenbach (1988))

6.1.3 Dilution Trends

The same parameters used in section 5.2.3 were used in the construction of the enthalpy – chloride diagram (Figure 6.8). An obvious mixing and dilution trend with a 'hot water' diluent is seen from the inferred reservoir chemistry and well and spring chemistry. The diagram suggests that mixing is occurring at depth between reservoir fluids and a diluent with a temperature of around 164 ^{o}C. This temperature is much higher than the previous estimated temperature of 105 ^{o}C (Sheppard & Lyon 1984) and similar to the diluent of 160 ^{o}C described at Waiotapu (Hedenquist & Browne 1989).

The maximum well temperature calculated from the quartz maximum steam loss geothermometer is 223 ^{o}C in both OK2 and OK6 with chloride concentrations ranging from 546 mg/l (OK2) to 319 mg/l (OK4). This is lower than any other studied geothermal fields in TVZ all of which have higher temperatures and chloride concentrations.

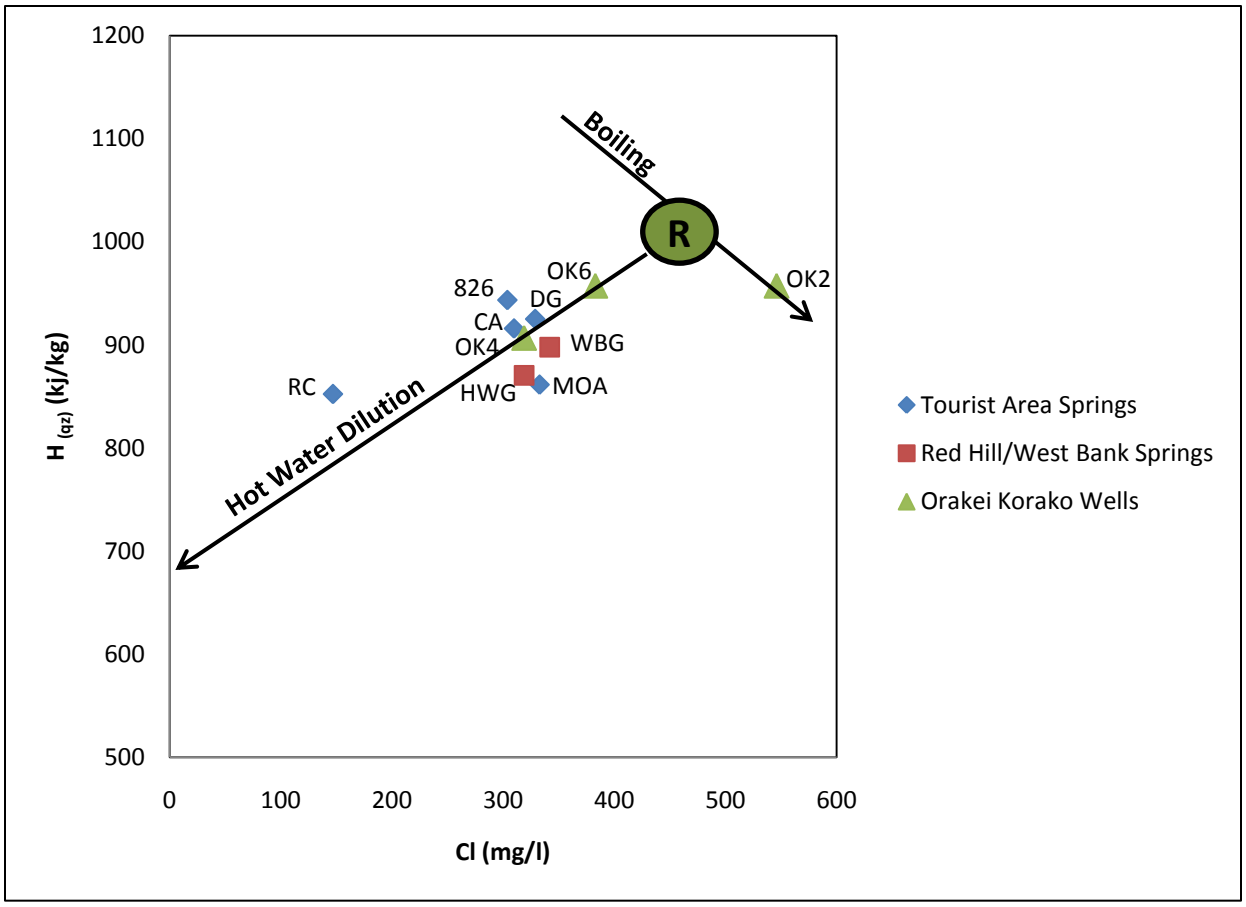

Figure 6.8: Enthalpy – chloride diagram for "reservoir' compositions of springs and wells at Orakei Korako. The green circle with the 'R' represents the inferred reservoir fluid (H = ~ 1000 kj/kg, Cl = 450 mg/l).

The enthalpy of all the samples varies around the dilution trend suggesting that some have more interaction with the diluent than others.

6.1.4 Stable Isotopic Compositions

Results from analysis of Tourist area and Red Hill/West Bank Springs are plotted in figure 6.9 below.

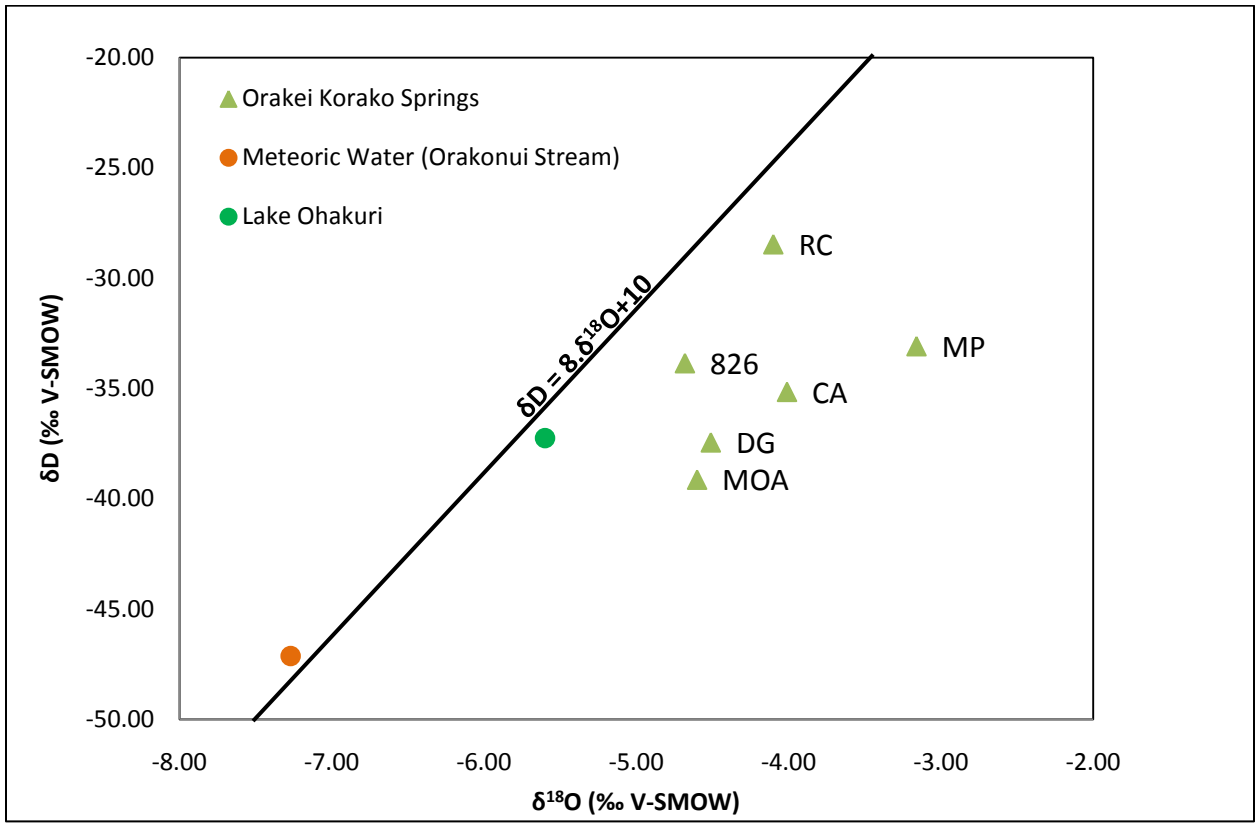

Figure 6.9: δD vs $\delta^{18}O$ graph for spring waters at Orakei Korako.

The springs show a reasonably positive linear trend from the meteoric water sample (Orakonui Stream) and the GMWL. This suggests there is mixing with local waters and a different fluid at depth causing samples to become enriched in ^{18}O and D. This may also be due to interaction with silicate minerals in the reservoir causing a positive shift in ^{18}O in the springs at the surface. Isotopic compositions of spring waters range from $\delta^{18}O$ = -4.6, δD = -39 (MOA) to $\delta^{18}O$ = -4.1, δD = -28 (RC).

Chapter 7: Discussion

7.1 Hydrogeochemistry at Ngatamariki and Orakei Korako

The following section describes the hydrology at Ngatamariki and Orakei Korako using geochemical constraints, along with interpreted subsurface geology and hydrology. Each area is discussed separately before a comparison is made between them in section 7.2.

7.1.1 Hydrogeochemistry of the Ngatamariki Geothermal Field

The direction of fluid flow at Ngatamariki has been outlined in several other studies (Hedenquist 1986; Brotheridge 1995; Urzua 2008) and in the past year (2009) the subsurface geology has become constrained from the drilling of wells NM5, 6 and 7. This section uses ratios of common ions, stable isotopes and measured flow from wells to describe the hydrology within the reservoir at Ngatamariki and the interactions that occur with the subsurface geology.

The ratio of HCO_3/SO_4 is used as an indicator of flow direction in geothermal fluids (see section 2.2.3). As fluids flow away from the reservoir they have more chance to interact with reservoir rocks increasing HCO_3 and decreasing H_2S. This creates an increase in the HCO_3/SO_4 ratio as fluids move away from the upflow zone.

Figure 7.1 shows the HCO_3/SO_4 ratios for the spring and well waters at Ngatamariki. There is a clear trend, with ratios increasing away from well NM3 and the springs located on the margins of the field showing the highest ratios. This means that the major upflow of hot fluids is located below NM3 and travels both north-west (Orakonui Stream springs and NM2) and south-east (NM5 and NM6) from NM3 towards Rotokawa.

The fluid flow is controlled by the host lithologies and zones of clay alteration which create aquitards and causes the lateral flow of the hot reservoir fluids (Urzua 2008; Bignall 2009).

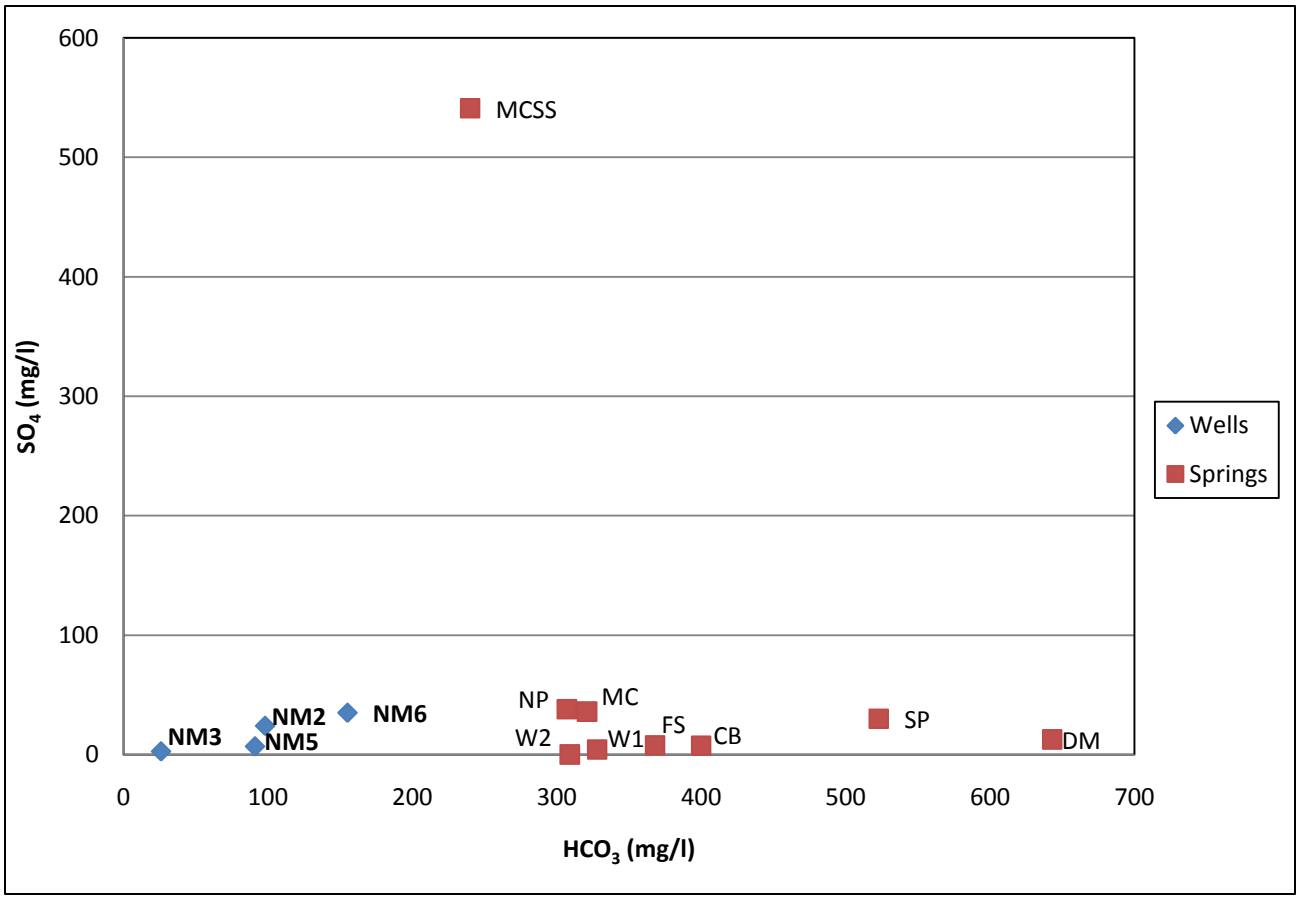

Figure 7.1: HCO_3/SO_4 ratios for well and spring waters at Ngatamariki.

The relationship between TDS and chloride (Figure 5.3), and bicarbonate and sulphate suggest that the spring, well and groundwater are derived from the same source (meteoric water), but are confined to different parts of the reservoir. The well waters represent the main reservoir, with the highest chloride and TDS content and high interpreted reservoir temperatures of around 295 ^{o}C (Table 5.1). Spring waters exhibit medium chloride and TDS content and have interpreted reservoir temperatures of between 160 – 180 ^{o}C (Table 5.1). Local meteoric waters and ground water exhibit very low TDS and chloride contents and have measured temperatures of around 17 ^{o}C at the surface (Orakonui Stream 2009, Appendix B).

From this it can be assumed that there are three separate aquifers at Ngatamariki:

1. The main reservoir where deep circulating geothermal fluids with high temperatures, chloride and TDS contents occur.
2. An 'Intermediate' aquifer where fluids derived from the main reservoir interact with a steam heated low chloride water, diluting the fluid and lowering the reservoir temperature to ~ 180 ^{o}C
3. A local groundwater 'shallow' aquifer containing local meteoric waters with low temperatures and low TDS and chloride concentrations.

Figure 7.2 shows the Ngatamariki conceptual (hydrological) model inferred from geophysical, geochemical and geological measurements taken during drilling and continued monitoring. The chemical data from this study supports the flow directions in the diagram with the relative north-west and south-east trends away from the main source (inferred to be below NM3).

The model shows that clays create a 'cap' on top of the main reservoir restricting it to > 900 m below the surface, also restricting the flow of fluids to the surface.

This in turn creates an 'intermediate aquifer' where fluids are confined between 200 – 500 m below the surface and flow laterally, interacting with steam heated low chloride, meteoric waters infiltrating from the outside of the field. Water flows across the top of the main reservoir beneath another clay cap about 200 m below the surface. Fluids from the intermediate aquifer re-equilibrate to a reservoir temperature of around 180 ^{o}C with the surrounding host rocks before travelling to the surface by lateral flow or using fault structures as conduits. This explains why the majority of the Ngatamariki springs are plotted in the 'partial equilibrium' area of the Na-K-Mg geothermometer diagram (Figure 5.6).

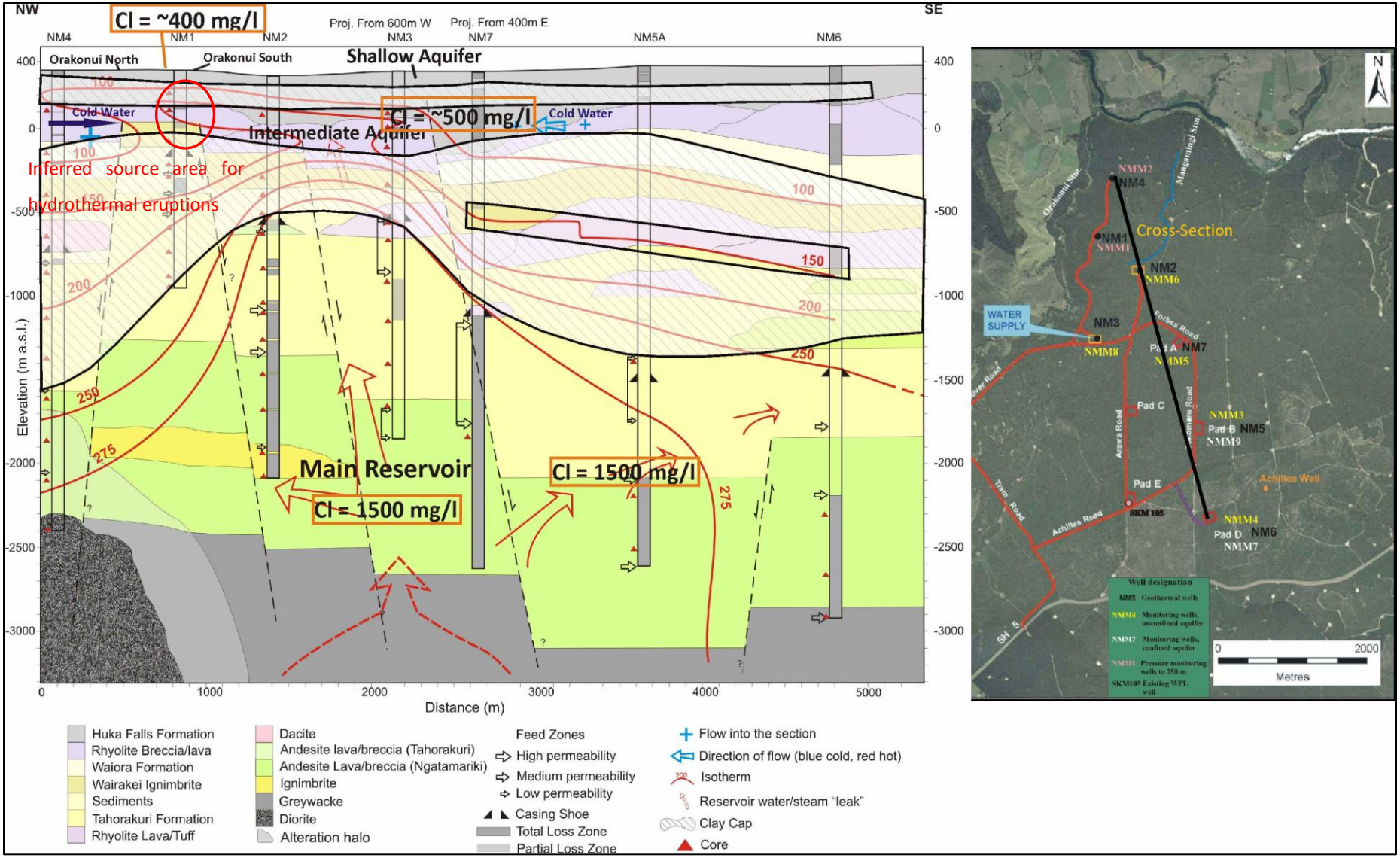

Figure 7.2: Conceptual hydrological model for the Ngatamariki geothermal system (courtesy of Mighty River Power). The model outlines the 3 different aquifers within the system and how the mixing with steam heated groundwater (two phase flow) in the intermediate aquifer causes chloride contents to drop before reaching the surface. The map to the right shows the line of section (Rae et al. 2009).

Above the upper clay cap (< 50 m below the surface) there is a meteoric water aquifer or 'shallow aquifer'. This aquifer appears to act completely independently of the rest of the field and represents groundwater in the area. Temperatures in this aquifer range from 20 – 60 ^{o}C (Bignall 2009) and the chemistry in surface waters (Orakonui Stream) is the same as the sub surface (monitoring wells) waters. This is reflected in the TDS vs chloride diagram (Figure 5.3).

It appears that the geothermal plume at Ngatamariki migrates south-east at depth towards Rotokawa and north-west near the surface towards Orakei Korako.

7.1.2 Hydrothermal Eruption Mechanisms at Orakonui South

Results from XRD analysis carried out on material erupted in the April 2005 eruption suggest that montmorillonite is the dominant form of hydrothermal alteration (Table 5.2). Using logs of clay alteration from NM1 and NM4 (wells in closest proximity to Orakonui South) the source depth of the material erupted can be inferred (Appendix A). Montmorillonite alteration occurs from 431-800 m below the surface in NM1 and from surface level to 1000 m below the surface in NM4 (Wood 1985, 1986). Orakonui South is closest to NM1 so it can be inferred that the source for the erupted materials is between 431 and 800 m below the surface, suggesting that the material is sourced from either the Wairakei Ignimbrite or rhyolite lavas/breccias (Figure 7.2). In this area a large fault is inferred by the geological model to account for the displacement of the reservoir lithologies between wells. Deep fluids may use this fault as a permeable conduit to rise towards the surface and pond (~ 300-350 m below the surface) above the clay cap before moving to the surface. A mix of perched lower temperature water and gas at this level subject to sudden pulses of hot reservoir fluids could trigger an eruption. However it is thought that low barometric pressures trigger hydrothermal eruptions (T.Powell pers comm, December 4, 2009); so in the case of the Main Crater at Ngatamariki it could be that perched fluids at depth within the intermediate aquifer subject to low barometric pressures allows the fluids to escape at a faster rate creating an

eruption at the surface that contains clasts from depth. However it must be considered that montmorillonite alteration may occur nearer to the surface at Orakonui South in different lithologies. In this case it is more likely that the source of the clasts is rhyolite closer to the surface. Without thin section analysis, the origin of the samples cannot be confirmed and samples collected in this study were unable to be prepared for thin section analysis due to their friable nature and small size.

7.1.3 Hydrogeochemistry at Orakei Korako

The hydrology of the Orakei Korako geothermal area has been discussed in several previous studies (Lloyd 1972; Sheppard & Lyon 1984; Leaver & Unsworth 2007) using water chemistry and subsurface geology of wells. This section uses the information from these studies and chemistry from the present study to describe the hydrology of the Orakei Korako field and the interactions occurring within it.

As mentioned in section 7.1.1 the HCO_3/SO_4 ratio is an indicator of flow direction. Thermal waters at Orakei Korako appear to be sourced from a deep reservoir and travel north towards the Waihunuhunu Springs and south away from the main source towards the Red Hill/West Banks area (Figure 7.3). The obvious exceptions are the Ruatapu Cave and 826 samples which are very rich in sulphate suggesting they are probably not connected to the major flow directions in the rest of the field.

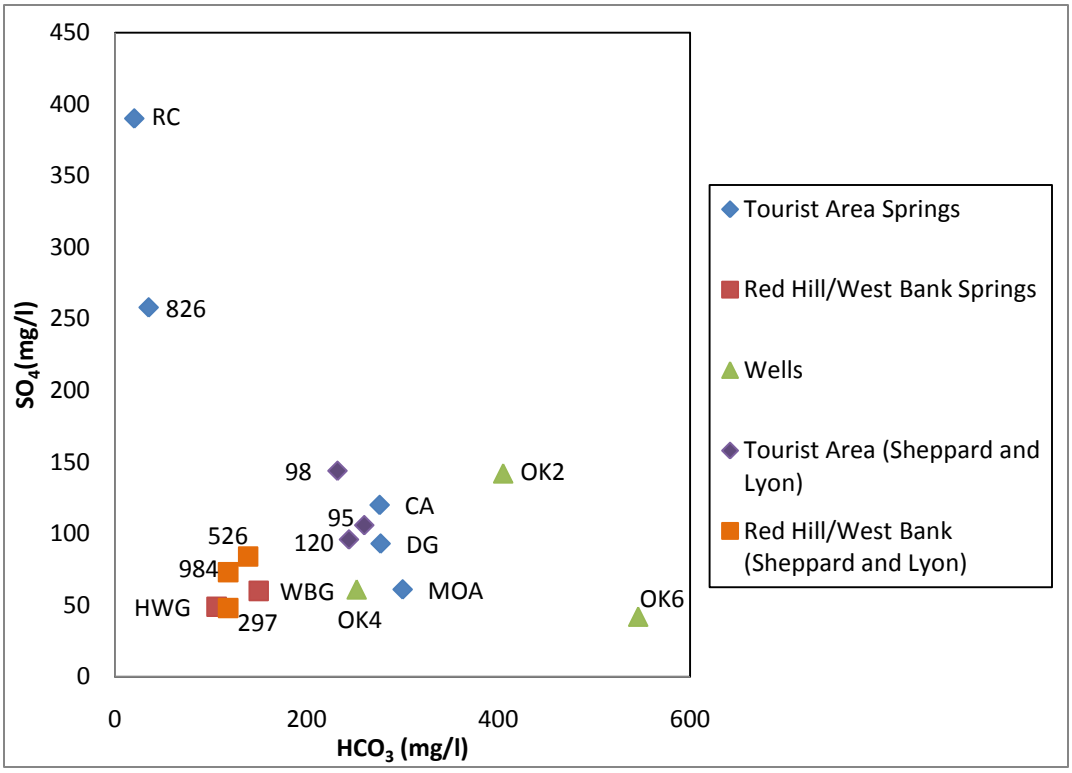

Figure 7.3: HCO_3/SO_4 ratios for spring and well waters at Orakei Korako.

The combination of the relationships between TDS and chloride (Figure 6.4) and bicarbonate and sulphate suggest that the waters at Orakei Korako are all derived from local meteoric waters. Hot geothermal waters appear to mix with colder meteoric waters at depth and create a very similar fluid chemistry at depth. This is clearly portrayed in the enthalpy-chloride diagram (Figure 6.8) where a trend suggesting dilution of deep fluids with a 'hot water' is evident. The hot meteoric waters ('hot waters', 164 ^{o}C) mix with deeper reservoir fluids at depth causing the chemistry of both water types to become very similar, as the waters supplying both the springs and the wells re-equilibrate at depth together before being discharged at the surface. Interpreted reservoir temperatures from the Na-K-Ca geothermometer (Table 6.1) for wells at Orakei Korako are ~230 ^{o}C with temperatures between 223-233 ^{o}C. Inferred reservoir temperatures for springs are ~220 ^{o}C with temperatures ranging from 164 to 248 ^{o}C. This suggests reservoir fluids are diluted by 'hot water' and this is supported by the Na-K-Mg diagram (Figure 6.7) which shows the majority of the spring waters are in partial equilibrium at Orakei Korako. This could be attributed to deep thermal waters being diluted by the cooler waters at depth, causing them to be unable to re-equilibrate before reaching the surface. A large range of temperatures is seen in the diagram which suggests that different springs are sourced from different places in the reservoir where differing intensities of dilution occur.

In the conceptual model of hydrology at Orakei Korako (Figure 7.4) it appears that fluid flow at depth is controlled by the infiltration of the colder fluids into the reservoir at depth. This creates two main plumes that reach the surface to the north close to OK6 and the Waihunuhunu Springs and to the south, nearing the surface close to OK1, and the tourist area reaching the surface near OK4 and the Red Hill/West Bank area. It appears that normal faults which concentrate the locations of spring features at the surface may control the flow of the fluids from depth and the locations of the geothermal plumes at Orakei Korako.

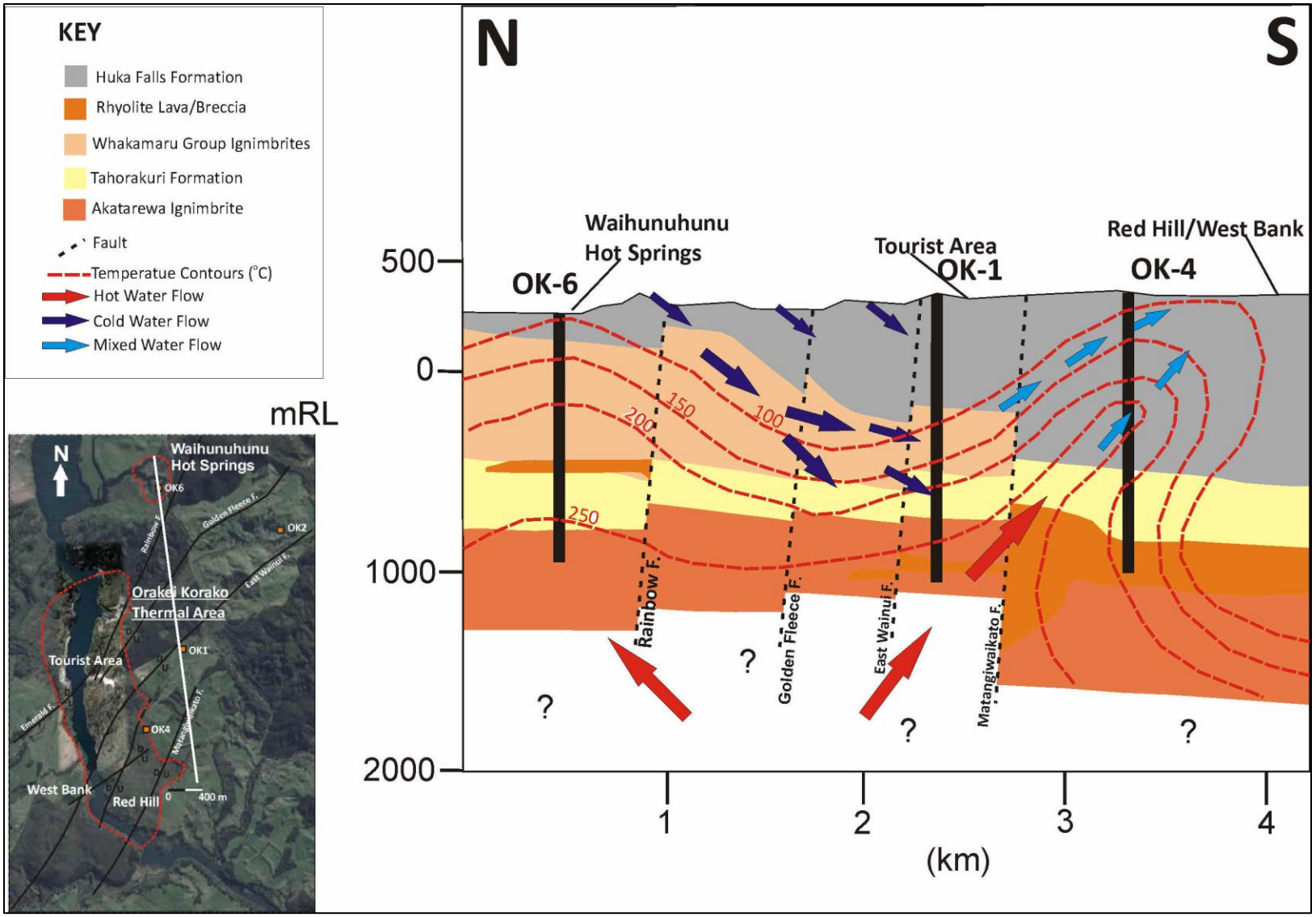

Figure 7.4: Conceptual hydrological model for the Orakei Korako geothermal field. The line of section is indicated by the white line in the map to the left. The model shows the dilution of the geothermal fluids by colder waters at depth creating a 'mixed' geothermal water indicated by the spring and well chemistry in the area. Whakamaru group ignimbrites represent the Te Kopia and Paeroa Ignimbrites (Adapted from Sheppard and Lyon, 1984 and Bignall, 2009). (OK2 is ignored because of its distance from the line of section).

Stable isotopic results suggest that there may be interaction with either altered host rock in the reservoir or mixing with a magmatic fluid at depth. A positive linear trend is seen between the springs and the local cold waters (Waikato River and Lake Ohakuri) (Figure 6.9). Interaction with either altered host rocks, magmatic fluids at depth or evaporation could explain the positive shift of the spring's samples relative to local cold water.

Hamlin (1999) modelled the near surface processes controlling fluid flow at Orakei Korako and reported that springs and mud pots are fed by their own independent conduits. Although most waters appear to be ascending along the local normal faults from depth, nearer to the surface, it appears that overlapping hydrothermal alteration haloes formed by the alteration of country rock by hot fluids create separate conduits for the ascending fluids (Figure 7.5).

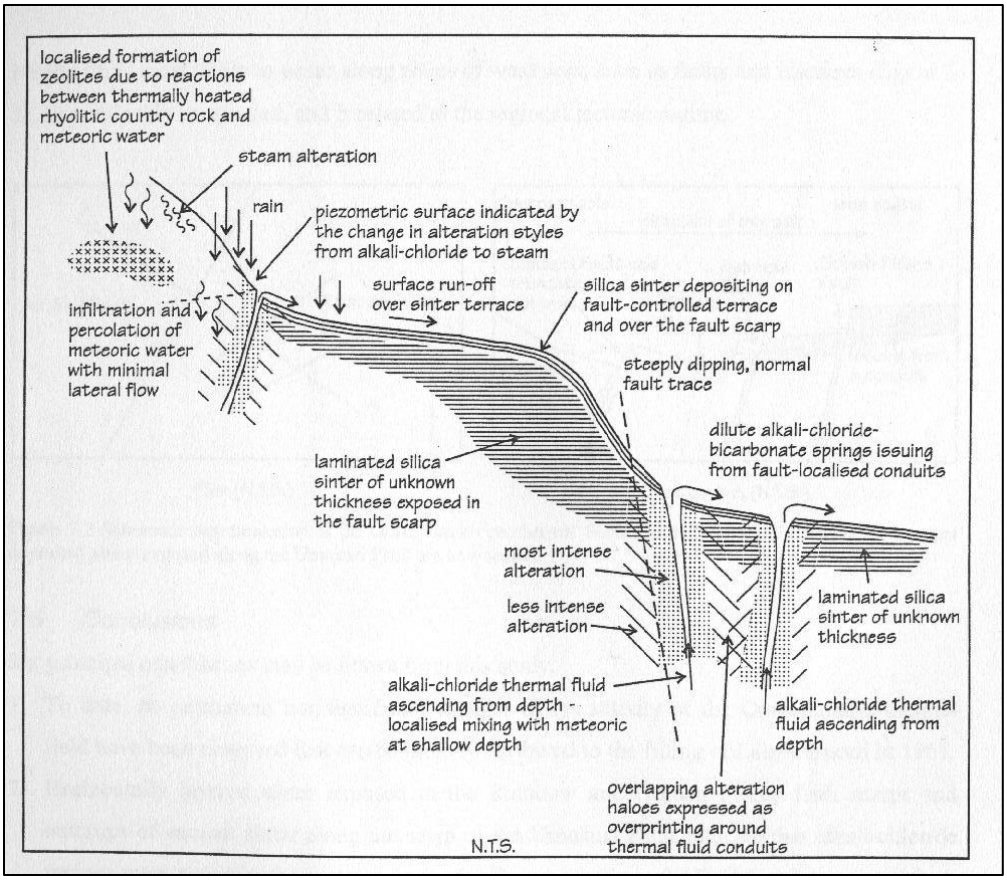

Figure 7.5: Schematic model of alteration and related hydrological processes at Orakei Korako (Hamlin 1999).

It also appears that meteoric waters percolate down fault zones with minimal lateral flow, at times maybe deep enough to be heated by the surrounding reservoir rock. This may account for the 164 ^{o}C dilutent that appears to be interacting with reservoir waters at depth.

Hamlin (1999) also suggests that the focus of geothermal activity at Orakei Korako is migrating eastward. This is supported by the lack of volatile features and distribution of thermally stressed vegetation in the western part of the field and the north-east orientation of the magnetic anomaly for the field (Soengkono 1993). Migration is most likely to occur along faults and fractures which act as zones of weakness related to the tectonic regime active in the area (Figure 7.6). The conduits of alkali-chloride springs which once deposited sinter in the western part of the field are now inactive.

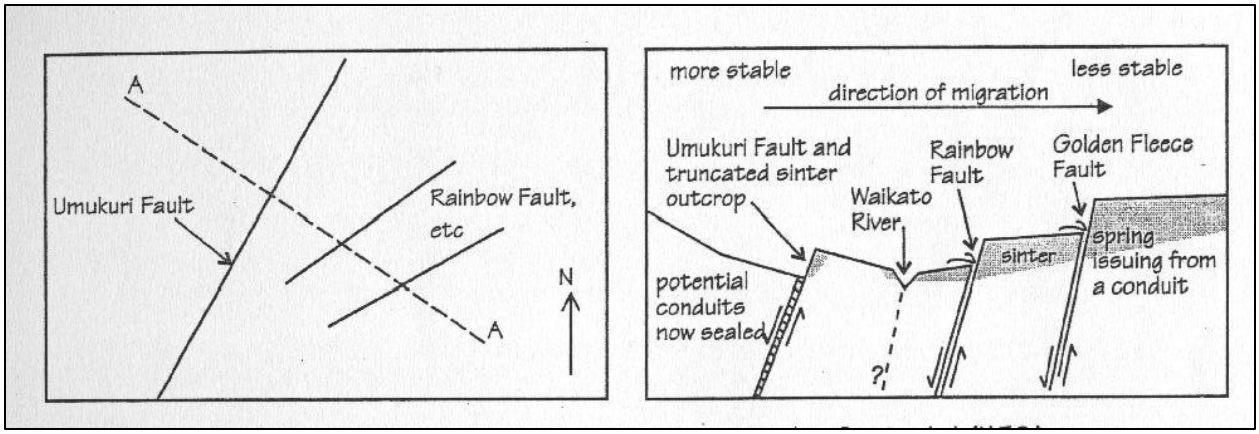

Figure 7.6: Schematic representation of the Orakei Korako geothermal field showing the eastward migration of the focus of geothermal activity (Hamlin 1999).

7.2 Hydrogeochemical model for the Ngatamariki – Orakei Korako Area

7.2.1 Geochemical Relationships

The geochemistry of each field has been described in chapters 5, 6 and 7.1. This section makes comparisons between the two to distinguish any similarities or differences.

Major ion chemistry can tell us a lot about the relationship between the two areas without having to use more advanced chemical relationships. The Cl-HCO_3-SO_4 ternary diagram (Figure 7.7) indicates that the composition of the waters from springs in both fields are slightly different, but the well water compositions are distinctly different. Spring waters at the Tourist Area and Red Hill/West Bank have higher sulphate concentrations than the springs at Ngatamariki, with the Red Hill/West Bank springs having the highest chloride concentrations.

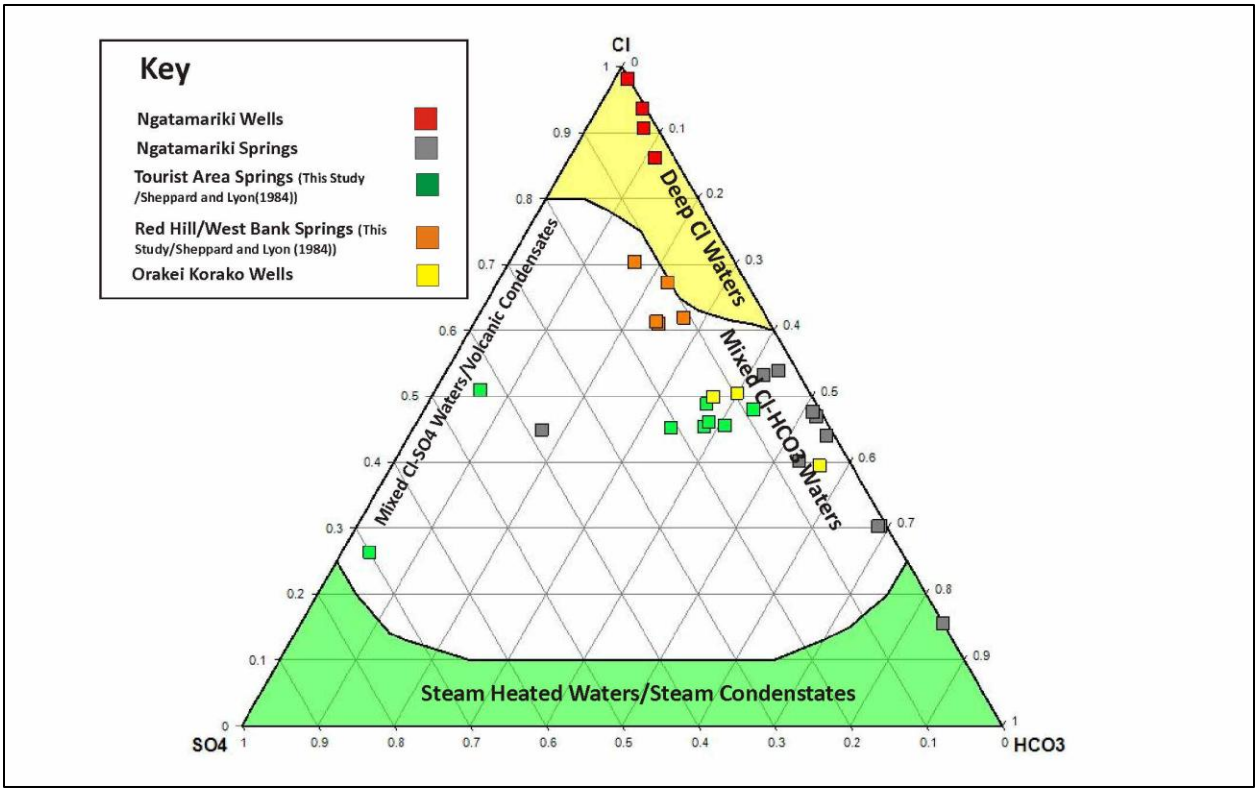

Figure7.7: Cl-HCO_3-SO_4 ternary plot for spring and well waters at Ngatamariki and Orakei Korako.

The high chloride content of the Red Hill/West Bank springs suggests a more direct pathway to the surface from depth compared to Ngatamariki and Tourist Area Springs. This, together with well chemistry, confirms the processes indicated in the conceptual hydrological models for both areas. The Orakei Korako wells exhibit a mixed chloride-bicarbonate signature suggesting mixing of the geothermal fluids with colder local meteoric waters at depth, which is anomalous in TVZ, while the Ngatamariki wells exhibit the typical deep chloride type water seen in other geothermal systems in the TVZ.

Although there are some similarities in the chemistry of the waters reflecting that the areas have similar host rocks, concentrations of conservative constituents (lithium and fluoride) in the waters at each location show that the waters at the two locations are different. The Cl-F-B ternary diagram (Figure 7.8) shows that the relative concentration of boron is similar for both fields but the concentration of fluoride is higher at Orakei Korako and the concentration of chloride is higher at Ngatamariki. This suggests different sources for each location.

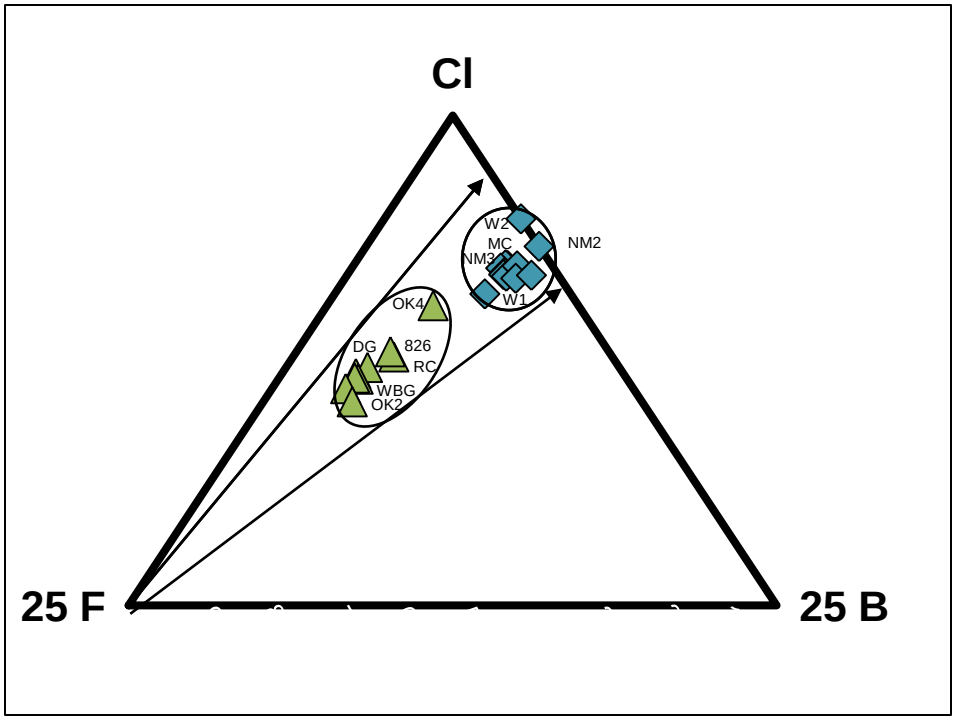

Figure 7.8: Cl-F-B ternary diagram for spring and well waters at Ngatamariki and Orakei Korako. Blue diamonds represent Ngatamariki springs and wells, green triangles represent Orakei Korako springs and wells.

Figure 7.9 is the Cl-Li-B ternary diagram for well and spring waters at the two areas, which cluster in distinct groups. Lithium contents in Ngatamariki waters are lower than in the Orakei Korako waters. This indicates that spring waters at Ngatamariki travel to the surface at a slower rate than at Orakei Korako. However the concentration of lithium is low at both areas (~50-30 %) which suggests that there is probably interaction with reservoir rocks during fluid ascent, where lithium is incorporated into hydrothermal alteration products. The low lithium contents can be attributed to the formation of clays within the volcanic reservoir rocks. Large clay caps form in volcanic sediments, breccias and domes/flows acting as aquitards preventing the direct flow of deep reservoir fluids to the surface. Significant amounts of hydrothermal alteration is noted at Orakei Korako (Bignall 1994) and Ngatamariki which accounts for the low concentrations of lithium in the spring and well waters.

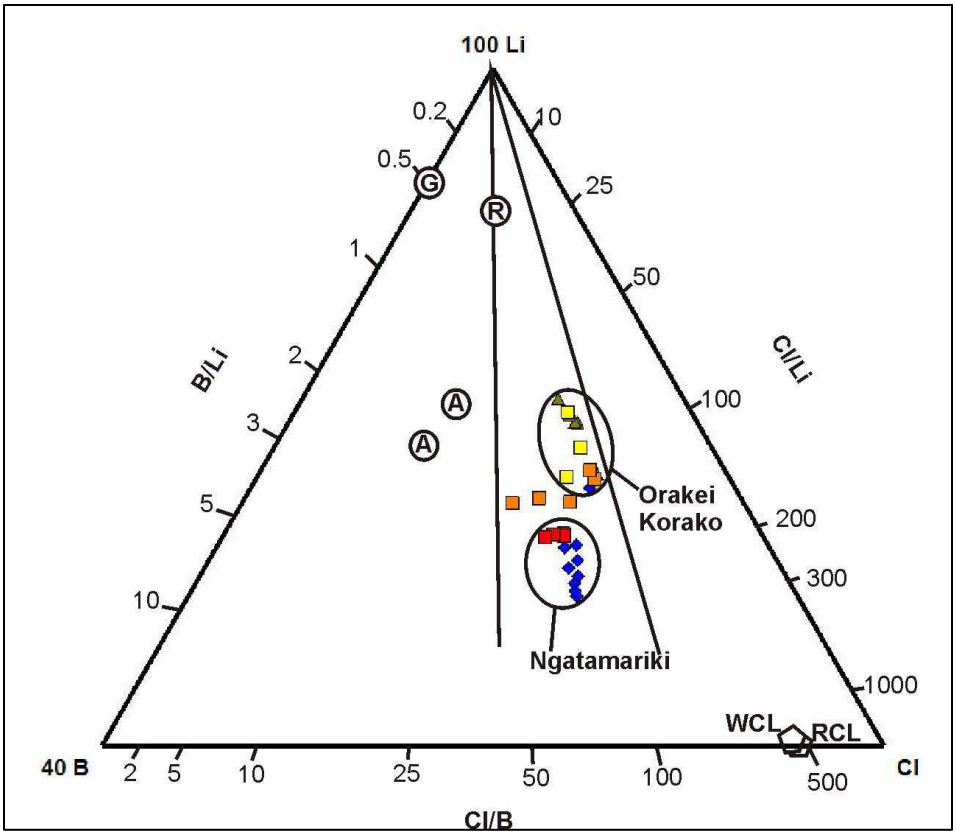

Figure 7.9: Cl-Li-B ternary diagram for spring and well waters at Ngatamariki and Orakei Korako. Ngatamariki springs are represented by blue diamonds, wells represented by red square. Red hill/West Bank springs are represented by orange squares. Tourist area springs are represented by green triangles and Orakei Korako wells are represented by yellow squares. G = TVZ greywacke, R = TVZ rhyolite, A = White Island andesite, WCL = White Island Crater Lake water and RCL = Ruapehu Crater Lake water (after Christensen et.al 2002).

The Na-K-Mg geothermometer diagram (Figure 7.10) shows that spring waters at Orakei Korako show higher reservoir temperatures than spring waters at Ngatamariki but do so over a broad range (~175 – 280 ^{o}C), mostly in partial equilibrium. This suggests that springs within the Orakei Korako field are sourced from different parts of the reservoir where subsurface temperature and water-rock interactions are different, supporting the conceptual model (Figure 7.4). The Ngatamariki waters appear have a consistent reservoir temperature of ~ 180 ^{o}C and are mostly in partial equilibrium. This supports the conceptual model (Figure 7.2) where the springs are sourced from an intermediate aquifer created by clay caps in the reservoir, allowing the interaction of steam heated groundwater and geothermal water.

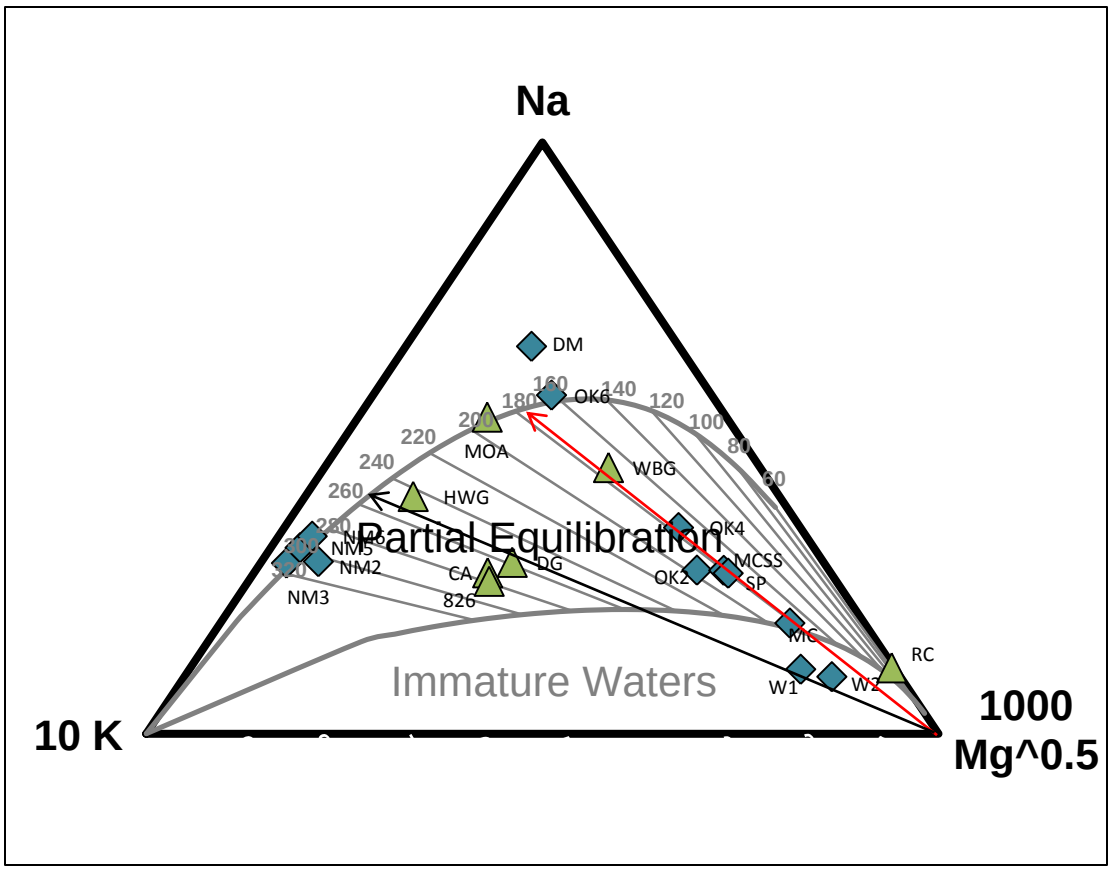

Figure 7.10: The Na-K-Mg geothermometer diagram for spring waters at Orakei Korako (green triangles) and spring and well waters at Ngatamariki (blue diamonds). The red arrow indicated the temperature the majority of features at Ngatamariki equilibrate at. The Black arrow shows the same for Orakei Korako (after Giggenbach, 1988).

The chloride enthalpy diagram (Figure 7.11) shows that waters at Ngatamariki are diluted with steam heated groundwater with a temperature of between 140 and 145 ^{o}C. This supports the model (Figure 7.2) that spring waters are sourced from the intermediate aquifer where cold groundwater mixes with deep geothermal waters from the main reservoir before being discharged at the surface. The waters at Orakei Korako shows two major trends suggesting dilution with hot water of around 164 ^{o}C and dilution by cold water of around 50 ^{o}C. This supports the conceptual model (Figure 7.4) for Orakei Korako where colder waters infiltrate into the reservoir diluting geothermal fluids at depth. It is also obvious that the parent fluids for each location are very different (Figure 7.11). The Waikato River Springs are anomalous in terms of

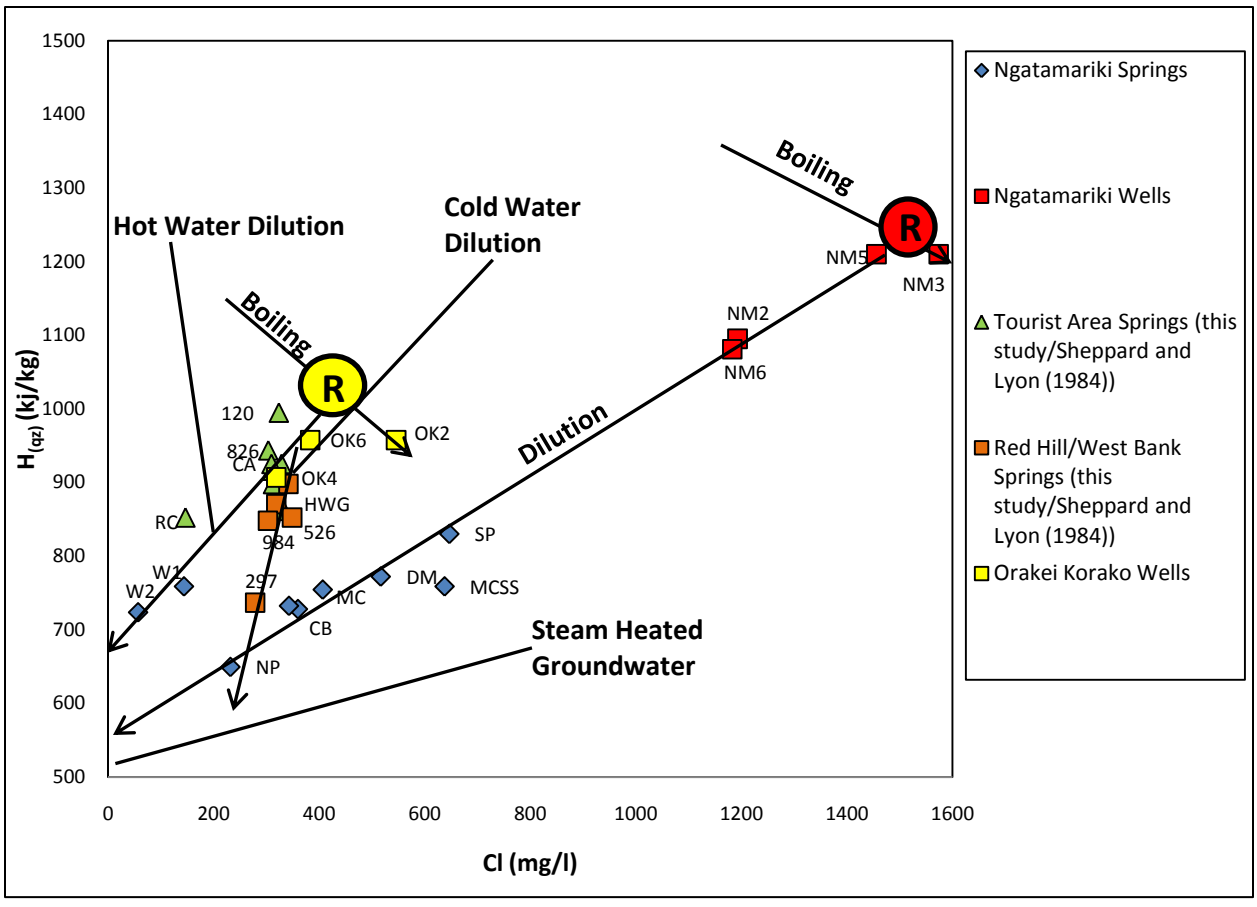

Figure 7.11: Enthalpy – chloride diagram for waters at Ngatamariki and Orakei Korako. The large red circle with the 'R' represents the inferred parent fluid at Ngatamariki and the yellow circle with the 'R' in it represents the Orakei Korako parent fluid.

Ngatamariki spring chemistry plotting with much lower chloride content than the rest of the springs in the field. This is likely due to steam condensing into the fluids before being discharged as seeps. This process is also evident in the Ruatapu Cave, Spring 826 and 120 samples at Orakei Korako.

7.2.2 Geological Relationships

As outlined in chapters 3 and 4 Ngatamariki and Orakei Korako have very similar subsurface geology dominated by volcanic tuffs, lavas, breccias, domes, lake sediments and ignimbrites. The key differences in the subsurface geology are the different ignimbrites and dome lava/breccias at each location. At Ngatamariki, the Wairakei Ignimbrite, intersected by wells, is the stratigraphic equivalent of the Te Kopia and Paeroa Ignimbrites in the north. These ignimbrites are grouped as the Whakamaru Group Ignimbrites across TVZ (see section 3.2.3).

At Ngatamariki the Tahorakuri formation is a thick sequence of fractured porphyritic andesite lava, whereas at Orakei Korako it is the Akatarewa Ignimbrite. Also at Ngatamariki greywacke basement was encountered in NM6, and the Ngatamariki diorite, the first pluton to be encountered in TVZ, was encountered in NM4. Erosional effects cannot explain the large vertical displacements of units seen between wells at Ngatamariki and Orakei Korako, suggesting that fault movements are the key to these displacements. Large north-east – south-west trending normal faults are mapped at the surface at Orakei Korako (Rainbow, Golden Fleece, East Wainui and Matangiwaikato Faults) as splays of the Paeroa Fault. No faults have been intersected by drilling at Ngatamariki.

7.2.3 Hydrogeological Model

The following hydrogeological model for the Ngatamariki Orakei Korako area (Figure 7.13) is based on all the above mentioned geochemistry and geology. From these constraints plus information from other studies, the evidence does not support there being a hydrological connection between the two systems. Although permeable breccia, tuff and formation contacts could facilitate fluid flow between the two areas (Bignall 2009), faults act as impermeable barriers to lateral fluid flow, and these stop any connection between the two fields. The other major difference between the two fields is their number of thermal features. Orakei Korako contains one of New Zealand's largest collections of thermal features, with more than 50 alkali-chloride discharges and the most active geysers in one location, whereas Ngatamariki only has around 12 spring features, a series of seeps and small sinter platforms.

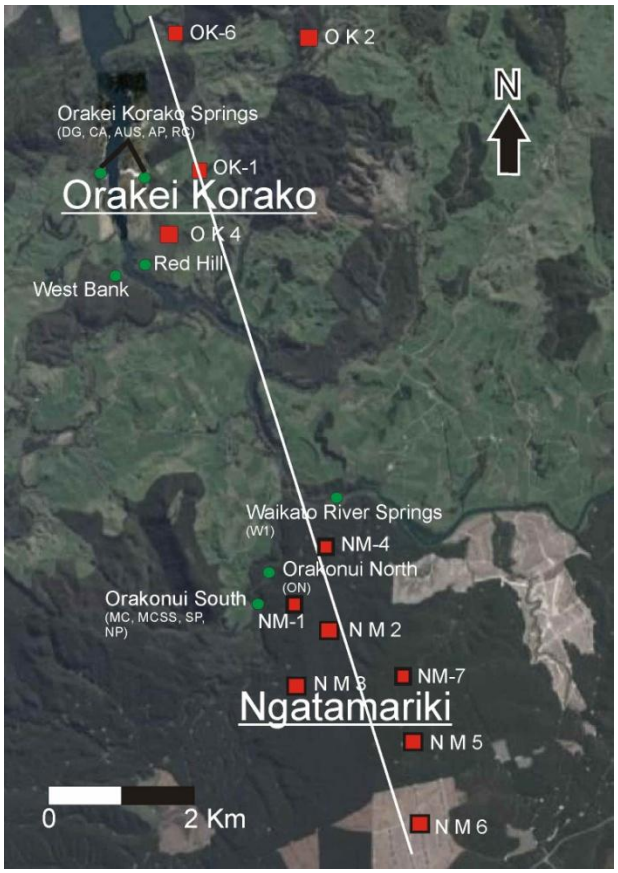

Figure 7.12: Locations of wells and springs at Ngatamariki and Orakei Korako. The Line of section for the hydrogeological model of the Ngatamariki-Orakei Korako area is represented by the white line (Satellite image sourced from Google Earth, 2009).

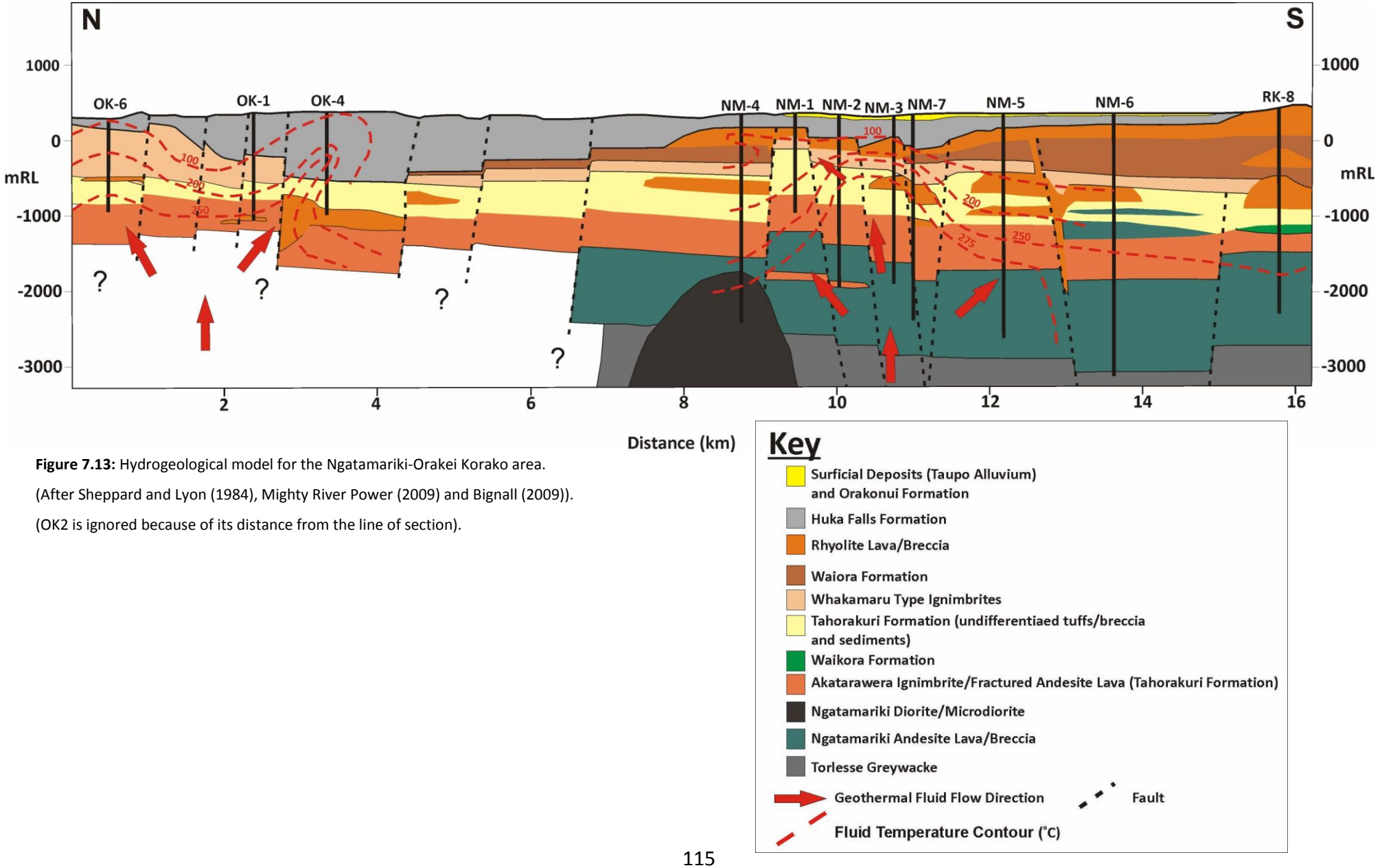

Figure 7.13: Hydrogeological model for the Ngatamariki-Orakei Korako area.

(After Sheppard and Lyon (1984), Mighty River Power (2009) and Bignall (2009)).

(OK2 is ignored because of its distance from the line of section).

7.3 Origins of Fluids

This section discusses what the chemistry of fluids at Ngatamariki and Orakei Korako tells us about their origins and the interactions and processes that occur as they move from their source to their final destination at the surface. The hydrological implications of major ion geochemistry for both Ngatamariki and Orakei Korako have been discussed in section 7.2. For the purpose of this section the Red Hill/West Bank Springs will be grouped with the Tourist Area Springs as the Orakei Korako Springs.

7.3.1 Major ion Indicators

Relative chloride, lithium and boron ratios (Figure 7.9) show that boron levels in waters at both areas is very low. This is likely derived from volcanic host lithologies as they are the richest in boron. Another source of boron could be greywacke, but it is released more rapidly from volcanic sediments (Ellis & Sewell 1963). Figure 7.9 shows that water compositions at both areas are most similar to that of the average TVZ rhyolite (Christenson et al. 2002), suggesting that the rhyolitic reservoir rocks may be the source of boron for both fields. Ngatamariki waters are slightly more enriched in boron than Orakei Korako suggesting that more boron may be leached out of host rocks at Ngatamariki. This is probably due to higher reservoir temperatures nearer to the surface at Ngatamariki allowing more boron to be leached from rhyolitic reservoir rocks. The W2 seep sample from Ngatamariki plots with the Orakei Korako waters in figure 7.9, with less chloride than the rest of the Ngatamariki springs. This is probably due to the interaction with the Waikato River, diluting the chemistry of the spring.

Lithium concentrations are significantly higher at Orakei Korako than Ngatamariki. This can be attributed to hydrothermal alteration, which is more abundant at Ngatamariki, taking up large amounts of lithium as mentioned above in section 7.2.

Fluoride concentrations are also very different at each location. Much higher relative concentrations of fluoride are obvious at Orakei Korako, with much higher chloride contents at Ngatamariki (Figure 7.8). This suggests either condensation of magmatic volatiles at around 400 ^{o}C or dissolution of fluoride bearing reservoir rocks at Orakei Korako. The latter requires

increased hydrolysis capability, which is consistent with elevated magmatic volatile contents (Christenson et al. 2002). As no information below around -1000 mRL is available for geology or fluid chemistry at Orakei Korako it is difficult to ascertain which of the above processes is more likely, but in either case it appears that waters at Orakei Korako are sourced from fluids which condense magmatic volatiles at higher temperatures than at Ngatamariki.

Chloride is the most conservative ion in geothermal systems, which makes it difficult to ascertain its source. Chloride can be leached from volcanic reservoir rocks like boron, but the reason for elevated chloride concentrations at Ngatamariki is that there is no deep mixing of colder fluids and geothermal fluids. This occurs at Orakei Korako where chloride contents are diluted throughout the reservoir. This process is clearly visible in the enthalpy-chloride diagram (Figure 7.11) where the Ngatamariki waters generally have higher concentrations of chloride until mixing with a steam heated groundwater, whereas the dominant process at Orakei Korako is mixing with a 'hot water' diluent.

However the environment of the deep reservoir needs to be considered, as the ultimate source for these constituents is unclear. Volcanic lithologies with similar Cl/B ratios only occur in the top 3.5 km of the reservoir at Ngatamariki and it is not known how deep the volcanic sequence at Orakei Korako continues. These volcanics are unlikely to contribute significantly large amounts to the original fluid composition. The greywacke basement could be a source for boron but the fluids passing through it are relatively depleted in chloride (Christenson et al. 2002). The lithologies which underlie greywacke in TVZ should be the equivalent of oceanic crust if tectonic models are correct; they could contribute to both the boron and chloride concentrations. Direct magmatic inputs as sources for most of these constituents cannot be over looked. For example boron, as H_3BO_3, is easily transported in high temperature vapours, and as temperature decreases boron partitions increasingly into its high temperature phase B (Christenson et al. 2002). Chloride is readily transported into high temperature systems as $HCL_{(g)}$, which contributes to the high content in deep geothermal brines as fluids boil separating the steam and vapour from the liquid.

7.3.2 Stable Isotopic Indicators

Stable isotopic compositions of oygen-18 and deuterium in water allow the determination of the origin of waters recharging a geothermal system. Well water samples taken from weir boxes have been corrected for steam separation to reservoir concentrations using the equation outlined in section 2.5.3.

Waters at Ngatamariki and Orakei Korako both appear to be derived from a meteoric source with different processes subsequently occurring to the fluids giving the springs different isotopic compositions. Figure 7.14 shows the relationship between δ ^{18}O and δ D for spring waters at both fields and well waters at Ngatamariki.

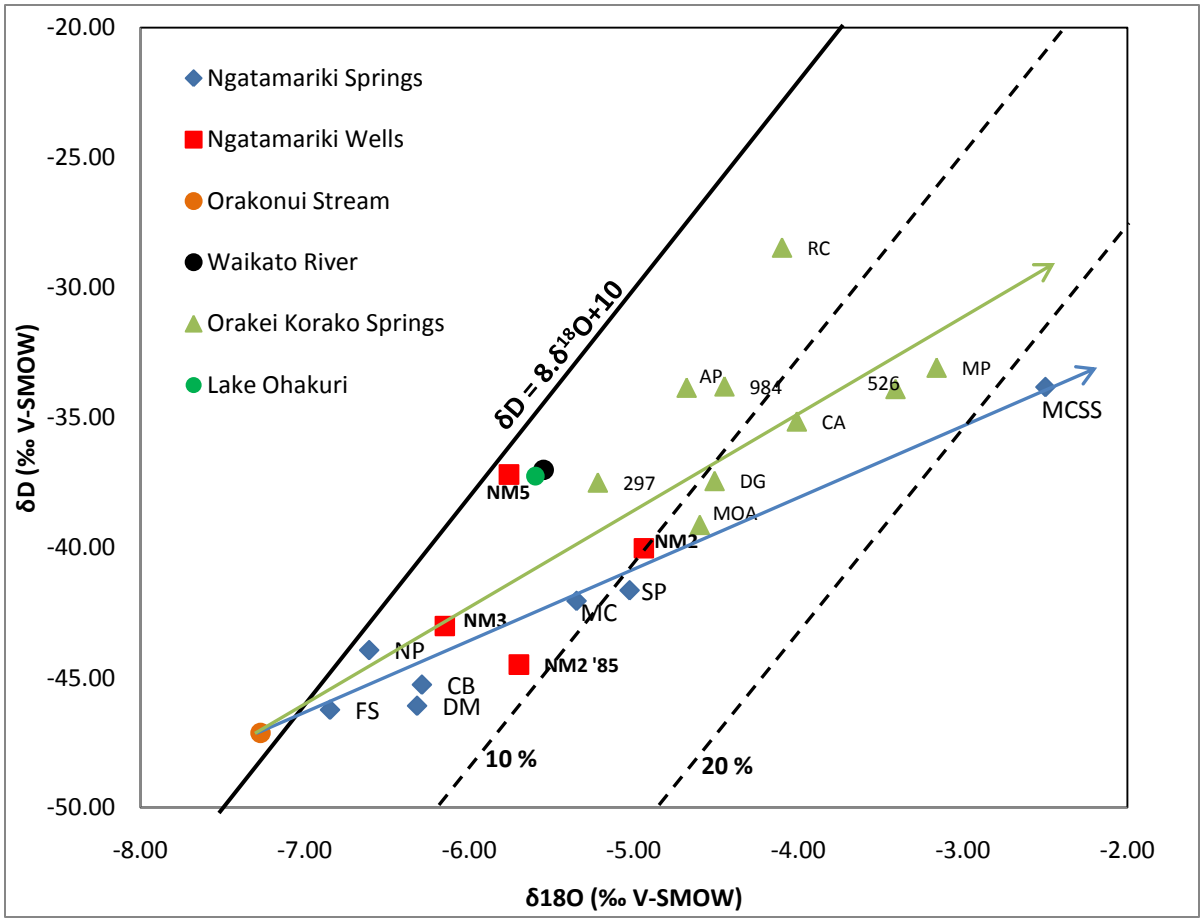

Figure 7.14: δ^{18}O vs δD for spring waters at Ngatamariki and Orakei Korako and well waters at Ngatamariki. The blue and green lines represent the mixing trends seen at Ngatamariki and Orakei Korako respectively. Dashed lines represent the magmatic influence on waters each line represents 10 % magmatic water input (after Giggenbach, 1995).

From this it appears that water from both fields is predominately of meteoric origin (Orakonui Stream) which is expected in geothermal systems (Craig 1963). A difference is seen between the two fields based on spring compositions, where the Ngatamariki springs have $\delta^{18}O$ values ranging from -5 to -7 ‰ and δ D values ranging from -41 to -46 ‰ and the Orakei Korako springs have $\delta^{18}O$ values ranging from -3 to -5 ‰ and δ D values ranging from -33 to -39 ‰. This suggests the meteoric waters are mixing with different fluids at depth to give the change in composition seen in spring waters.

The exceptions in both fields are Ruatapu Cave at Orakei Korako and Main Crater Side Spring at Ngatamariki, both of which are heavily enriched in $\delta^{18}O$ and δ D when compared with the rest of their respective fields. The Ruatapu Cave sample can be explained by an evaporation effect (kinetic fractionation) as the water sits in the bottom of the cave and evaporates slowly with very slow recharge. The MCSS sample could also possibly be explained by the effect of evaporation, but the sample sits almost directly on the mixing line between meteoric water and andesitic water (Figure 7.15). This could be explained by the spring having its own separate conduit to a different part of the reservoir compared with the other springs. However on the $Cl\text{-}SO_4\text{-}HCO_3$ ternary diagram (Figure 7.7) it plots close to a volcanic condensate which may also explain the enrichment by evaporation and condensation.

Well Waters from NM2, 3 and 5 show very similar signatures to spring waters. NM2 and NM5 are more enriched in δ D (-36 and -37 ‰ respectively) and $\delta^{18}O$ (-4.6 and -5.8 ‰ respectively) than NM3 (δ D = -43, $\delta^{18}O$ = -6.1) and the springs. As mentioned earlier NM3 is inferred to represent the main upflow source for the reservoir and sits in tightly with the Ngatamariki springs. This suggests that NM3 is the most representative of the field and can be used as a comparison for mixing processes. NM2 plots more tightly with the Orakei Korako springs and NM5 plots close to the Waikato River and Lake Ohakuri. Water rock interaction with silicate minerals could explain the enrichment in oxygen-18 in NM2 and 5 but the enrichment in deuterium can only be explained by more intense mixing with magmatic water or evaporation. The steep gradient between local meteoric water and NM5 suggests this may be an evaporation effect caused by

boiling at depth. The enrichment in oxygen-18 and deuterium in the NM2 sample suggests more mixing with magmatic water at depth (~10 %). A possible explanation for this could be the fact that NM2 is closest to the diorite intrusion and the greywacke basement which may allow a more direct link to magmatic fluids. The NM2 sample taken in 1985 (Giggenbach 1995) has been added to the data to constrain any changes over time. It appears that the sample taken for NM2 during this study is more enriched in oxygen-18 and deuterium. This may be due to change in the field over time and the extraction of fluids causing deeper fluids rise higher in the reservoir. The most enriched sample at Orakei Korako is the Manganese Pool suggesting that about 17 % mixing with magmatic water is occurring. This high enrichment could also be due to a slight contribution from evaporation as the majority of samples suggest between 10 and 13 % mixing for the field (Figure 7.15).

Magmatic Mixing

As mentioned in section 2.5.3 enrichment in oxygen-18 and deuterium is seen when deep circulating meteoric water interacts with magmatic water. The mixing line for Ngatamariki (Figure 7.15) Ignores the NM5 sample as it is affected by evaporation and suggests that the waters at Ngatamariki are mixed with andesitic water. It appears that Orakei Korako waters are mixed with an end member with a ^{18}O value of about 12 ‰ and a D value of about 10 ‰ which could possibly be rhyolitic or 'mantle-type'. This would be consistent with the model for volcanism in TVZ (Cole 1990; Wilson et al. 1995; Spinks et al. 2005) because Ngatamariki is further to the south, on the edge of the Whakamaru Caldera and MVC, closer to the andesitic front. Orakei Korako is located further to the north within the Whakamaru Caldera and MVC, dominated by rhyolitic volcanism. Assuming that because andesitic water is more enriched in oxygen-18 and deuterium than basaltic water, it could be that rhyolitic water is more enriched than andesitic water. In this case it would make sense for Orakei Korako to show more enriched signatures than are seen at Ngatamariki.

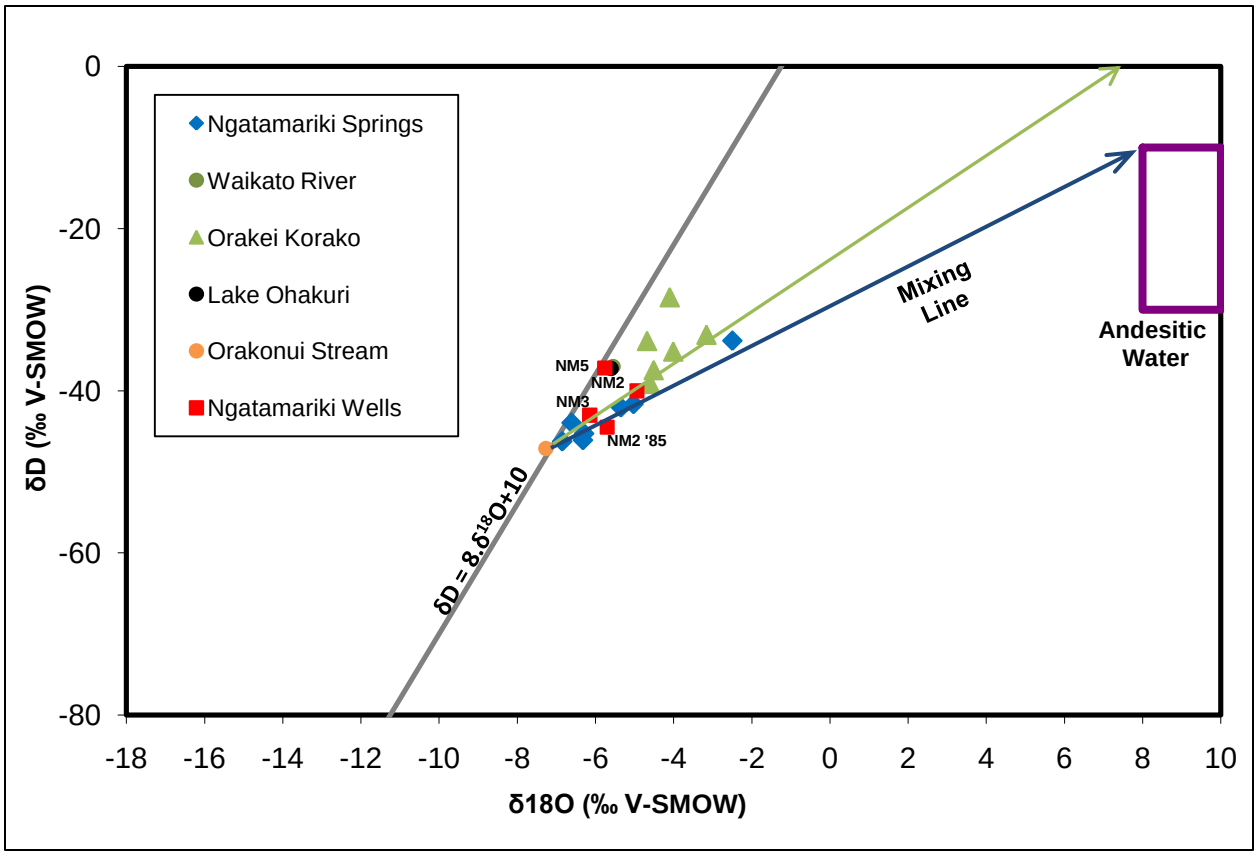

Figure 7.15: $\delta^{18}O$ vs δD magmatic mixing trends for waters at Ngatamariki and Orakei Korako.

Cl vs $^{18}O/D$ Relationships

A positive relationship between Cl and ^{18}O is seen between the Ngatamariki springs and wells, which suggests mixing of deep fluids with a dilute fluid about 1 ‰ heavier than local meteoric water (Figure 7.16). This causes the springs to be enriched in oxygen-18 compared with meteoric water, suggesting that the diluent may be in isotopic equilibrium with reservoir rocks. This is consistent with the enthalpy-chloride diagram (Figure 7.11) which suggests that the deep Ngatamariki waters are mixed with a steam heated groundwater from the intermediate aquifer. Ngatamariki well waters show a slight mixing trend with andesitic water.

Orakei Korako spring waters are more enriched in oxygen-18 and cluster in a tight, almost vertical, linear group suggesting boiling of a high temperature fluid > 240 ^{o}C .This suggests that waters may be sourced from a relatively enriched reservoir fluid, but as no data is available from well discharges this is conjecture.

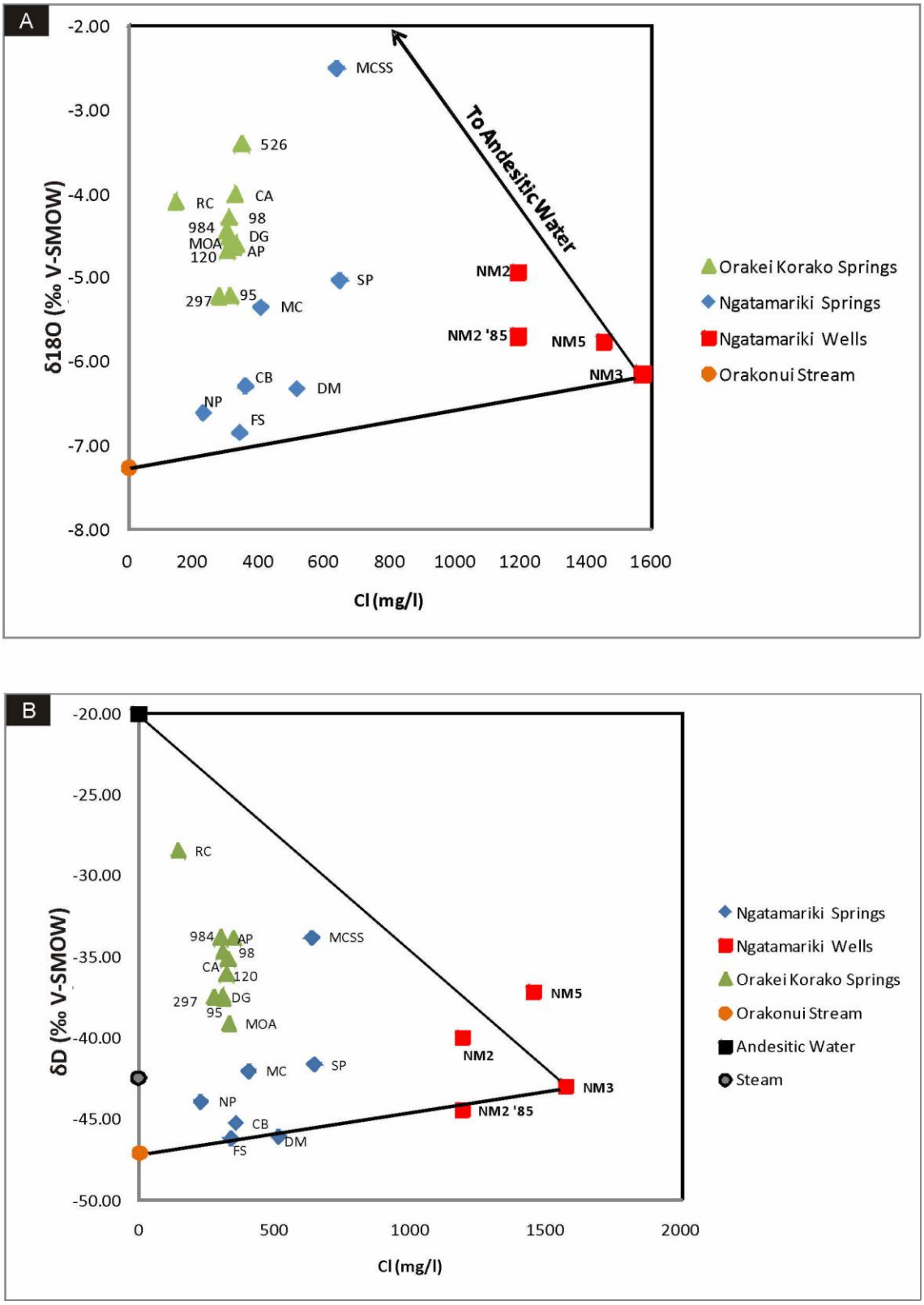

Figure 7.16: A) δD vs Cl and B) $\delta^{18}O$ vs Cl for Ngatamariki springs and wells and Orakei Korako Springs. Waters are compared to steam and andesitic or 'arc-type' water (after Christensen et.al, 2002). NM3 is considered as the closest to a 'source water' for the reservoir which is why the mixing lines are connected to it.

The relationship between Cl and D shows very similar traits to the relationship between Cl and ^{18}O. As δ D signatures are not significantly affected by water rock interaction it can be assumed that only mixing relationships determine the concentrations of δ D. Ngatamariki waters show a positive trend between a diluent about 1 ‰ (δ D) heavier than meteoric water (Orakonui Stream) and deep waters (Figure 7.16). Steam is plotted on the diagram at about 1 ‰ heavier than meteoric water which suggests that the majority of spring waters are mixing with steam at some point during their ascent to the surface. This again supports the model suggesting that deep fluids are mixed with steam heated groundwater before reaching the surface (Figure 7.2). Well waters show a slight mixing trend with andesitic waters shown by NM2 and NM5 plotting close to the mixing line.

Orakei Korako waters are again relatively enriched in deuterium when compared to Ngatamariki ranging from -40 to -28 ‰. The waters also show an almost vertical trend of enrichment in both ^{18}O and D suggesting that boiling of a fluid > 240 ^{o}C is occurring within the reservoir. This suggests they are from a more enriched source fluid but without deep fluid data this is only speculation.

7.3.3 Summary

Analysis of water chemistry at Ngatamariki and Orakei Korako has illustrated that waters evolve differently at each location. The hydrogeochemistry at each location suggests that both fields are independent of each other, with Ngatamariki waters derived from a high temperature reservoir typical of geothermal systems in TVZ and Orakei Korako waters derived from a mixed low chloride reservoir different to other geothermal systems in TVZ.

Geothermal Fluids at Ngatamariki move up through the deep reservoir and migrate south east towards Rotokawa at depth and north-west towards Orakei Korako near the surface. Spring waters at Ngatamariki are sourced from an intermediate aquifer created by clay caps where deep geothermal waters mix with steam heated groundwater and then proceed towards the surface. During this process the water becomes isotopically lighter ($\delta^{18}O$ -5 to -6.85 ‰, δ D -40 to -46 ‰) and chloride content drops (~1200 to ~600 mg/l) (Figure 7.17).

Orakei Korako waters are sourced from a mixed reservoir where colder waters interact with hot geothermal fluids. Spring waters are sourced from the reservoir with low chloride contents (~400 mg/l) and ascend to the surface along a series of normal faults acting as conduits. The geothermal plume nears the surface at the Waihunuhunu Springs in the north and at the Red Hill/West Bank area in the south.

Isotope chemistry of waters at both areas suggests they are meteoric waters which interact with magmatic waters in the reservoir causing enrichment in the isotopic signatures. The enrichment at Ngatamariki suggests mixing with andesitic 'arc-type' water, whereas Orakei Korako waters appear to be mixed with a more enriched fluid at depth which may represent a rhyolitic 'mantle-type' end member.

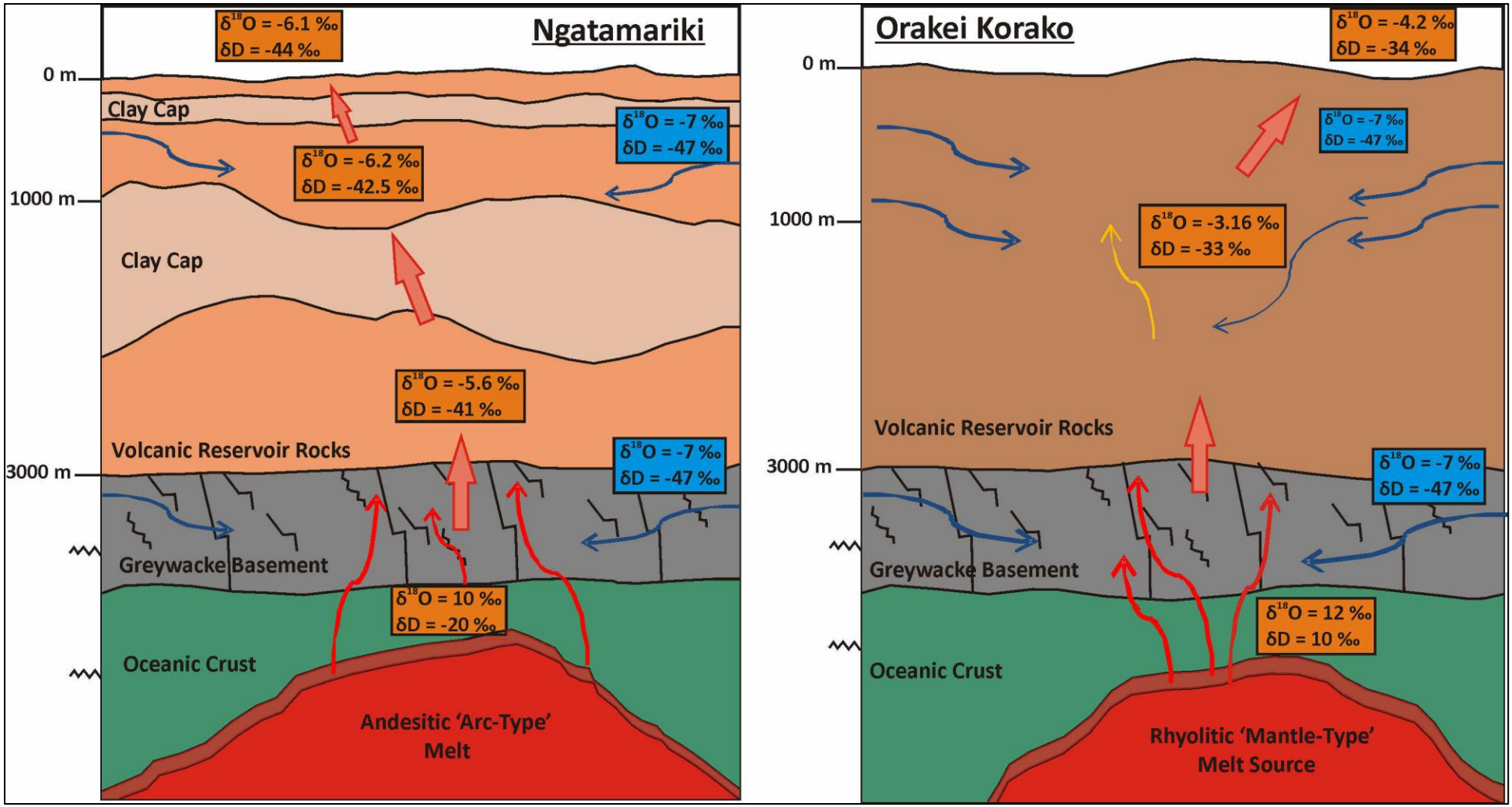

Figure 7.17: Schematic models for isotopic fractionation within the Ngatamariki and Orakei Korako Geothermal Fields. Orange boxes represent the composition of geothermal fluids and blue boxes represent the composition of meteoric water. Measured values are used for the surface, deep reservoir and meteoric waters at Ngatamariki, andesitic water is from Giggenbach (1992) and the intermediate aquifer values are inferred. Measured values for surface and meteoric waters are used for Orakei Korako, the rest of the values are inferred from isotopic results. The scale below 3000 m in the models is not accurate.

Chapter 8: Conclusions

The 12 km^2 Ngatamariki Geothermal Field (Urzua 2008) has a small amount of thermal activity located on its western boundary along the Orakonui Steam and in the northern part of the field along the Waikato river. The objective of this study was to describe the physical nature and chemistry of these features and compare them to the water chemistry from wells drilled into the field for electrical power generation, to gain an understanding of the geochemical nature of the geothermal system at Ngatamariki. The same was done for the Orakei Korako Field located 7 km to the north and comparisons were drawn between the two. From this six main conclusions can be made:

1. Features alongside the Orakonui Stream at Orakonui South have changed considerably since the last published survey of the area in 2002 (Campbell et al. 2002) prior to the April 2005 eruption at Orakonui South. The outflow for the Main Crater has shifted to the north and Pavlova Spring (mentioned in previous studies) was not clearly evident. No active deposition of sinter is currently occurring at Orakonui North, but small high temperature springs occur on both banks of the Orakonui Stream with sinter platforms on the eastern bank. The nature of features at Orakei Korako has not changed significantly since last reported by Hamlin (1999).

2. Orakei Korako exhibits anomalous deep water chemistry (low Cl) and temperatures compared to other systems in the TVZ, due to a high degree of mixing with colder fluids deep in the reservoir. Reservoir fluids at Ngatamariki exhibit high Cl contents and temperatures typical of other TVZ systems.

3. Surface spring chemistries at Ngatamariki and Orakei Korako exhibit more subtle geochemical differences, but still maintain the chemical signature (Cl, B, F, Li) of local deep fluids.

4. Greater temperatures of partial equilibrium of the Orakei Korako waters suggest a better connection between the surface and fluids at depth than at Ngatamariki. This is due to the mixing of fluids at depth and their more direct route to the surface via a series of large normal faults. Ngatamariki springs are mixed and re-equilibrated at a lower temperature in an intermediate reservoir created by hydrothermal clay alteration of reservoir rocks before being discharged at the surface.

5. Comparisons of major ion chemistry, stable isotope chemistry and sub surface geology suggest there is **no** hydraulic connection between the two fields.

6. Geothermal fluids at Ngatamariki and Orakei Korako are dominated by meteoric water with variable amounts of magmatic influence. The source of the magmatic fluid component appears to differ between the two systems. The magmatic fluid component at Ngatamariki appears to be andesitic, whereas more enriched isotopic signatures at Orakei Korako suggest that the waters may be mixed with a rhyolitic end member.

References

Arehart GB, Christenson BW, Wood CP, Foland KA, Browne PRL 2002. Timing of volcanic, plutonic and geothermal activity at Ngatamariki, New Zealand. Journal of Volcanology and Geothermal Research 116(3-4): 201-214.

Arnórsson S 1985. The use of mixing models and chemical geothermometers for estimating underground temperatures in geothermal systems. Journal of Volcanology and Geothermal Research 23(3-4): 299-335.

Ballantyne JM, Moore JN 1988. Arsenic geochemistry in geothermal systems. Geochimica et Cosmochimica Acta 52(2): 475-483.

Bennie SL 1983. Geophysical Investigations of the Ngatamariki Geothermal Area. Wellington, New Zealand, D.S.I.R. 35 p.

Beresford SW, Cole JW 2000. Kaingaroa Ignimbrite, Taupo Volcanic Zone, New Zealand: evidence for asymmetric caldera subsidence of the Reporoa Caldera. New Zealand Journal of Geology and Geophysics 43: 471-481.

Bibby HM, Caldwell TG, Davey FJ, Webb TH 1995. Geophysical evidence on the structure of the Taupo Volcanic Zone and its hydrothermal circulation. Journal of Volcanology and Geothermal Research 68(1-3): 29-58.

Bignall G 1994. Thermal Evolution and Fluid-Rock Interactions in the Orakeikorako-Te Kopia Geothermal System, Taupo Volcanic Zone, New Zealand. Unpublished PhD thesis, Auckland University, Auckland. 400 p.

Bignall G 2009. Ngatamariki Geothermal Field Geoscience Overview. *GNS Science Consultancy Report 2009/94*. 41 p.

Brotheridge JMA 1995. Surface Manifestations - Past and Present - Of The Ngatamariki Geothermal Field, Taupo Volcanic Zone, New Zealand. Unpublished M.Sc thesis, University of Auckland. 154 p.

Brown SJA, Wilson CJN, Cole JW, Wooden J 1998. The Whakamaru group ignimbrites, Taupo Volcanic Zone, New Zealand: evidence for reverse tapping of a zoned silicic magmatic system. Journal of Volcanology and Geothermal Research 84(1-2): 1-37.

Browne PRL 1979. Minimum age of the Kawerau geothermal field, North Island, New Zealand. Journal of Volcanology and Geothermal Research 6(3-4): 213-215.

Browne PRL, Lawless JV 2001. Characteristics of hydrothermal eruptions, with examples from New Zealand and elsewhere. Earth-Science Reviews 52(4): 299-331.

Browne PRL, Rodgers KA 2006. Occurrence and significance of anomalous chloride waters at the Orakei Korako geothermal field, Taupo Volcanic Zone, New Zealand. Geothermics 35(3): 211-220.

Browne PRL, Graham IJ, Parker RJ, Wood CP 1992. Subsurface andesite lavas and plutonic rocks in the Rotokawa and Ngatamariki geothermal systems, Taupo Volcanic Zone, New Zealand. Journal of Volcanology and Geothermal Research 51(3): 199-215.

Bruckner MZ 2009. Ion Chromatography. Retrieved 23/02/2010 2010, from http://serc.carleton.edu/microbelife/research_methods/biogeochemical/ic.html

Campbell KA, Rodgers KA, Brotheridge JMA, Browne PRL 2002. An unusual modern silica-carbonate sinter from Pavlova spring, Ngatamariki, New Zealand. Sedimentology 49: 835-854.

Chandrasekharam D, Bundschuh J 2008. Low-enthalpy geothermal resources for power generation. Leiden, The Netherlands, CRC Press/Balkema.

Christenson BW, Mroczek EK, Kennedy BM, van Soest MC, Stewart MK, Lyon G 2002. Ohaaki reservoir chemistry: characteristics of an arc-type hydrothermal system in the Taupo Volcanic Zone, New Zealand. Journal of Volcanology and Geothermal Research 115(1-2): 53-82.

Cole JW 1972. Distribution of high-alumina basalts in Taupo Volcanic Zone. Publication of Geology Department, Victoria University of Wellington.

Cole JW 1990. Structural control and origin of volcanism in the Taupo volcanic zone, New Zealand. Bulletin of Volcanology 52: 445-459.

Cole JW, Lewis KB 1981. Evolution of the Taupo-Hikurangi subduction system. Tectonophysics 72(1-2): 1-21.

Craig H 1961. Standard for reporting concentrations of deuterium and oxygen-18 in natural waters Science 133: 1833-1934.

Craig H 1963. The isotopic geochemistry of waters and carbon in geothermal areas. Neuclear Geology on Geothermal Areas. CNR, Pisa. Pp. 17-53.

Ellis AJ 1979. Chemical geothermometry in geothermal systems. Chemical Geology 25(3): 219-226.

Ellis AJ, Sewell JR 1963. Boron in Waters and Rocks of New Zealand hydrothermal areas. New Zealand Journal of Science 6: 589-606.

Ellis AJ, Mahon WAJ 1977. Chemistry and Geothermal Systems. New York, Academic Press INC. 392 p.

Faure G 1977. Principles of Isotope Geology. New York N.Y, John Wiley and Sons, Inc.

Fournier RO 1977. Chemical Geothermometers and mixing models for geothermal systems. Geothermics 5: 41-50.

Fournier RO 1981. Application of water geochemistry to geothermal exploration and reservoir engineering; in Geothermal systems. In: Rybach L, Muffler LJP ed. Geothermal systems: Principals and Case Histories;. New York, John Wiley and Sons. Pp. 109-143.

Fournier RO, White DE, Truesdell AH 1974. Geochemical indicators of subsurface temperature. J.Res. U.S Geological Surver 2: 259-261.

Fournier RO, Truesdell AH 1973. An empirical Na---K---Ca geothermometer for natural waters. Geochimica et Cosmochimica Acta 37(5): 1255-1275.

Fournier RO, Potter Ii RW 1979. Magnesium correction to the Na---K---Ca chemical geothermometer. Geochimica et Cosmochimica Acta 43(9): 1543-1550.

Friedman I, O'Neill JR 1977. Compilation of stable isotope fractionation factors of geochemical interest. In: Fleischer M ed. Data of geochemistry, U.S Geological Survey Prof. Paper, 440-KK.

Gamble JA, Smith IEM, McCulloch MT, Graham IJ, Kokelaar BP 1993. The geochemistry and petrogenesis of basalts from the Taupo Volcanic Zone and Kermadec Island Arc, S.W. Pacific. Journal of Volcanology and Geothermal Research 54(3-4): 265-290.

Gamble JA, Smith IEM, Graham IJ, Peter Kokelaar B, Cole JW, Houghton BF, Wilson CJN 1990. The petrology, phase relations and tectonic setting of basalts from the taupo volcanic zone, New Zealand and the Kermadec Island arc - havre trough, SW Pacific. Journal of Volcanology and Geothermal Research 43(1-4): 253-270.

Giggenbach WF 1988. Geothermal solute equilibria. Derivation of Na-K-Mg-Ca geoindicators. Geochimica et Cosmochimica Acta 52(12): 2749-2765.

Giggenbach WF 1995. Variations in the chemical and isotopic composition of fluids discharged from the Taupo Volcanic Zone, New Zealand. Journal of Volcanology and Geothermal Research 68(1-3): 89-116.

Giggenbach WF, Soto RC 1992. Isotopic and chemical composition of water and steam discharges from volcanic-magmatic-hydrothermal systems of the Guanacaste Geothermal Province, Costa Rica. Applied Geochemistry 7(4): 309-332.

Google INC 2009. Google Earth (Version 5.1.3533.1731) [Software].

GNS 2009. Analytical Report WAL091105001.

Goff F, Janik CJ 2000. Geothermal Systems. In: Sigurdsson H ed. Encyclopaedia of Volcanoes, Academic Press. Pp. 817-834.

Grange LI 1937. The Geology of the Rotorua-Taupo Subdivision, Rotorua and Kaimanawa Divisions. Survey NZG ed. Wellington, Department of Scientific and Industrial Research.

Grindley GW 1960. Geological map of New Zealand - Sheet 8 Taupo. New Zealand Geological Survey, D.S.I.R.

Grindley GW 1965. The geology, structure and exploitation of the Wairakei geothermal field, Taupo, New Zealand. New Zealand Geological Survey Bulletin Vol. 75. DSIR.

Hamlin KA 1999. Geological studies of the Orakeikorako geothermal field, Taupo Volcanic Zone. Unpublished M.Sc thesis, University of Auckland. 118 p.

Healy J 1974. Ngatamariki Geothermal Field. New Zealand Geological Survey Report 38, Minerals of New Zealand, Part D, Geothermal Resources, DSIR, Wellington.

Hedenquist JW 1986. Chemistry of the Ngatamariki Geothermal Field: Preliminary Assesment prior to discharge of wells NM1-NM4. DSIR Chemisrty Division Technical Note 86/4

Hedenquist JW, Browne PRL 1989. The evolution of the Waiotapu geothermal system, New Zealand, based on the chemical and isotopic composition of its fluids, minerals and rocks. Geochimica et Cosmochimica Acta 53(9): 2235-2257.

Henley RW, Truesdell AH, Barton Jr. PB 1985. Fluid-Mineral Equilibria in Hydrothermal Systems Robertson JM ed, Society of Economic Geologists.

Hochstein MP, Browne PRL 2000. Surface Manifestations of Geothermal Systems with Volcanic Heat Sources. In: Sigurdsson H ed. Encyclopaedia of Volcanoes Academic Press. Pp. 835-855.

Hochstetter FV 1864. Geologie von Neu Seeland: Beitrage zur Geologie der Provinzen Auckland und Nelson, Novara Exped. Unpublished thesis, Translated and edited by Dr. C. A Felming, 1959, Government Printer, Wellington. 274 p.

Houghton BF, Wilson CJN, Lloyd EF, Gamble JA, Kolelaar BP 1987. A Catalouge of Basaltic Deposits within the Central Taupo Volcanic Zone. New Zealand Geological Survey Record 18: 95-101.

Houghton BF, Wilson CJN, McWilliams MO, Lanphere MA, Weaver SD, Briggs RM, Pringle MS 1995. Chronology and dynamics of a large silicic magmatic system: Central Taupo Volcanic Zone, New Zealand. Geology 23(1): 13-16.

Jackson KW, Mahmood TM 1994. Atomic Absorption, Atomic Emission, and Flame Emission Spectrometry. Analytical Chemistry 66(12): 252R-279R.

Karig DE 1970. Ridges and Basins of the Tonga-Kermadec Island Arc System. J. Geophys. Res. 75.

Keam RF 1955. Volcanic Wonderland - the scenery and spectacle of the New Zealand thermal region. published by G. B Scott. Auckland, New Zealand.

Kissling WM, Weir GJ 2005. The spatial distribution of the geothermal fields in the Taupo Volcanic Zone, New Zealand. Journal of Volcanology and Geothermal Research 145(1-2): 136-150.

Leaver JD, Unsworth CP 2007. System dynamics modelling of spring behaviour in the Orakeikorako geothermal field, New Zealand. Geothermics 36(2): 101-114.

Leonard GS 2003. The Evolution of Maroa Volcanic Centre, Taupo Volcanic Zone, New Zealand. Unpublished P.hD thesis, University of Canterbury, Christchurch.

Lloyd EF 1972. Geology and Hot Springs of Orakeikorako. Wellington, New Zealand Geological Survey. 164 p.

Mahon WAJ 1964. Flourine in the natural thermal waters of New Zealand. New Zealand Journal of Science 7: 3-28.

Mahon WAJ 1972. The Chemistry of the Orakeikorako Hot Spring Waters. In: Lloyd EF ed. Geology and Hot Springs of Orakeikorako. Wellington, New Zealand Geological Survey.

Nicholson K 1993. Geothermal Fluids: Chemistry and Exploration Techniques. Berlin, Springer-Verlag. 263 p.

Rae AJ, Ramirez LE, Bardsley C 2009. Geology of Exploration Well NM6, Ngatamariki Geothermal Field. *GNS Science Consultancy Report* 2009/130. 68 p.

Ramirez LE, Rae AJ 2009. Geology of Injection Well NM5, NM5a, Ngatamariki Geothermal Field. *GNS Science Conslutancy Report* 2009/41. 29 p.

Ramirez LE, Rae AJ, Boseley C 2009. Geology of Exploration Well NM7, Ngatamariki Geothermal Field. *GNS Science Consultancy Report* 2009/289. 57 p.

Risk GF, Caldwell TG, Bibby HM 2003. Tensor time domain electromagnetic resistivity measurements at Ngatamariki geothermal field, New Zealand. Journal of Volcanology and Geothermal Research 127(1-2): 33-54.

Sharp ZD, Atudorei V, Durakiewicz T 2001. A rapid method for determination of hydrogen and oxygen isotope ratios from water and hydrous minerals. Chemical Geology 178(1-4): 197-210.

Sheppard DS, Lyon GL 1984. Geothermal fluid chemistry of the Orakeikorako field, New Zealand. Journal of Volcanology and Geothermal Research 22(3-4): 329-349.

Soengkono S 1993. Interpretation of aeromagnetic data over the Orakeikorako geothermal field, Central North Island, New Zealand. In: Lee KC, Dunstall MG, Hochstein MP ed. *Proceedings of the 15th New Zealand Geothermal Workshop*. Pp. 207-212.

Spinks KD, Acocella V, Cole JW, Bassett KN 2005. Structural control of volcanism and caldera development in the transtensional Taupo Volcanic Zone, New Zealand. Journal of Volcanology and Geothermal Research 144(1-4): 7-22.

Stewart MK, Taylor CB 1981. Environmental isotopes in New Zealand hydrology: 1 Introduction: The role of oxygen-18, deuterium, and tritium in hydrology. New Zealand Journal of Science 24: 295-311.

Urzua LA 2008. Intergration of a preliminary one-dimensional MT analysis with geology and geochemistry in a conceptual model of the Ngatamariki Geothermal Field. Unpublished MSc thesis, Auckland University. 128 p.

Werner C, Cardellini C 2006. Comparison of carbon dioxide emissions with fluid upflow, chemistry, and geologic structures at the Rotorua geothermal system, New Zealand. Geothermics 35(3): 221-238.

White DE 1970. Geochemistry applied to the discovery, evaluation and exploitation of geothemal energy resources. Geothermics Special Issue 2(1): 58-80.

Wilson CJN, Houghton BF, Lloyd EF 1986. Volcanic history and evolution of the Maroa-Taupo area, Central North Island. In: Smith IEM ed. Late Cenozoic Volcanism in New Zealand, R.Soc, New Zealand, Bulletin 23. Pp. 194-223.

Wilson CJN, Gravely DM, Leonard GS, Rowland JV 2009. Volcanism in the central Taupo Volcanic Zone, New Zealand: tempo styles and controls. In: Thordarson Tea ed. Studies in Volcanology: The Legacy of George Walker, IAVCEI Proceedings in Volcanology 2.

Wilson CJN, Houghton BF, McWilliams MO, Lanphere MA, Weaver SD, Briggs RM 1995. Volcanic and structural evolution of Taupo Volcanic Zone, New Zealand: a review. Journal of Volcanology and Geothermal Research 68(1-3): 1-28.

Wood CP 1985. Stratigraphy and Petrology of NM1, NM2, NM3 Ngatamariki Geothermal Field. DSIR Report.

Wood CP 1986. Stratigraphy and Petrology of NM4 Ngatamariki Geothermal Field. DSIR Report.

Appendices

Appendix A: Deep Stratigraphy at Ngatamariki

Stratigraphy for wells NM1-4 at Ngatamariki (Wood 1985, 1986; Urzua 2008)

ID	From	to	Lithology	Circulation Loss
NM1	0	23	Pumice and Sands	Complete at 23 m
NM1	23	50	Coarse Gravels	
NM1	50	200	Silstone,Sandstone, minor gravels	Circulation loss at 69 m
NM1	200	315	Rhyolite	Complete at 226 m
NM1	315	325	Sands	
NM1	325	460	Crystal lithic tuff (ignimbrite)	
NM1	460	650	Crystal tuff	
NM1	650	740	no cuttings	Complete at 650-735 m
NM1	740	1115	Sediments and tuffs	
NM1	1115	1302	Crystal tuff (ignimbrite)	
NM2	0	20	Pumice lapilli and Gravel	
NM2	20	115	Sands and gravels	
NM2	115	305	Sediments, silstones, sandstones	33 l/s circ loss
NM2	305	470	Rhyolite	Complete at 339 m
NM2	470	685	Crystal tuff (ignimbrite), Q rich	
NM2	685	785	Black mudstone and grey tuff	
NM2	785	855	Crystal tuff (ignimbrite), Q rich	
NM2	855	875	Black mudstone and grey tuff	12 l/s at 870m
NM2	875	905	Greenish tuff	
NM2	905	953	no cuttings	10 l/s at 935
NM2	953	995	Breccia (andesitic)	
NM2	995	1110	Tuffs	
NM2	1110	1155	No cuttings returned	
NM2	1155	1205	Welded crystal Tuff (ignimbrite) Q poor	
NM2	1205	1355	Grey Tuff	
NM2	1355	1354	no cuttings	
NM2	1354	1356	Crystal lithic tuff (ignimbrite)	
NM2	1415	1417	Pumice breccia (ignimbrite) Q poor	Complete at 1575 m-***Main feedzone***
NM2	1582	1586	Lithic pumice breccia (ignimbrite) Q free	***Main feedzone***
NM2	1786	1788	Andesitic breccia	
NM2	2000	2255	Andesitic breccia	
NM2	2255	2403	Welded crystal Tuff (ignimbrite) Q rich	
NM3	0	40	Pumice Tephra, sands and gravel	
NM3	40	115	Gravels (rhyolitic)	
NM3	275	590	Rhyolite	Complete 324-340-367m
NM3	590	695	Crystal Tuff (ignimbrite); Q-rich	
NM3	695	785	Sediments: dominated by black mudstone	
NM3	785	995	Dacite	
NM3	995	1200	Sediments and tuff: mixed sequence	***Main feedzone***
NM3	1200	1950	Ignimbrites	
NM3	1950	2194	Andesitic lava and breccia	
NM4	0	40	Gap	
NM4	40	150	Gravelly silstones over gravel and sands	
NM4	150	190	Gravelly rhyolitic detritus	
NM4	190	435	Rhyolite	Complete at 287-318-378 m
NM4	435	650	Tuffaceous clastic deposits	Complete at 552 m
NM4	650	740	Unwelded lithic crystal Tuff (Q-rich ignimbrite)	
NM4	740	785	Welded lithic crystal tuff (Q-rich ignimbrite)	
NM4	785	835	Crystal tuff (Q-rich ignimbrite)	
NM4	835	900	Sediments: Much black silstone	
NM4	900	1090	Lava and Tuffs (dacitic?)	
NM4	1090	1130	Tuffs and black silstone	
NM4	1130	1170	no cuttings	
NM4	1170	2100	Rhyolite-Ignimbrite?	6.5 l/s at 1301 m
NM4	2100	2650	Ignimbrite?	
NM4	2650	2749	Quartz diorite	

Clay alteration in wells NM1-4 (Wood 1985, 1986; Urzua 2008)

Well	Core depth	Hydrothermal Alteration
NM1	150	I-S
NM1	260	I-S
NM1	431	M
NM1	580	M
NM1	650	M
NM1	800	I-S
NM1	915	I-S
NM1	952	I
NM1	1100	I
NM1	1250	I
NM1	1305	I
NM2	300	I-S
NM2	598	I (IS?)
NM2	700	Ch-S
NM2	834	I
NM2	953	I
NM2	1155	I
NM2	1354	I
NM2	1415	I
NM2	1582	I
NM3	261	I-S
NM3	332	M
NM3	452	M
NM3	672	I-S
NM3	903	I-S
NM3	1009	I-S
NM3	1246	I
NM3	1495	I
NM3	1743	I
NM4	260	M
NM4	505	M
NM4	752	M
NM4	1000	I-S
NM4	1225	I-S
NM4	1476	I-S
NM4	1730	I
NM4	1962	I
NM4	2209	I

Alteration types are: I = Illite, S = Smectite, M = Montmorillonite and Ch = Chlorite.

Stratigraphy for well NM5 at Ngatamariki (Ramirez & Rae 2009).

NM5 - NM5A		*Formation*	*Lithology*
Depth (mCHF)	**Depth** (mRL)		
0 to 10	381 to 371	**Surficial Deposits**	Pumice breccia, with common volcanic lithics and crystal fragments of quartz and minor feldspar.
10 to >40	371 to 341	**Oruanui Formation**	White-cream to pinkish vitric-lithic tuff, with vesicular pumice and minor/common lava lithics and crystals of quartz, feldspar and rare pyroxene.
45 to 90		**No Returns**	-
<95 to >165	286 to 216	**Huka Falls Formation**	Coarse to medium gained sandstone, minor fine gravel and siltstone.
170 to 200		**No Returns**	-
<205 to ~215	176 to 166	**Waiora Formation**	Pumice-rich vitric tuff, with volcanic lithics, quartz, rare biotite and pyroxene crystals.
220		**No Returns**	-
~225 to ~370	156 to 11	**Rhyolite lava**	Glassy rhyolite lava, with a perlitic texture. Phenocrysts are quarz, feldspar, pyroxene and magnetite.
370		**No Returns**	-
~370 to 590	11 to -209	**Waiora Formation**	Pale grey - greenish grey pumice rich - vitreous tuff, intercalated with crystal tuff (quartz, feldspar and rare pyroxene), tuffaceous coarse sandstone and tuffaceous siltstone.
590 to 785	-209 to -404	**Wairakei Ignimbrite**	Quartz-rich, crystal-lithic tuff/breccia, with abundant quartz, minor feldspar, rare biotite and pyroxene crystals, and minor volcanic lithics and pumice, set in a fine matrix.
785 to 1070	-404 to -689	**Rhyolite lava**	Hard porphyritic quartz-rich rhyolite lava with phenocrysts of quartz, minor feldspar and minor/rare ferromagnesian minerals.
1070 to 1220	-689 to -839	**Tahorakuri Formation**	Pale grey to white lithic tuff/breccia with lithics of dark grey lava, argillite and sandstone, along with pale grey rhyolite and pumice fragments.
1220 to 1375	-839 to -994	**Rhyolite breccia**	Pale grey, rhyolite breccia with angular to subangular rhyolite clasts in a glassy vitric matrix.
1375 to 2457	-994 to -2084	**Tahorakuri Formation**	White to pale grey, lithic tuff/breccia containing lithic clasts of dark grey to brown lava, argillite, greywacke and sandstone, with pale grey rhyolite and pumice fragments in a sand-silt matrix
2457 to 2987	-2084 to -2606	**No Returns**	-

Stratigraphy for well NM6 at Ngatamariki (Rae et al. 2009)

Depth (mCHF)	Depth (mRL)	Stratigraphic Formation
0 to 200	372.5 to 172.5	**No returns.**
200 to 205	172.5 to 167.5	**Huka Falls Formation** Pale grey siltstone intercalated with silty sandstone.
205 to 240	167.5 to 132.5	**No returns.**
240 to 325	132.5 to 47.5	**Rhyolite Lava** Weakly porphyritic rhyolite lava with spherulitic and flow banded textures.
325 to 585	47.5 to -212.5	**No returns.**
585 to 825	-212.5 to -452.5	**Waiora Formation** Light grey to white pumice-rich tuff, volcanic breccia, sediments and lithic-crystal tuff. Lithics include pumice, porphyritic rhyolite and ignimbrite. Crystals are quartz, plagioclase and pyroxene.
825 to 980	-452.5 to -607.5	**Wairakei Ignimbrite** Quartz-rich, crystal-lithic ignimbrite with abundant crystals of quartz, plagioclase, amphibole and pyroxene. Lithics are rhyolite and pumice.
980 to 1205	-607.5 to -832.5	**Rhyolite Lava** Hard, porphyritic quartz-rich rhyolite lava with phenocrysts of quartz, plagioclase and ferromagnesian minerals.
1205 to 1270	-832.5 to -897.5	**Tahorakuri Formation (crystal-lithic tuff)** Pale grey to white bleached crystal-lithic tuff with quartz and plagioclase crystals and lithics of rhyolite and possible andesite in a silicified matrix.
1270 to 1350	-897.5 to -977.5	**Tahorakuri Formation (andesite lava and breccia)** Porphyritic andesite lava with phenocrysts of plagioclase and pyroxene. The top 15 m is brecciated.
1350 to 1450	-977.5 to -1077.5	**Tahorakuri Formation (non-welded vitric tuff)** Pale grey to white non-welded, fine vitric tuff with sparse silicified lithics and andesite clasts and minor plagioclase and chlorite-altered ferromagnesian crystals.
1450 to 1630	-1077.5 to -1307.5	**Tahorakuri Formation (andesite/dacite lava and breccia)** Dark grey, porphyritic andesite/dacite lava with phenocrysts of plagioclase and pyroxene in a glassy matrix. Below ~1535mRF the unit is a breccia with clasts of lava (andesite/dacite), tuff and rhyolite and crystals of plagioclase and pyroxene.
1630 to 2210	-1307.5 to -1837.5	**Tahorakuri Formation (non- to partially-welded ignimbrite)** Greenish grey to pale grey partially welded ignimbrite with abundant flattened pumice and lithics of andesite, tuff, rhyolite, dacite, greywacke and argillite. Crystals include quartz, plagioclase and possible pyroxene.
2210 to 2565	-1837.5 to -2192.5	**Andesite Lava** Pale grey porphyritic andesite lava. Phenocrysts of feldspar, clinopyroxene and minor hornblende.
2565 to 2676	-2192.5 to -2303.5	**No returns.**
2676 to 2679 (Core #1)	2303.5 to -2306.5	**Andesite Lava** Green to purple grey, porphyritic andesite lava with phenocrysts of plagioclase, clinopyroxene and minor hornblende.
2769 to 3022	-2306.5 to -2649.5	**No returns.**
3022 to 3025 (Core #2)	-2649.5 to -2652.5	**Andesite Lava** Green to purple grey, porphyritic andesite lava with phenocrysts of plagioclase, clinopyroxene and minor hornblende.
3025 to 3385	-2652.5 to -3012.5	**No returns.**
3385 to 3388 (TD) (Core #3)	-3012.5to -3015.5 (TD)	**Greywacke basement** Pale grey, massive meta-sandstone and siltstone.

Stratigraphy for well NM7 at Ngatamariki (Ramirez et al. 2009)

NM7		Stratigraphic Formation
Depth (mCHF)	Depth (mRL)	
0 to 40	0 to 328	**NO CUTTINGS COLLECTED**
<40 to 75	>328 to 293	**ORUANUI FORMATION** Pumice-crystal tuff/breccia with a mud matrix. Abundant crystals of quartz, plagioclase, hornblende, pyroxene and magnetite. Minor lithics include dark to pale grey volcanic, possible greywacke and obsidian.
75 to >98	293 to <270	**HUKA FALLS FORMATION** Fine, sand sized lithics (volcanics, greywacke, rhyolite and pumice) and crystal fragments (quartz, plagioclase and hornblende) in a pale brown mud matrix.
98 to 397	270 to -29	**NO RETURNS**
<397 to 480	> -29 to -112	**HUKA FALLS FORMATION** Sand sized lithics of rhyolite, pumice, possible andesite and silicified clasts, along with abundant crystals of quartz and plagioclase in a mud matrix.
480 to 520	-112 to -152	**RHYOLITE BRECCIA** Rhyolite breccia with clasts of rhyolite lava and minor fragments of mudstone and siltstone.
520 to 645	-152 to -276	**WAIORA FORMATION** A non-welded, pumice–crystal–lithic ignimbrite with pumice, rhyolite and lithic fragments, and abundant quartz, plagioclase and biotite crystals.
645 to 680	-276 to -311	**RHYOLITE BRECCIA** Rhyolite breccia with spherulitic, porphyritic, perlitic and flow banded rhyolite clasts.
680 to 940	-311 to -571	**WAIRAKEI IGNIMBRITE** Crystal-rich, non-welded ignimbrite with abundant crystals of quartz, plagioclase, and minor biotite and pyroxene. Lithics are rhyolite, pumice and dark grey volcanics.
940 to 1185	-571 to -816	**RHYOLITE LAVA** Weakly porphyritic rhyolite lava with minor, rounded quartz and plagioclase phenocrysts that increase in abundance with depth. Laminated carbonaceous sediments occur throughout.
1185 to 1380	-816 to -1011	**TAHORAKURI FORMATION** Finely laminated, pumiceous, tuffaceous sediments (siltstones and sandstones). Clasts of pumice, porphyritic volcanics and greywacke.
1380 to >1457	-1011 to < -1088	**VOLCANIC BRECCIA** Weakly porphyritic volcanic breccia with plagioclase phenocrysts in a silicified matrix.
1457 to 2169	-1088 to -1799	**NO RETURNS**
<2169 to >2174	> -1799 to < -1804	**ANDESITE BRECCIA** Subrounded to rounded clasts of porphyritic andesite, greywacke, granite, diorite and rhyolite, with common crystals of plagioclase, pyroxene, hornblende and rare quartz. Drillcore #1 2169-2184 mRF
2174 to 2953 (TD)	-1804 to -2560	**NO RETURNS**

Appendix B: Field Notes

Fieldwork 04/02/09 – 18/02/09

04/02/09

NM2 & NM3

NM3 well is being bled. Bleed sample taken from weir box. Temp = 73.1^{o}C, pH = 8

NM2 well is flowing sample taken from weir box. Temp Weir Box = 96^{o}C, pH = 8.5, Sample temp = 73.9^{o}C.

05/02/09

Orakonui Stream South

Main Crater – the nature of the crater appears to have changed significantly since Spinks, 2006. The main bubbling side spring looks as if it may have erupted subsequent to the 2005 eruption; the water level in the side spring is lower than the outflow channel for the crater.

As you head down the track from the farm gate you can see a large cliff section on the eastern bank of the stream which appears to be a section of white pyroclastic deposits, probably Taupo. It appears that the Taupo holds up the cliffs on the eastern bank.

Overnight rain on the 5th made the soil too saturated for soil flux measurements.

06/02/09

Orakonui Stream South (with Clinton)

1/1 - Water sample taken from the main crater pool (002), Water Temp: 53.8 ^{o}C, Air temp: 21.3 ^{o}C. (E2786604, N6291772)

(001)E2786623, N6291776 -Orakonui Stream temp measurement 15.5 ^{o}C (upstream of crater outlet, 001), at this point the temp of the mud in the stream is 82.8 ^{o}C at 30cm depth.

1/2. – Water sample from confluence of pool and outflow channel (003), temp – 53.8 ^{o}C. (E2786605, N6291792)

1/3 – Water sample from just above confluence with stream (004), temp – 53.6 ^{o}C. (E2786615, N6291798)

1/4. – Water sample at confluence of stream and crater outflow. (005), Temp of water – 19^{o}C, soil temp 30cm below stream bed at confluence – 96.0^{o}C. (E2786634, N6291822)

1/5 – Water and sub soil temperature in stream to the south of 1/1 (006), Water Temp = 16.2^{o}C, 30cm soil temp = 62.8^{o}C, temperature in the bank on the western side is 39 ^{o}C at 30cm depth. (E2786624, N6291772)

Orakonui Stream North

1/6 – Clear Black: Spring found along track at base of stream. Two large Pine trees obscure the stream (116 Clint). Temp of spring = 94.5 ^{o}C, Temp upstream = 17.6 ^{o}C, Temp downstream = 17.8 ^{o}C (main channel), 20.1 ^{o}C (mouth of spring), 15cm soil temp in channel = 43.4 ^{o}C. (NZTM E1876641, N5730660)

1/7 – Little Clear Black: Another spring found about 10m downstream of C.B (117 Clint). Spring Temp = 83.8 ^{o}C, Soil Temp in spring = 78.6 ^{o}C (15cm), 83.0 (30cm), Temp smaller spring just to

south = 77.3 ^{o}C, Water Temp just downstream = 17.9 ^{o}C, 20 cm stream bank temp = 69.3 ^{o}C, 20 cm mid stream temp = 72.1 ^{o}C, 5 cm eastern bank temp = 69.3 ^{o}C. (NZMT E1876658, N5730674).
1/8: (007), (118 Clint). O.N spring 4 Spinks 2006, spring temp = 94.4 ^{o}C, associated boiling mud pot ~15 cm x 15cm just to the south, mud temp = 75.8 ^{o}C, 5cm soil temp = 35.3 ^{o}C, 15 cm soil temp = 41.4 ^{o}C, 30 cm soil temp = 58 ^{o}C. (NZMG: E2786717, N6292221. NZMT: E1876651, N5736624).
1/9: (119 Clint). Outcrop of partially welded pumice with a silt and clay matrix. Hot water is seeping out of the base of the outcrop. The pumice appears to have elongated vesicles. Upper part of the outcrop is poorly sorted pumice which is indurated. The lower part is hydrothermally altered. Pumice clasts throughout the outcrop are sub-angular to sub-rounded. (NZMT: E1876605, N5730559).
1/10: (008), (120 Clint). Rock under ledge in western bank is acting as a spring. Aquifer rocks are warm and altered (33.4 ^{o}C). It appears that the rock unit is the only one hosting the fluid as there are intensely altered bands of rock which may be the permeable layer at a large scale. (NZMG: E2786680, N6292134, NZMT: E1876590, N5730549).
1/11: Another spring feature (121 Clint). 20 cm soil temp in steam = 33.1 ^{o}C. Water is bubbling out of the sediment in the stream bed at this temperature. (NZMT: E1876574, N5730557).
1/12: (122 Clint). Must come back! Impermeable rock layer sits above aquifer layer in a punga grove. The rock here may be similar to that above where the car is parked in the paddock. (NZMT: E1876583, N5730544).
1/13: (123 Clint). Confluence of Spinks northern most mapped spring and Orakonui Stream. (NZMT: E1876660, N5730690).
1/14: (124 Clint). Point of hot spring at the top of most northern mapped spring by Spinks, it is Calc alkaline. Temp = 83.1 ^{o}C. (NZMT: E1876697, N5730607)
1/15: (125 Clint). Another alkaline spring, temp 64 ^{o}C. (NZMT: E1876682, N5730622).
1/16: (009). Water sample from downstream of the northern most spring, sample temp 18.2 ^{o}C. (NZMG: E2786770, N6292258).

09/02/09

<u>South Orakonui Main Crater</u>
All springs are bubbling rigorously in the crater today, altered and unaltered hydrothermal eruption material collected, altered from the north side of crater outlet unaltered from south side.

10/02/09

NM2 and NM3 Water Samples
New Glass Jars

NM2: Water sample taken from weir, well flowing. Temp of fluid in weir = 96.5 ^{o}C, pH = 8.5, Temp of sample 74.1 ^{o}C.

NM3: Water sample taken from weir, well bleeding. Temp of fluid in weir = 72.7 ^{o}C, pH = 7.75, Temp of sample = 68.9 ^{o}C.

17/02/09

Water Sampling Orakonui South Crater (with Jimmy)

(039). Sample 1) Main Crater pH: 8, Temp ~58 ^{o}C
Sample 2) Main Crater Side Spring pH: <6.2, Temp ~55 ^{o}C
18/02/09

Orakei Korako

5/1: Sample taken from Ruatapu Cave, pH = substantially less than 6.2. Rock sample also taken.
5/2: Surface spring sample (O.K 1) (NZMG: E2784750, N6298523), pH = 8.5, temp = 90+ ^{o}C.
5/3: Water sample taken at the confluence of Lake Ohakuri and the thermal outflow. (041) (NZMG: E2784567, N6298487).
5/4: Lake Ohakuri sample take from ~500m upstream of thermal area. (042) (NZMG: E2784479, N6298648).
5/5: Taupo pyroclastics in quarry opposite where point is taken on the road, the unit is 4 m+ thick. (043) (NZMG: E2784196, N6298648).
Orakonui Stream Confluence
5/6: Sample taken from beside jetty on upstream side of Orakonui Stream on the Waikato River. (044) (NZMG: E2787206, N6293496), sample also taken downstream of the confluence from beneath the bridge.
Ngatamariki
5/7: Outcrop of insitu bedrock above Orakonui Stream on farmland. Outcrop creates a peak in the hillside. The rock is well indurated and light grey, it has phenocrysts of feldspar and olivine or hornblende. Possibly a rhyolite dome or ignimbrite (refer to Lloyd). (045) (NZMG: E2786169, N6291612).
Orakonui Stream South
5/8: Water sample taken upstream of crater and southern most pool. (046) (NZMG: E2786651, N6291705)

5/9: GPS (047) of Taupo in farm paddock. (NZMG: E2786525, N6291699)

Fieldwork 18/05/09 – 21/05/09

18/05/09

Orakonui North Spring Sampling.

Samples being taken for analysis at GNS Wairakei

1) Clear Black (pH invalid) T = 93.7 ^{o}C
2) Sample taken from Devils Mouth (pH invalid) T = 83 ^{o}C (called northern most spring in February field work) (E 2786791, N 6292177)
3) The northern most sinter mapped was found no active springs but a lot of seepage draining down to the stream is evident. (E 2786792, N 6292286).
4) Spring with associated mud pot, now called Father and Son spring (pH invalid) T = 94.4 ^{o}C.

19/05/09

Orakonui South Spring and Stream Samples

Rain overnight – samples for analysis at GNS Wairakei being taken

1) Northern most geothermal pool pH = 7.2, T = 30 ^{o}C (E 2786593, N 6291838)
2) Confluence Orakonui Stream and Main Crater outflow pH = 6.84, T = 15.5 ^{o}C (E 2786613, N 6291811)
3) Main Crater sample pH = 7.3, T = 49.8 ^{o}C (E 2786586, N 6291785)
4) Main Crater Side Spring sample pH = 5.84?; T = 46.8 ^{o}C.
5) Southern most spring/pool pH = 7.2, T = 72.3 ^{o}C (E 2786614, N 6291711)
6) Orakonui Stream sample south of thermal area pH = 6.89?; T = 13.0 ^{o}C (E 2786638, N 6291507)

20/05/09

Orakei Korako

Rain overnight – samples for analysis as GNS Wairakei

1) Ruatapu Cave sample pH = 2.67, T = 35 ^{o}C (E 2784855, N 6298344).

2) Artists Palette sample taken from northern end of palette near Pyramid of Geysers pH (invalid), T = 75.1 ^{o}C (E 2784892, N 6298467)
3) Sample from The Cauldron (Base of Golden Fleece scarp) pH = (invalid) T = 86.7 ^{o}C (E 2784761, N 6298516)
4) Diamond Geyser sample (Rainbow Fault) pH = (invalid) T = 83.4 ^{o}C (E 2784621, N 6298565)
5) Map of Australia (Western Bank pool/Spring) pH = 7.25, T = 80.5 ^{o}C (E 2784263, N 6298543)

Ngatamariki

6) Orakonui Stream Sample ~15 m upstream of Waikato Confluence pH = 7.42, T = 15.3 ^{o}C (E 2787128, N 6293452)

21/05/09

Nga Tamariki MRP Well/Drill Sites

1) NM5 – Testing Well pH = 7.9, T = 97 ^{o}C (Sample taken at 91 ^{o}C)
2) NM3 – Flowing well for water pH = 7.9, T = 96.5 ^{o}C

Fieldwork 1/12/09 – 7/12/09

1/12/09

Orakei Korako Spring Sampling

1/1 – Sample taken from Devils Throat (DT/1)

1-2 – Kakuki Basalt sample taken from road cutting south of Orakei Korako. It is a high alumina basalt, primitive in terms of the TVZ.

6/12/09

Waikato River to Orakei Korako Sampling (With MRP team)

6/1 – At hottest spring on southern bank, spring is flooded with river water but is still high temperature (60 – 70 ^{o}C). W.P 004 – NZMG E2787942, N6293426 (Sample W1)

6/2 – 20m towards cliff from last spring is a spring of the same temperature. W.P 005 – NZMG E2787924, N6293413 (sample W2)

6/3 – Dome breccia seen in river cliff W.P 006 – NZMG E2786860, N6294297

6/4 – Contact between Huka Falls and dome breccia W.P 007 – NZMG E2786746, N6294514

6/5 – Red Hill Springs – Geyser above Tutukau Bath, Water at boiling point, they geyser appears to only have small spurts in a 5x5m radius around the pool. W.P 008 – NZMG E2785034, N6296830 (sample TBG)
6/6 – West Bank Springs, Most southern of the springs which is a geyser, outflow from pool exits to the Waikato river, pool at boiling point, W.P 009 – NZMG E2784606, N6297090

7/12/09
Orakonui North
7/1 – Clear Black appears much smaller, sample take from LCB which appears to have a larger pool than in previous visits (Sample LCB)
7/2 – Spring on left hand side of main sinter (Sample taken SSS)
7/3 – Most southern sinter found, NZMG W.P 011 and 012 E2784315, N6298533; E2786739, N6292158. Sinter flows down towards the Orakonui Stream.
7/4 – Most Northern sinter, split into two areas which are very overgrown, W.P 013, E2786792, N6292303.

Appendix C: Locations of thermal features at Orakei Korako Tourist Area (Hamlin 1999).

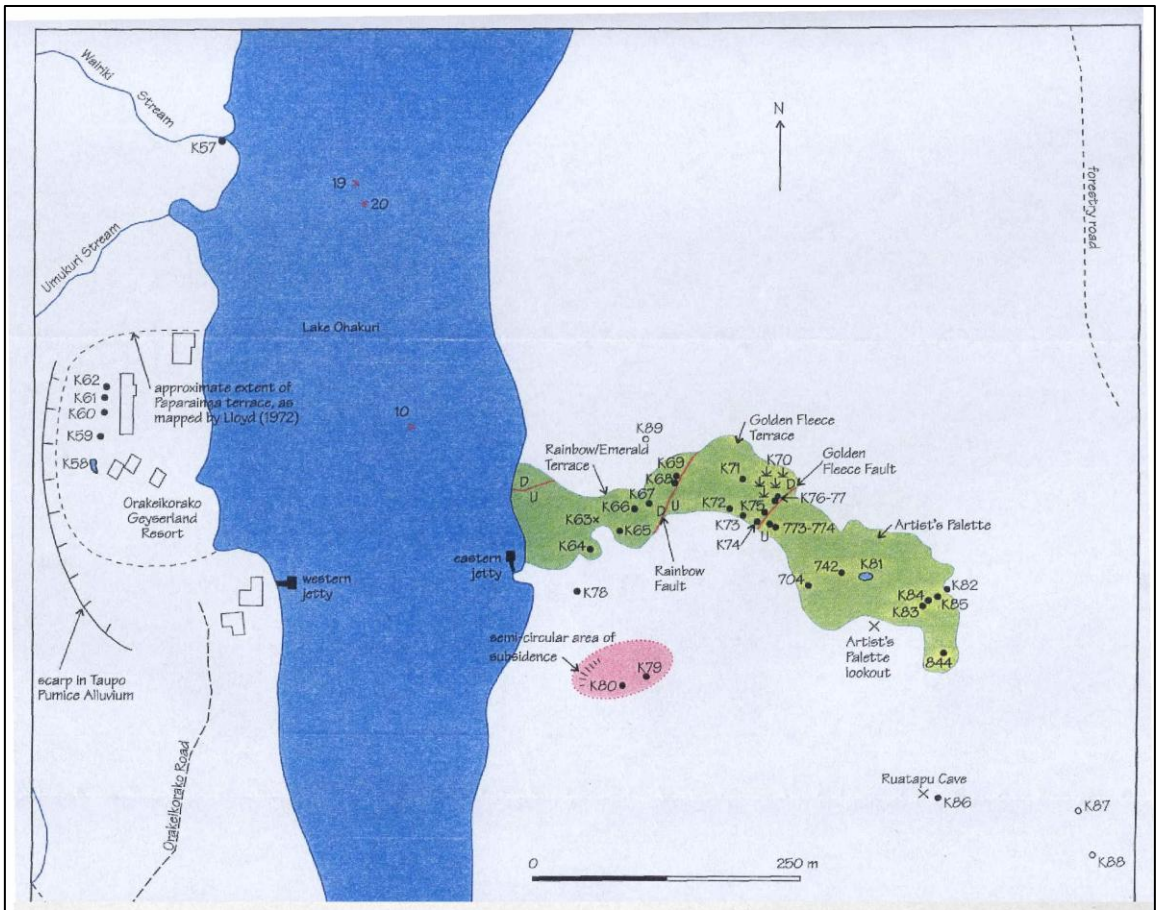

Key to springs and locations shown in figures 3-1 and 3-2 and described in the text

number	feature	number	feature	number	feature
K1-29	westernmost mud pots	K66	Hochstetter Pool	K84	Still Pool
K30-50	mud pots straddling arcuate ridge	K67	Map of Africa	K85	Invisible Spring
K51	Acid Spring	K68	Tim and Terry Springs	K86	Waiwhakaata
K52	Bramble Pool	K69	Devil's Throat	K87	coalesced mud pots
K53	Kanuka Pool	K70	Diatom Marsh	K88	separate mud pot
K54	Pool 4	K71	Fred and Maggie Pool	K89	small mud pot
K55	Apron Pool	K72	Manganese Pool	K90	Sinter Island
K56	Mannanin Pool	K73	Wairiri Geyser	K91	Hot waterfall geyser
K57	Umukuri Spring	K74	Dreadnought Geyser	K92	Breccia Number Twelve
K58	Map of Australia	K75	Cauldron	Features	referred to in Lloyd (1972)
K59	Utility Pool	K76-77	Twin Springs	10	Te mimi-a-Homaiterangi
K60	Bracken Pool	K78	Soda Fountain	19	Minginui
K61	Green Pool	K79	Kurapai	20	Rahurahu
K62	Brown Pool	K80	Ellan Vannin	23	Rameka
K63	channel on Rainbow Terrace	K81	Palette Pool	704	Psyche's Bath
K64	Diamond Geyser	K82	Pyramid of Geysers	742	Square Pool
K65	Sapphire Geyser	K83	Muddy Waters	773-774	Twin Pools

Appendix D: Methods used for analysis of major ions at GNS Wairakei.

WAIRAKEI ANALYTICAL LABORATORY
Private Bag 2000, Taupo
Phone: (07) 374 8211
Fax: (07) 374 8199
e.mail: w.labmanager@gns.cri.nz

Appendix to REPORT WAL090520001

Summary of Methods Used and Detection Limits

The following table gives a brief description of the methods used to conduct the analyses on this report.
The detection limits given below are those attainable in a relatively clean matrix. Detection limits may be higher for individual samples should insufficient sample be available, or if the matrix requires that dilutions be performed during analysis

	PARAMETER	METHOD USED	DETECTION LIMIT
	Bicarbonate (total)	HCO3 Titration Method ASTM Standards D513-82 Vol.11.01 of 1988	20 mg/L
	Boron	ICP-OES APHA 3120-B 21st Edition 2005	0.3 mg/L
	Bromide	Ion Chromatography APHA 4110-B 21st Edition 2005	0.04 mg/L
	Calcium	ICP-OES APHA 3120-B 21st Edition 2005	0.05 mg/L
	Cesium	Flame Emission Spectrometry APHA 3500-Cs 21st Edition 2005	0.02 mg/L
	Chloride	Ion Chromatography APHA 4110-B 21st Edition 2005	0.04 mg/L
	Chloride	Potentiometric Method APHA 4500-Cl D 21st Edition 2005	20 mg/L
	Fluoride	Ion Selective Electrode APHA 4500-F C 21st Edition 2005	0.1 mg/L
	Fluoride	Ion Chromatography APHA 4110-B 21st Edition 2005	0.005 mg/L
	Lithium	ICP-OES APHA 3120-B 21st Edition 2005	0.01 mg/L
	Magnesium	ICP-OES APHA 3120-B 21st Edition 2005	0.01 mg/L
	pH	Electrometric Method APHA 4500-H+ B 21st Edition 2005	1
	Potassium	ICP-OES APHA 3120-B 21st Edition 2005	0.90 mg/L
	Rubidium	Flame Emission Spectrometry APHA 3500-Rb 21st Edition 2005	0.01 mg/L
	Silica (as SiO_2)	ICP-OES APHA 3120-B 21st Edition 2005	0.6 mg/L
	Sodium – 818.326 nm	ICP-OES APHA 3120-B 21st Edition 2005	1.5 mg/L
	Sulphide (total as H2S)	Methylene Blue Method APHA 4500-S2 D 21st Edition 2005	0.01 mg/L
	Sulphate	Ion Chromatography APHA 4110-B 21st Edition 2005	0.03 mg/L

If you have any queries with regard to the above please contact the Laboratory Manager, Dr B Mountain, ph. 07-3748211, mob. 027-220 9647, Email: b.mountain@gns.cri.nz

Appendix E: Measured Well pressures, steam fractions and enthalpies for Ngatamariki wells.

Well	Date	CP (bg)	SF (%)	H (kj/kg)
NM2	13/03/2009	27.8	17	1238
NM3	3/07/2009	6.25	26	1235
NM5	28/04/2009	7.6	22	1182
NM6	28/04/2009	8.3	16	1060

(Data courtesy of Mighty River Power)

Appendix F: Water Chemistry

Composition of waters discharged from springs and wells at Ngatamariki.

Ngatamariki																				
Springs (O'Brien 2010)	**IDENT**	**pH**	**Li**	**Na**	**K**	**Ca**	**Mg**	**SiO2**	**B**	**Cl**	**F**	**SO4**	**HCO3**	**As**	**Rb**	**Cs**	**TDS**	**δ18O (‰ V-SMOW)**	**δD (‰ V-SMOW)**	**H (Qz) Kj/Kg**
M.C	MC	7.3	2.1	365	22	4.4	0.54	193	5.6	407	1.6	36	321		0.18	0.33	1359	-5.35	-42.05	754.4
M.C Side Spring	MCSS	6.44	3.7	679	30	24	0.94	195	8.6	638	2.6	541	240		0.26	0.51	2364	-2.50	-33.83	758.8
O.S South Pool	SP	7.53	3.2	623	22	0.94	0.06	244	9.2	647	3.1	30	523		0.21	0.52	2106	-5.03	-41.64	830
O.S North Pool	NP	7.61	1.5	260	13.1	9.2	1	132	3.1	232	1.1	38	307		0.1	0.22	998	-6.61	-43.94	649.5
Clear Black	CB	7.4	1.6	359	17.3	7.1	0.59	177	5.1	360	1.7	7.4	400		0.13	0.26	1337	-6.29	-45.27	728
Father and Son	FS	7.3	1.6	351	16.8	5.4	0.6	180	4.9	343	1.7	7.7	368		0.13	0.29	1281	-6.85	-46.24	732.4
Devils Mouth	DM	7.36	3.4	584	16.6	0.66	0.02	204	7.6	517	2.5	12.7	643		0.13	0.26	1992	-6.32	-46.08	772.1
W1	W1	7.18	0.81	184	20.2	5.6	1.7	195	2.1	144	1.2	4.2	328		0.01	0.03	887			758.8
W2 (GNS, 2009)	W2	6.78	0.5	129	11.6	3.7	1.2	174	0.61	57		0.1	309		0.14	0.02	687			723.6
Stream, River and Lake Waters (O'Brien 2010)																				
Waikato RIver	WR																	-5.55	-37.01	
Lake Ohakuri	LO																	-5.60	-37.25	
Orakonui Stream	OS	7.7	0.12	28.5	2.4	4.7	2.3	78	0.39	5.3	0.2	4.6	49		0.06	0.03	176	-7.27	-47.13	
Wells																				
NM2 (Hedenquist, 1986)	NM2	8.4	10.7	876	191	4.9	0.31	830	21.9	1463		23	55		1.82	1.65	3479			
NM2 (Hedenquist, 1986)	NM2 '85	6.7	8.6	703	154	4.3	0.03	710	17.4	1193		24	98		1.47	1.35	2915	-5.70	-44.50	1095
NM2 (O'Brien 2010)	NM2									1193								-4.94	-40.03	
NM3 (O'Brien 2010)	NM3	8.99	11.2	884	208	3.7	0.01	945	23	1574	4.9	2.6	26		2.1	1.7	3686	-6.15	-43.02	1210
NM5 (MRP, 2009)	NM5	5.83	9.4	750	152	3	0.02	787	19.6	1227	4.8	10.3	110		0.91		3074			
NM5 (O'Brien 2010)	NM5	8.8	10.8	853	176	3.1	0.01	936	23	1456	6	6.8	91		1.7	1.7	3565	-5.76	-37.19	1210
NM6 (MRP, 2009)	NM6	6.27	8.8	787	147	4.2	0.01	680	20	1183	2.9	35	155		0.83		3024			1081
Monitoring Wells																				
NMM5 (Ricketts, 2009)	NMM5	10.1	0.019	25	6	34	1.5	78	21.9	7.2		10	77	0.0054			261			
NMM6 (Ricketts, 2009)	NMM6	7.5	0.053	18	3	5.6	2.7	79	17.4	3.1		5.1	68	0.059			202			
NMM6 (Plume) (Ricketts, 2009)	NMM6 P	6.6	3.6	360	48	52	24	350	23	790		5.3	38	0.27			1694			
NMM7 (Ricketts, 2009)	NMM7	8	0.059	19	1.3	5.3	3	48	19.6	4.3		6.8	72	0.065			179			
NMM8 (Ricketts, 2009)	NMM8	7	0.41	55	12	9.6	5.7	84	23	32		1	170	0.051			393			
NMM9 (Ricketts, 2009)	NMM9	8	0.12	34	7.1	9.2	3.1	70	20	29		7.1	94	0.18			274			

Composition of waters discharged from springs and wells at Orakei Korako.

Orakei Korako																			
Tourist Area (O'Brien 2010)	**IDENT**	**pH**	**Li**	**Na**	**K**	**Ca**	**Mg**	**SiO2**	**B**	**Cl**	**F**	**SO4**	**HCO3**	**Rb**	**Cs**	**TDS**	**δ18O (‰ V-SMOW)**	**δD (‰ V-SMOW)**	**H (Qz) Kj/Kg**
Map of Australia	MOA	8.19	3.1	330	18.6	0.56	0.01	269	3.2	333	11.6	61	300	0.27	0.59	1331	-4.60	-39.13	861.5
Diamond Geyser	DG	7.36	4	317	43	2.8	0.12	314	3.2	310	9.9	93	277	0.61	0.58	1375	-4.51	-37.44	916
The Cauldron	CA	7.24	4.3	333	53	1.9	0.13	319	3.5	329	11.8	120	276	0.57	0.61	1453	-4.01	-35.15	925.2
Ruatapu Cave	RC	2.57	2.3	154	0.49	4.7	1.5	261	1.8	147	3.9	390	20	0.49	0.28	987	-4.10	-28.46	852.4
Artists Palette (Spring 826)	826	5.9	4.2	294	50	1.7	0.12	338	3.4	304	7.9	258	35	0.55	0.54	1297	-4.68	-33.85	943.6
Manganese Pool	MP																-3.16	-33.08	
Red Hill/West Bank (O'Brien 2010)																			
Hot Waterfall Geyser	HWG	9.46	2.9	295	34	0.97	0.01	276	3.2	319	11.5	49	106	0.24	0.5	1098			870.5
O'Brien's Geyser	OBG	8.01	3.3	308	13.1	2.6	0.06	299	3.5	342	13.7	60	150	0.1	0.3	1196			897.8
Tourist Area (Sheppard and Lyon 1984)																0			
95	95	8.6	4.4	339	45	1.5	0.39	297	4.1	313	14	106	260	0.46	0.59	1385	-5.21	-37.6	897.8
98	98	7.9	4	300	46	2	0.52	322	3.1	310	11.8	144	232	0.47	0.56	1376	-4.28	-34.7	925.2
120	120	8.6	4.3	321	57	2	0.25	381	3	324	11	96	244	0.49	0.59	1445	-4.64	-36.1	994.8
Red Hill/West Bank (Sheppard and Lyon, 1984)																			
526	526	7.6	3.4	334	10	1.1	0.02	263	6	349	13	84	139	0.17	0.49	1203	-3.41	-33.9	852.4
984	984	7.4	2.6	275	11	3.2	0.12	258	4	303	11.5	73	118	0.14	0.22	1060	-4.45	-33.8	847.9
297	297	8.9	2.9	249	4	1.5	0.02	182	6	279	9.8	48	118	0.07	0.18	900	-5.22	-37.5	736.8
Orakei Korako Wells (Sheppard and Lyon 1984)																			
OK2	OK2	9.1	3.1	550	54	1		480		546	5.7	142	405			2187			957.5
OK4	OK4	9.2	3.2	300	35	1.3		410	4.2	319	13.7	61	252			1399			906.9
OK6	OK6	8.9	4.3	430	49	3.9		480	4.1	383	5.6	42	546			1948			957.5
OK6	OK6	8.8	2	257	19.3	12.1		250	1.6	142	3.1	20	490			1197			

Appendix G: Geothermometers used in this study.

Geothermometer	Equation and Restrictions
Chalcedoney	t ^{o}C =(1032/4.69 – log c) -273.15 (0-250 ^{o}C)
Quartz no steam loss	t ^{o}C =(1309/5.19 – log c) -273.15 (0-250 ^{o}C)
Quartz max steam loss	t ^{o}C =(1522/5.19 – log c) -273.15 (0-250 ^{o}C)
Na-K-Ca	t ^{o}C =(1647/log (Na/K)+β[log(√Ca/Na)+2.06]+2.47) -273.15 (<100 ^{o}C if β = 4/3 and >100 ^{o}C if β = 1/3)
Na-K-Ca Mg Correction	T.Na-K-Ca - TΔMg (T.Na-K-Ca> 70 ^{o}C and R<50)

Chalcedony: (Fournier 1981)

Quartz no steam loss: (Fournier 1981)

Quartz maximum steam loss: (Fournier 1981)

Na-K-Ca: (Fournier & Truesdell 1973)

Na-K-Ca Mg Correction: (Fournier & Potter Ii 1979)

If R> 50 it is assumed that the temperature is equal to the water sample temperature.

Appendix H: XRD diffraction patterns for samples OSU and OSA.

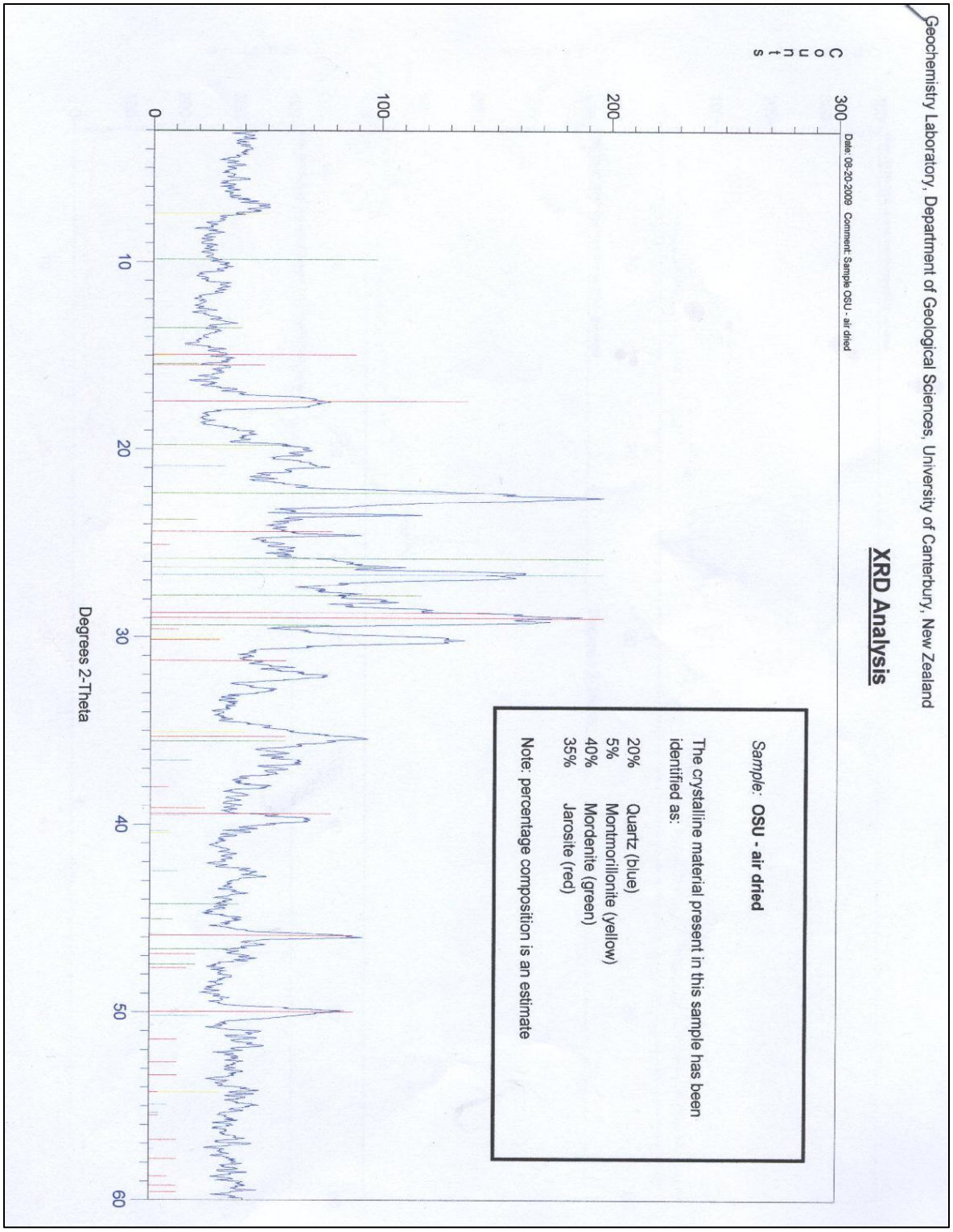

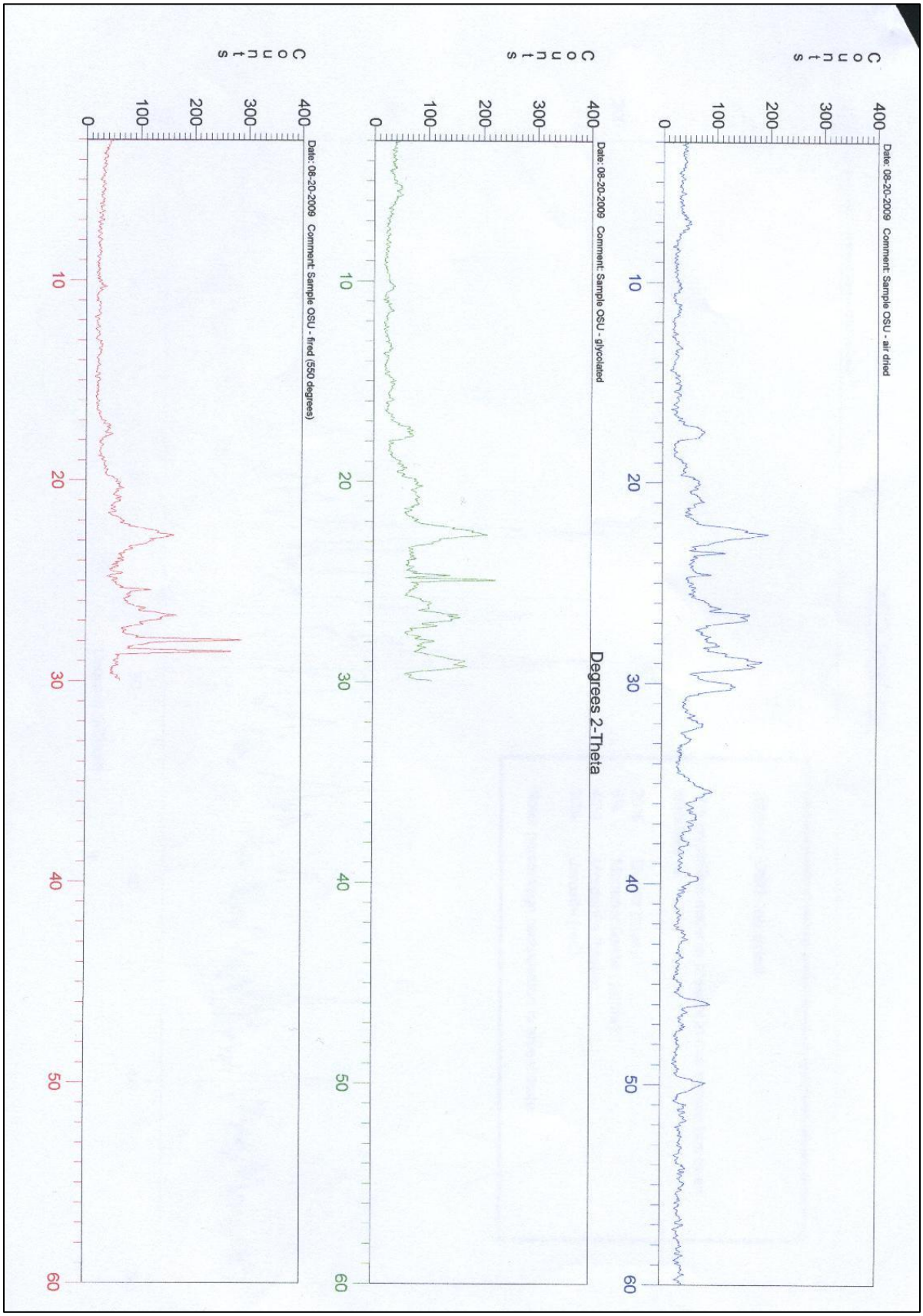
Counts
Date: 08-20-2009 Comment: Sample OSU - air dried
Date: 08-20-2009 Comment: Sample OSU - glycolated
Degrees 2-Theta
Date: 08-20-2009 Comment: Sample OSU - fired (550 degrees)

Geochemistry Laboratory, Department of Geological Sciences, University of Canterbury, New Zealand

XRD Analysis

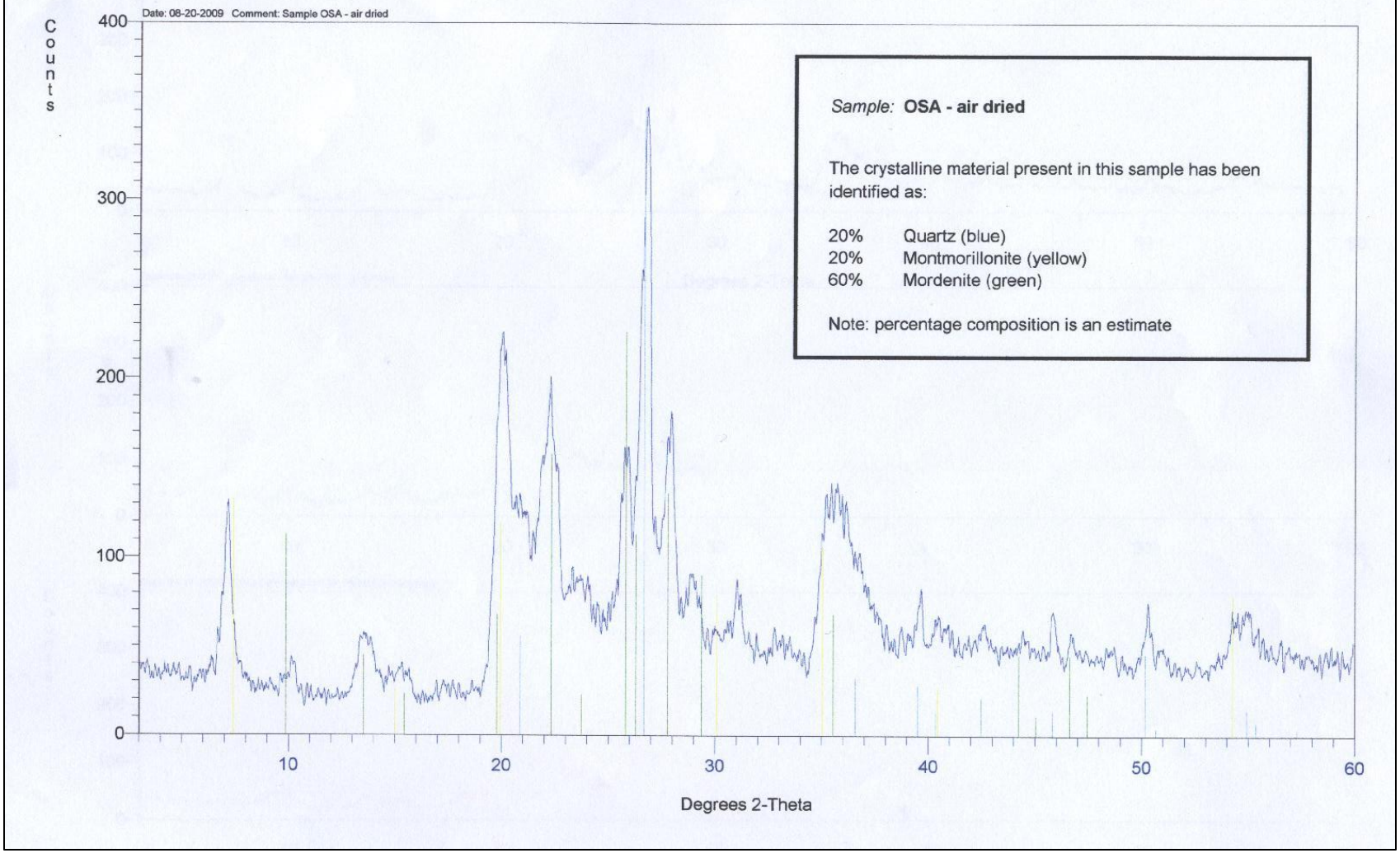

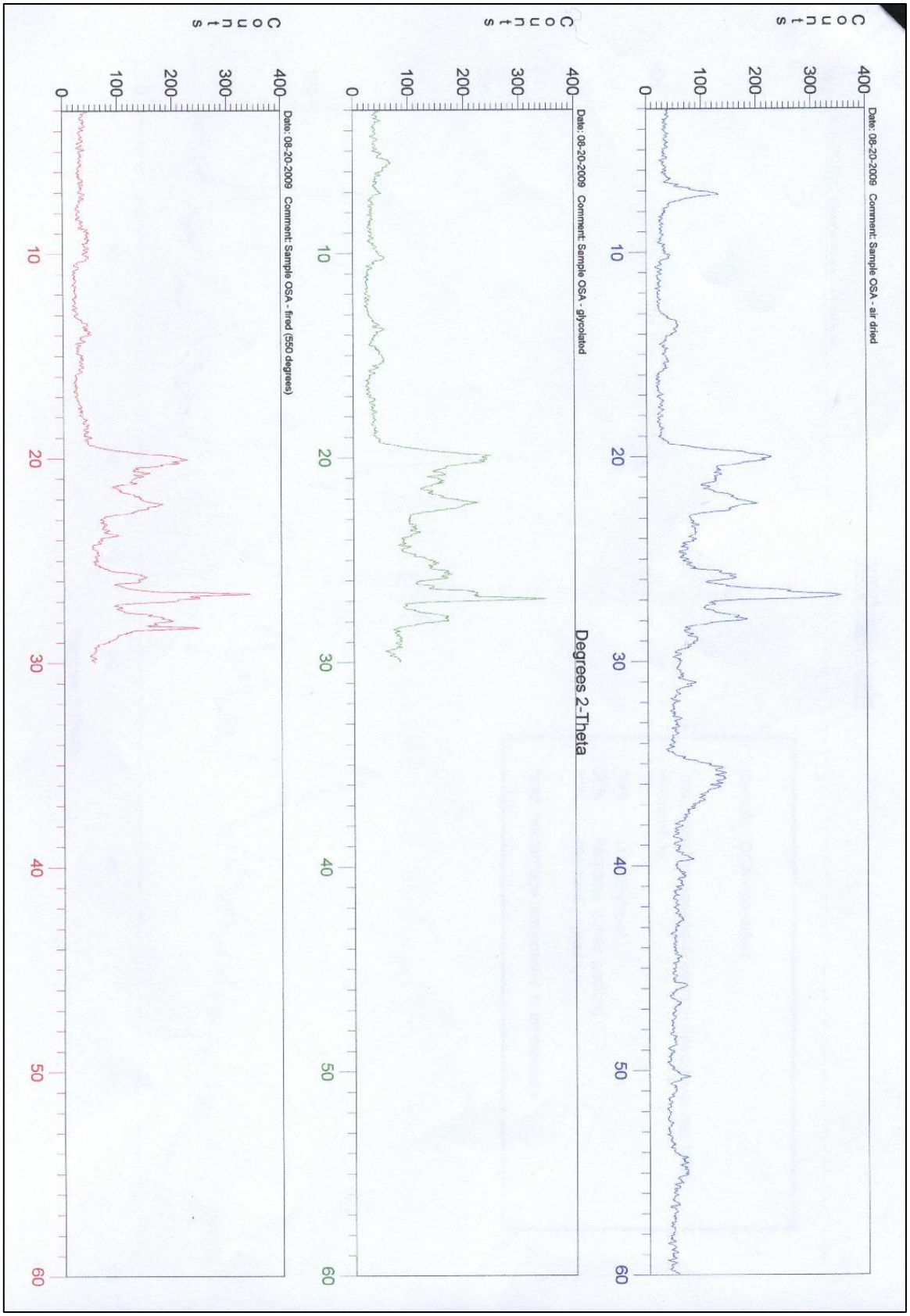
Counts
Date: 08-20-2009 Comment: Sample OSA - air dried
Date: 08-20-2009 Comment: Sample OSA - glycolated
Degrees 2-Theta
Date: 08-20-2009 Comment: Sample OSA - fired (550 degrees)

Appendix I: Locations and sample numbers for previous studies at Orakei Korako (Sheppard & Lyon 1984)